



**University of  
Nottingham**

UK | CHINA | MALAYSIA

**EXPLORATION OF MICROALGAL CULTURE USING A SEMI-  
CLOSED THIN LAYER CASCADE PHOTOBIOREACTOR FOR  
BIODIESEL SYNTHESIS AND PROTEIN PRODUCTION**

Tan Chung Hong

Main Supervisor: Dr. Show Pau Loke

Co-Supervisor: Dr. Lam Hon Loong

Thesis submitted to the University of Nottingham for the degree of Doctor of  
Philosophy

May 2019

# ABSTRACT

---

The expanding aquaculture industry increases the prices of fishmeal, the main protein source in fish diet. A promising alternative is microalgal protein. Therefore, the protein production capacities of two green microalgae species, *Chlorella sorokiniana* CY1 and *Chlorella vulgaris* ESP-31, were investigated. After optimization, the maximum biomass and protein productivities of *Chlorella sorokiniana* CY1 reached high values of  $4.35 \pm 0.09$  and  $0.856 \pm 0.025$  g/L/d, while that of *Chlorella vulgaris* ESP-31 also reached high values of  $4.636 \pm 0.10$  and  $0.946 \pm 0.065$  g/L/d. The cultivation time for both species was only 2 days, wherein *Chlorella sorokiniana* CY1 and *Chlorella vulgaris* ESP-31 amassed moderate protein contents of  $25.9 \pm 1.3\%$  and  $26.8 \pm 1.3\%$ . The optimum conditions for both species were 50% initial nitrate concentration of Basal medium, 5% CO<sub>2</sub> aeration, and 750  $\mu\text{mol}/\text{m}^2/\text{s}$  light intensity. The high biomass and protein productivities of both species indicated their capability as potential protein sources.

After studying protein production from microalgae, a second microalgae-derived commodity that received global attention was microalgal biofuels, in particular biodiesel. Microalgae is widely regarded as the most promising source of green and sustainable fuel for the future, with microalgal biodiesel widely seen as a replacement for diesel fuel. Compared to biodiesel from terrestrial crops such as palm oil and rapeseed, the benefits of microalgal biodiesel include rapid growth rate of microalgal cells, higher carbohydrate and lipid content, higher productivity per unit land area, and utilisation of wastewater for growth. Therefore, five indigenous microalgae species from Taiwan were selected to determine their potential for lipid production, namely *Chlamydomonas* sp. Tai-01, Tai-03 and Pin-01, as well as *Scenedesmus* sp. ESP-05 and ESP-07. *Chlamydomonas* sp. Tai-03 proved to be the best strain, achieving biomass growth and productivity of  $3.48 \pm 0.04$  g/L and  $0.43 \pm 0.01$  g/L/d, accompanied by an oil content and oil productivity

of  $28.6 \pm 1.41\%$  and  $124.1 \pm 7.57$  mg/L/d. This was attained by inoculating 0.12 g/L biomass into BG-11 medium with 25% initial nitrate concentration and light-emitting diode (LED) light intensity of  $200 \mu\text{mol}/\text{m}^2/\text{s}$ . The fatty acid methyl esters (FAMES) obtained from the *Chlamydomonas* sp. Tai-03 strain consisted mainly of palmitic acid, oleic acid and linoleic acid, making this microalga a suitable feedstock for biodiesel synthesis.

The microalga species *Chlamydomonas* sp. Tai-03, which was previously optimised for maximal lipid production for biodiesel generation, received further optimization by investigating the effects of different CO<sub>2</sub> concentration and different medium replacement strategy using semi-batch operation. The optimum conditions were found as 5% CO<sub>2</sub> concentration and semi-batch operation with 25% medium replacement ratio, which further enhanced the biomass growth and productivity to  $4.15 \pm 0.12$  g/L and  $1.23 \pm 0.02$  g/L/d, with lipid content and productivity of  $19.4 \pm 2.0\%$  and  $239.6 \pm 24.8$  mg/L/d. Under the medium replacement strategy, 25% of the microalgal biomass could be replaced/harvested daily after the culture entered the medium replacement phase of the cultivation process (which was 8 days after the start of cultivation). Upon analysis, the major fatty acid methyl esters (FAMES) were palmitic acid (C16:0), oleic acid (C18:1), and linoleic acid (C18:2). These short-chain FAMES combined with high growth rate make *Chlamydomonas* sp. Tai-03 a suitable candidate for biodiesel synthesis.

Although microalgae can be turned into numerous valuable commodities, their large-scale cultivation still poses a great challenge to the current microalgal industries. Open systems are cheap to install and operate, easy to clean and maintain, and have high surface area to volume ratio, suitable for microalgal culture. But they are susceptible to contamination, evaporative losses, and unfavourable weather conditions. In contrast, closed photobioreactor systems have high productivity, control of growth parameters, and minimum risk of contamination. But photobioreactors are expensive to install and difficult to operate and maintain. Therefore, an integration of thin layer cascade photobioreactors with a semi-closed

## *Abstract*

setup was proposed that could be used to cultivate greater volumes of different microalgal species and generate different products such as proteins and lipids. This semi-closed photobioreactor system would have the benefits of both open systems and closed systems. An improved concept design had been illustrated and computational fluid dynamics (CFD) analysis using a simulation program (ANSYS) had also been performed to visualise the functionality and mechanism of the concept design. The CFD analysis revealed that the improved concept design of thin layer cascade semi-closed photobioreactor performed satisfactorily and was suitable for the cultivation of different microalgal species to produce proteins for fish feed and lipids for biodiesel.

# ACKNOWLEDGEMENT

---

The person I am most grateful to is my primary supervisor, Dr. Show Pau Loke. If not for him, I would not be where I am now. Dr. Show has given me ample support in most of my Ph.D. endeavours. I would also like to thank my family for supporting me all the way in undertaking a PhD degree. My housemates (Yan, Billie, CN), my juniors (Kit Wayne, Shir Reen, Isabelle), and all my PhD colleagues (you all know who you are) helped me through a lonely journey called PhD with frequent laughter, games, and adventures. I would never forget Shikin, Yoges, and Muna for their help. Especially Shikin, when she doesn't give up on me even when I have given up on me. No single word can describe the moment the thesis is submitted.

The technicians are forever my heroes – Andrew, Fareez, Bob, Faizal, Asyraf, and Irshad in Block N, as well as Kak Siti in Bioscience and Yusof and colleagues in Mechanical. Lastly, I would like to offer my most sincere gratitude to my mentors in NCKU, Prof. Chang (co-supervisor) and Dr. Chen, as well as my Taiwan colleagues/friends for all their support when I just started on my journey.

# PUBLICATIONS

---

## A. Journal Papers

1. Tan CH, Show PL, Lam MK, Fu XT, Ling TC, Chen CY, Chang JS 2020. Examination of indigenous microalgal species for maximal protein synthesis. *Biochemical Engineering Journal*, 154, pp. 107425.
2. Tan CH, Show PL, Ling TC, Nagarajan D, Lee DJ, Chen WH, Chang JS 2019. Exploring the potency of integrating semi-batch operation into lipid yield performance of *Chlamydomonas* sp. Tai-03. *Bioresource Technology*, 285, pp. 121331.
3. Tan CH, Show PL, Ling TC & Lam HL 2017. Genetic Manipulation to Increase Lipase Production in Microorganisms – A Recent Review. *Current Biochemical Engineering*, 4, no. 1, pp. 34-42.
4. Tan CH, Chen C-Y, Show PL, Ling TC, Lam HL, Lee D-J & Chang J-S 2016. Strategies for enhancing lipid production from indigenous microalgae isolates. *Journal of the Taiwan Institute of Chemical Engineers*, 63, pp. 189-194.
5. Tan CH, Cheah W, Tau C, Show PL, Juan JC & Chang J-S 2015a. Algae cultivation in wastewater for biodiesel—a review. *Chemical Engineering Transactions*, 45, pp. 1393-1398.
6. Tan CH, Show PL, Chang J-S, Ling TC & Lan JC-W 2015b. Novel approaches of producing bioenergies from microalgae: A recent review. *Biotechnology Advances*, 33, no. 6, pp. 1219-1227.
7. Tan CH, Show PL, Ooi CW, Ng EP, Lan JCW & Ling TC 2015c. Novel lipase purification methods—a review of the latest developments. *Biotechnology Journal*, 10, no. 1, pp. 31-44.

8. Lee SY, Sankaran R, Chew KW, Tan CH, Krishnamoorthy R, Chu D-T & Show P-L 2019. Waste to bioenergy: a review on the recent conversion technologies. *BMC Energy*, 1, no. 4, pp. 1-22.
9. Phong WN, Show PL, Teh WH, Teh TX, Lim HMY, Nazri NSb, Tan CH, Chang J-S & Ling TC 2017. Proteins recovery from wet microalgae using liquid biphasic flotation (LBF). *Bioresource Technology*, 244, pp. 1329-1336.
10. Choong WP, Tan CH, Show PL, Lam HL, Mohamad Annuar MSB, Juan JC, Chang J-S & Ling TC 2016. Efficient enzyme-catalysed transesterification of microalgal biomass from *Chlamydomonas* sp. *Energy*, 116, pp. 1370-1373.
11. Lung Y-T, Tan CH, Show PL, Ling TC, Lan JC-W, Lam HL & Chang J-S 2016. Docosahexaenoic acid production from crude glycerol by *Schizochytrium limacinum* SR21. *Clean Technologies and Environmental Policy*, 18, no. 7, pp. 2209-2216.
12. Chen C-Y, Kao P-C, Tan CH, Show PL, Cheah WY, Lee W-L, Ling TC & Chang J-S 2016. Using an innovative pH-stat CO<sub>2</sub> feeding strategy to enhance cell growth and C-phycoerythrin production from *Spirulina platensis*. *Biochemical Engineering Journal*, 112, pp. 78-85.
13. Chen C-Y, Lee P-J, Tan CH, Lo Y-C, Huang C-C, Show PL, Lin C-H & Chang J-S 2015. Improving protein production of indigenous microalga *Chlorella vulgaris* FSP-E by photobioreactor design and cultivation strategies. *Biotechnology Journal*, 10, no. 6, pp. 905-914.

## **B. Conference Papers**

1. Tan CH, Cheah WY, Ling TC, Show P., Juan JC, and Chang JS (2015). Algae cultivation in wastewater for biodiesel – A review. In: 3rd Postgraduate Colloquium for Environmental Research (POCER) 2015. Kuching: AIDIC, pp. 1393-1398.

2. Tan CH, Show PL, and Lam HL (2015). Drying Processes for Microalgal Biomass – A Mini Review. In: The 8th Asia-Pacific Drying Conference (ADC). Kuala Lumpur.
3. Lung YT, Tan CH, Show PL, Lam HL, and Lan JCW (2015). Docosaehaenoic Acid Production from Crude Glycerol by *Schizochytrium limacinum* SR21. In: Conference Process Integration, Modelling and Optimisation for Energy Saving and Pollution Reduction (PRES'15). Kuching: AIDIC, pp. 967-972.

### **C. Book Chapters**

1. Tan CH, Motavasel Z, Vijiaretnam NR, Show PL (2019). Chapter 9 – Drying. In: Show PL, Ooi CW & Ling TC (eds.) *Bioprocess Engineering – Downstream Processing*. CRC Press, pp. 189-207.
2. Chang JS, Show PL, Ling TC, Chen CY, Ho SH, Tan CH, Nagarajan D & Phong WN (2017). Chapter 11 – Photobioreactors. In: Larroche C, Sanromán MÁ, Du G & Pandey A (eds.) *Current Developments in Biotechnology and Bioengineering*. Elsevier, pp. 313-352.



# TABLE OF CONTENTS

---

<b>TABLE OF FIGURES</b>	<b>xv</b>
<b>TABLE OF TABLES</b>	<b>xix</b>
<b>ACRONYMS AND ABBREVIATIONS</b>	<b>xx</b>

## **CHAPTER 1 - INTRODUCTION**

1.1. Brief Overview of Research	1
1.1.1. The importance and hurdles of microalgal protein as fishmeal replacement in aquaculture	2
1.1.2. The importance and hurdles of microalgal biofuels	3
1.1.3. The importance and hurdles of photobioreactor design	4
1.2. Aim	5

## **CHAPTER 2 - LITERATURE REVIEW**

2.1. A brief background of cyanobacteria and microalgae	6
2.2. A brief summary of photosynthesis in cyanobacteria and microalgae	8
2.3. Microalgal biodiesel synthesis	9
2.3.1. Acid/base catalysis	10
2.3.2. Direct transesterification of wet biomass	11
2.3.3. Supercritical fluid method	12
2.4. Microalgal protein in aquaculture	13
2.4.1. Brief summary of aquaculture	13
2.4.2. Fishmeal production and utilisation	14
2.4.3. Microalgal protein as potential fishmeal replacements	15
2.5. Factors affecting microalgal growth	16
2.5.1. Light Utilisation	16
2.5.2. CO <sub>2</sub> assimilation	18

*Table of Contents*

2.5.3.	pH	19
2.5.4.	O <sub>2</sub> removal	20
2.5.5.	Mixing	21
2.5.6.	Temperature	22
2.6.	Microalgae cultivation systems	24
2.6.1.	Open system	26
2.6.1.1.	Circular pond	27
2.6.1.2.	Raceway pond	27
2.6.1.3.	Thin layer cascade	29
2.6.2.	Closed system	32
2.6.2.1.	Stirred tank photobioreactor	33
2.6.2.2.	Horizontal tubular photobioreactor	34
2.6.2.3.	Vertical tubular photobioreactor	35
2.6.2.3.1.	Bubble column photobioreactor	36
2.6.2.3.2.	Air-lift photobioreactor	37
2.6.2.4.	Flat plate photobioreactor	39
2.6.2.5.	Internally illuminated photobioreactor	40
2.6.2.6.	Fermenter type photobioreactor	42
 <b>CHAPTER 3 - MATERIALS AND METHODS</b>		
3.1.	Study 1	44
3.1.1.	Microalgae strain, medium composition, and culture conditions	45
3.1.2.	Determination of microalgae cell concentration	45
3.1.3.	Determination of medium nitrate concentration	46
3.1.4.	Operation of photobioreactor	46
3.1.5.	Preparation of different initial nitrate concentrations	47
3.1.6.	Preparation of different CO <sub>2</sub> concentrations	47
3.1.7.	Preparation of different light intensities	47
3.1.8.	Preparation of microalgal biomass for protein determination	47

*Table of Contents*

3.1.9.	Determination of protein content by Lowry assay	48
3.1.10.	Determination of microalgal biomass and protein productivities	49
3.1.11.	Statistical analysis	49
3.2.	Study 2	49
3.2.1.	Microalgae strain and medium composition	50
3.2.2.	Determination of microalgae cell concentration	51
3.2.3.	Determination of medium nitrate concentration	52
3.2.4.	Determination of light intensity	52
3.2.5.	Determination of oil/lipid content	52
3.2.6.	Operation of photobioreactor	53
3.2.7.	Adjustment of initial nitrate concentration	54
3.2.8.	Statistical analysis	54
3.3.	Study 3	54
3.3.1.	Microalga strain, medium composition, and culture conditions	55
3.3.2.	Determination of microalgae cell concentration	55
3.3.3.	Determination of medium nitrate concentration	55
3.3.4.	Determination of light intensity	56
3.3.5.	Determination of oil/lipid content	56
3.3.6.	Operation of photobioreactor	56
3.3.7.	Addition of organic carbon sources	57
3.3.8.	Operation of semi-batch culture with medium replacement	58
3.3.9.	Statistical analysis	58
3.4.	Study 4	58
3.4.1.	Design of photobioreactor	58
3.4.2.	Simulation of photobioreactor	59
3.4.3.	Governing equations in ANSYS CFX	59

*Table of Contents*

3.4.3.1.	Transport Equations	59
3.4.3.2.	Buoyancy	60
3.4.3.3.	The Homogeneous Model	60
3.4.3.4.	The <i>k</i> -epsilon Turbulence Model	61
3.4.3.5.	Mesh Adaption	62

**CHAPTER 4 - RESULTS AND DISCUSSION**

4.1.	Study 1 - Investigation of the performance of <i>Chlorella sorokiniana</i> CY1 and <i>Chlorella vulgaris</i> ESP-31 in protein production	64
4.1.1.	Aim and objectives of study	64
4.1.2.	Growth curves of microalgal species	64
4.1.3.	Effects of different medium and initial nitrate concentrations on microalgal biomass and protein productions	65
4.1.4.	Effects of different CO <sub>2</sub> concentrations on microalgal biomass and protein productions	68
4.1.5.	Effects of different light intensity on microalgal biomass and protein productions	71
4.2.	Study 2 – Strategies for enhancing lipid production from indigenous microalgae isolates	76
4.2.1.	Aim and objective of study	76
4.2.2.	Microalgae selection	77
4.2.3.	Effects of initial nitrate concentration on the cell growth and lipids production of <i>Chlamydomonas</i> sp. Tai-03	79
4.2.4.	Effects of light intensity on the cell growth and lipids production of <i>Chlamydomonas</i> sp. Tai-03	81
4.2.5.	Effects of initial cell concentration on the cell growth and lipids production of <i>Chlamydomonas</i> sp. Tai-03	83
4.3.	Study 3 – Exploring the potency of integrating semi-batch operation into lipid yield performance of <i>Chlamydomonas</i> sp. Tai-03	86

## Table of Contents

4.3.1.	Aim and objective of study	86
4.3.2.	Effects of organic and inorganic carbon on microalgal biomass and lipid production of <i>Chlamydomonas</i> sp. Tai-03	86
4.3.3.	Cost analysis of the use of different organic carbon and CO <sub>2</sub> concentrations on microalgal biomass and lipid production of <i>Chlamydomonas</i> sp. Tai-03	91
4.3.4.	Effects of different medium replacement ratio on microalgal biomass and lipid production of <i>Chlamydomonas</i> sp. Tai-03	92
4.4.	Study 4 – Design of semi-closed thin layer cascade photobioreactor for microalgal culture	97
4.4.1.	Aim and objective of study	97
4.4.2.	Initial design concept of semi-closed thin layer cascade photobioreactor	97
4.4.3.	CFD simulation of initial concept	105
4.4.3.1.	Drawing of upper and lower platforms in ANSYS	105
4.4.3.2.	Meshing of drawing in ANSYS	106
4.4.3.3.	Setup of simulation in ANSYS	108
4.4.3.4.	Results of simulation in ANSYS	110
4.4.4.	Improvement of the initial concept of semi-closed thin layer cascade photobioreactor	111
4.4.4.1.	Meshing and setup of the proposed improvements in ANSYS	112
4.4.4.2.	Simulation results of the proposed improvements in ANSYS	113
4.4.4.3.	Mesh independence study of improved PBR concept design	114
4.4.4.4.	Effects of dense microalgal cultures on simulation results	116

*Table of Contents*

**CHAPTER 5 - CONCLUSIONS** **120**

**REFERENCES** **123**

# TABLE OF FIGURES

---

Figure 1 – Open pond with rotating arm for mixing the microalgal cultures (Hamed, 2016) .....	27
Figure 2 – Schematic diagram of raceway pond with paddlewheel to circulate the microalgal cultures (Bahadar and Bilal Khan, 2013) .....	28
Figure 3 – Schematic diagram of thin layer cascade photobioreactor (model Dahlia), where the number represents: (1) sloping platforms, (2) retention tank, (3) pump, (4) CO <sub>2</sub> inlet, (5) measurement and control sensors (pH, dissolved O <sub>2</sub> , temperature, and liquid level), (6) return pipe to upper platform, (7) flow distributor (spreads culture flow across upper platform), (8) connecting trough, (9) elevated platform, (10) screen (helps to degas excess O <sub>2</sub> produced by the microalgae), and (11) valve for harvesting (Masojídek et al., 2015) .....	30
Figure 4 – Schematic diagram of stirred tank photobioreactor (Rorrer and Cheney, 2004) .....	33
Figure 5 – Schematic diagram of horizontal tubular photobioreactor (Bahadar and Bilal Khan, 2013) .....	35
Figure 6 – Schematic diagram of (a) airlift photobioreactor and (b) bubble column photobioreactor (Krichnavaruk et al., 2005) .....	37
Figure 7 – Schematic diagram of flat plate photobioreactor (Bahadar and Bilal Khan, 2013) .....	40
Figure 8 – Schematic diagram of internally illuminated bubble column photobioreactor (Yadavalli et al., 2014) .....	41
Figure 9 – Schematic diagram of fermenter type bioreactor (Goldrick et al., 2015) .....	43
Figure 10 - The phylogenetic tree of 5 isolated microalgal strains .....	51

Table of Figures

Figure 11 - Biomass concentration, nitrate concentration, and protein content evolution of *Chlorella sorokiniana* CY1 (a, c, e) and *Chlorella vulgaris* ESP-31 (b, d, f). All growth graphs were from optimized conditions in each optimization step. Both species become increasingly optimized when viewed vertically from left to right. .... 65

Figure 12 - Effects of different initial nitrate concentration on biomass and protein productions of *Chlorella sorokiniana* CY1 (C) and *Chlorella vulgaris* ESP-31 (E) using BG-11 medium (BG) and Basal medium (B). The number of cultivation days marked in red are parameters where the microalgal strains did not reach nitrogen starvation and were harvested during stationary phase. .... 67

Figure 13 - Effects of different CO<sub>2</sub> concentration on biomass and protein productions of *Chlorella sorokiniana* CY1 (C) and *Chlorella vulgaris* ESP-31 (E) using Basal medium with 50% initial nitrate concentration..... 69

Figure 14 - Effect of different CO<sub>2</sub> concentrations on the biomass and pH of (a) *Chlorella sorokiniana* CY1 and (b) *Chlorella vulgaris* ESP-31. .... 70

Figure 15 - Effects of different light intensity (LI) on biomass and protein productions of *Chlorella sorokiniana* CY1 (C) and *Chlorella vulgaris* ESP-31 (E) using Basal medium with 50% initial nitrate concentration..... 72

Figure 16 - Influence of differing initial nitrate concentration on (a) biomass and biomass productivity; (b) oil content and oil productivity of *Chlamydomonas* sp. Tai-03. .... 80

Figure 17 - Influence of differing light intensity on (a) biomass and biomass productivity; (b) oil content and oil productivity of *Chlamydomonas* sp. Tai-03. .... 82



Table of Figures

Figure 18 - Influence of differing initial cell concentration on (a) biomass and biomass productivity; (b) oil content and oil productivity of *Chlamydomonas* sp. Tai-03. .... 83

Figure 19 - Comparison of *Chlamydomonas* sp. Tai-03 biomass and lipid production when supplemented with different concentrations of organic carbons (OCs) and inorganic CO<sub>2</sub> gas, where 2 and 4 = OC concentrations in g C/L (grams of carbon equivalent per litre of culture) (PS = Previous study, Glu = Glucose, Su = Sucrose, Gly = Glycerol, Ac = Acetate, Fru = Fructose) ..... 88

Figure 20 - Biomass growth and medium nitrate profile of *Chlamydomonas* sp. Tai-03 under semi-batch operation with medium replacement ratios of (a) 25%, (b) 50%, and (c) 75% (Arrows show the days of medium replacements) ..... 94

Figure 21 - Trimetric view of semi-closed thin layer cascade photobioreactor design ..... 98

Figure 22 - Trimetric view of upper platform ..... 99

Figure 23 - Trimetric view of lower platform ..... 99

Figure 24 - Trimetric view of retention tank ..... 100

Figure 25 - Dimensions of upper platform ..... 101

Figure 26 - Dimensions of lower platform..... 101

Figure 27 - Dimensions of retention tank ..... 102

Figure 28 - Drawing of initial concept of semi-closed thin layer cascade photobioreactor in ANSYS DesignModeler ..... 106

Figure 29 - Meshing of initial concept of semi-closed thin layer cascade photobioreactor in ANSYS Meshing ..... 107

Figure 30 - Green highlight of initial concept of semi-closed thin layer cascade photobioreactor in ANSYS Meshing ..... 107

Figure 31 - The four main boundaries in ANSYS CFX-Pre, namely (a) FreeTop, (b) Outlet, (c) Walls, (d) WaterInlet ..... 109

*Table of Figures*

Figure 32 – A clear representation of water volume fraction in ANSYS CFD-Post..... 110

Figure 33 – Water velocity of (a) the upper platform and (b) the lower platform in ANSYS CFD-Post ..... 111

Figure 34 – Improved concept design by addition of more mixing rods, slight elevation of the opening of inlet tube, and cutting away of portions of the photobioreactor below the inlet tube (to minimise the stagnant flow behind the inlet tube) ..... 112

Figure 35 – Mesh of the improved photobioreactor concept design ..... 113

Figure 36 – Simulation results of the improved photobioreactor concept design where (a) represents the upper platform and (b) represents the lower platform..... 114

Figure 37 – Refined mesh of improved photobioreactor concept design for mesh independence study ..... 115

Figure 38 – Simulation results of improved photobioreactor concept design with refined mesh where (a) represents the upper platform and (b) represents the lower platform ..... 116

Figure 39 – Simulation results of improved concept design with moderate viscosity ( $1.2 \times 10^{-3}$  Pa.s) microalgal culture where (a) represents the upper platform and (b) represents the lower platform ..... 118

Figure 40 – Simulation results of improved concept design with high viscosity ( $2.6 \times 10^{-3}$  Pa.s) microalgal culture where (a) represents the upper platform and (b) represents the lower platform ..... 119

# TABLE OF TABLES

---

Table 1 - A comparison of the advantages and disadvantages of open and closed systems in microalgal cultivation .....	24
Table 2 - The concentrations of different organic carbons (OCs) used in Study 2.....	57
Table 3 - Comparison of biomass and protein productions of <i>Chlorella sorokiniana</i> CY1 and <i>Chlorella vulgaris</i> ESP-31 with other studies.....	74
Table 4 - Comparison of oil productivity with recent research in lab-scale cultures .....	76
Table 5 - Biomass and oil analysis of five microalgae in BG-11, Basal and BBM .....	78
Table 6 - Fatty acid methyl ester (FAME) profile of <i>Chlamydomonas</i> sp. Tai-03 .....	85
Table 7 - Analysis of cost for organic carbons (OCs) and CO <sub>2</sub> in 1 L batch operation (as of July 2018), and comparison of biomass and lipid production yields using 5% CO <sub>2</sub> condition as a reference.....	92
Table 8 - Comparison of different medium replacement ratio (MRR) on biomass and lipid production of <i>Chlamydomonas</i> sp. Tai-03.....	95
Table 9 - FAME (fatty acid methyl ester) profile of <i>Chlamydomonas</i> sp. Tai-03.....	96

# ACRONYMS AND ABBREVIATIONS

---

2-OC	2 grams carbon equivalent (organic carbon)
4-OC	4 grams carbon equivalent (organic carbon)
3N BBM	3-fold concentration of NaNO <sub>3</sub> in Bold's Basal medium
Ac	Acetate
ADP	Adenosine diphosphate
ANOVA	Analysis of variance
atm	Atmosphere (unit)
ATP	Adenosine triphosphate
BBM	Bold's Basal medium
CaCl <sub>2</sub> .2H <sub>2</sub> O	Calcium chloride dihydrate
CaCO <sub>3</sub>	Calcium carbonate
CCM	Carbon concentrating mechanism
CFD	Computational fluid dynamics
CO <sub>2</sub>	Carbon dioxide
Co(NO <sub>3</sub> ) <sub>2</sub> .6H <sub>2</sub> O	Cobalt(II) nitrate hexahydrate
CuSO <sub>4</sub> .5H <sub>2</sub> O	Copper(II) sulphate pentahydrate
DCW	Dry cell weight
DIC	Dissolved inorganic carbon
DOW	Deep ocean water
DSW	Deep seawater
EDTA.2Na	Ethylenediaminetetraacetic acid disodium salt
FAME	Fatty acid methyl ester
FeSO <sub>4</sub> .7H <sub>2</sub> O	Iron(II) sulphate heptahydrate
FFA	Free fatty acid
FID	Flame ionization detector

*Acronyms and Abbreviations*

Fru	Fructose
Glu	Glucose
Gly	Glycerol
H <sup>+</sup>	Hydrogen ion/Hydrion/Proton
H <sub>2</sub> S	Hydrogen sulphide
H <sub>2</sub> SO <sub>4</sub>	Sulphuric acid
H <sub>3</sub> BO <sub>3</sub>	Boric acid
H <sub>3</sub> PO <sub>4</sub>	Phosphoric acid
HSM	High salt medium
K <sub>2</sub> HPO <sub>4</sub>	Di-potassium hydrogen phosphate
KH <sub>2</sub> PO <sub>4</sub>	Potassium dihydrogen phosphate
KNO <sub>3</sub>	Potassium nitrate
KOH	Potassium hydroxide
LED	Light-emitting diode
MgSO <sub>4</sub> .7H <sub>2</sub> O	Magnesium sulphate heptahydrate
MnCl <sub>2</sub> .4H <sub>2</sub> O	Manganese(II) chloride tetrahydrate
MW	Molecular weight
Na <sub>2</sub> MoO <sub>4</sub> .2H <sub>2</sub> O	Sodium molybdate dihydrate
NaCl	Sodium chloride
NADP <sup>+</sup>	Nicotinamide adenine dinucleotide phosphate
NADPH	Reduced nicotinamide adenine dinucleotide phosphate
NaMeO	Sodium methoxide
NaNO <sub>3</sub>	Sodium nitrate
NaOH	Sodium hydroxide
NO <sub>x</sub>	Nitrogen oxides
O <sub>2</sub>	Oxygen
OC	Organic carbon
PAR	Photosynthetically active radiation

## *Acronyms and Abbreviations*

PBR	Photobioreactor
PCR	Polymerase chain reaction
P <sub>i</sub>	Phosphate ion (PO <sub>4</sub> <sup>3-</sup> )
Pr.	Productivity
PS	Previous study (refers to Study 1 in this thesis)
PUFA	Polyunsaturated fatty acid
rDNA	Ribosomal deoxyribonucleic acid
ROS	Reactive oxygen species
RSM	Response surface methodology
Rubisco	Ribulose-1,5-bisphosphate carboxylase/oxygenase
SC-CO <sub>2</sub>	Supercritical carbon dioxide
SO <sub>x</sub>	Sulphur oxides
Su	Sucrose
SW	Seawater
TAP medium	Tris-Acetate-Phosphate medium
TFA	Total fatty acid
TLC	Thin layer cascade
VFA	Volatile fatty acid
W	Watt (energy)
WLEP	Wet lipid extraction procedure
ZnSO <sub>4</sub> .7H <sub>2</sub> O	Zinc sulphate heptahydrate

# CHAPTER 1

## INTRODUCTION

### 1.1. Brief Overview of Research

In the past few decades, microalgal biotechnology has garnered a lot of attention due to the ability of microalgae to generate a variety of valuable metabolites, such as carbohydrates, proteins, lipids, carotenoids, vitamins, and minerals. Due to its product diversity, microalgal biomass has been utilised in different industries such as biofuels, fertiliser, aquaculture, nutraceutical, and wastewater treatment (Cardozo et al., 2007). To generate these metabolites, microalgae can be cultured using carbon dioxide (CO<sub>2</sub>) and different types of industrial waste as nutrient media, thereby helping to alleviate the environmental issues caused by these effluents. The types of industrial waste can also be chosen based on the application of the microalgal biomass. If microalgal biofuel is being produced, waste streams unsuitable for discharge into rivers or lakes (containing higher levels of toxic chemicals or trace metals) may be suitable for microalgal culture after undergoing proper filtration and dilution. In this case, the microalgae can be used to produce biofuels and minimise contamination levels in wastewater. On the other hand, if microalgal-derived food, supplement, or fertilisers are targeted, food waste from kitchens, agriculture, or food-packaging industries can be used. Despite the benefits of microalgal biomass, the high production cost associated with microalgal biomass (compared to forestry and agricultural biomass) remains one of the main hurdles for large-scale application (Costa and de Morais, 2014). To overcome the high production cost, development of efficient and affordable photobioreactor (PBR) is a necessity (Wang et al., 2012). Since the field of research regarding microalgae

is very diverse, it is essential to narrow down the scope of research in this thesis, which is to focus on the upstream process of microalgal biomass production. The upstream process includes identification and characterisation of suitable microalgal species, optimisation of culture conditions to high yields of targeted products, and photobioreactor design. Therefore, in this section, two different products (microalgal protein and biodiesel) have been selected due to the demand for these products as alternative sources of fishmeal and fossil fuel in the modern world. Section 1.1.1 and 1.1.2 discusses the importance and hurdles of microalgal protein and biodiesel. Section 1.1.3 explains the importance of a new photobioreactor design which would be able to accommodate different microalgal species to produce different products. After this, Section 1.2 would list the aims of this thesis and Section 4 would elaborate the experimental results in detail according to the order in which the aims were listed.

#### **1.1.1. The importance and hurdles of microalgal protein as fishmeal replacement in aquaculture**

As our population increases, our need for more food also rises. One particular aspect is higher demand for protein, and fish is not only a protein-rich food source, but also rich in essential fatty acids. It has been estimated that the average per capita consumption of fish may increase in the future (Fisheries and Aquaculture Department (FAO), 2018). This can be due to an increase in healthy mind sets of developed countries (Kris-Etherton et al., 2009) and higher income growth of developing countries (Rana et al., 2009). The yield of wild fisheries has been controlled at around 90 million tonnes (Mt) annually to allow the wild fish stocks to recover and prevent over-fishing. The additional demands for fish are being satisfied by aquaculture industry, whereby in 2016, the total aquaculture production reached 80 Mt (Fisheries and Aquaculture Department (FAO), 2018). The rise of the aquaculture industry has increased the demand of fishmeal, the main protein source used in fish diets. As fishmeal is made by processing wild fish



and wild fish catches has become consistent, the supply of fishmeal is getting more strained and this has drove up the price of fishmeal (Guedes et al., 2015).

In regards to this concern, microalgal protein has caught the attention of researchers as a potential fishmeal replacement. Partial replacement of fishmeal using protein-rich microalgal biomass in fish diets have been successful in the cultures of various fish such as Atlantic salmon, whiteleg shrimp, common carp (Kiron et al., 2012), sea bream juveniles (Vizcaíno et al., 2014), and Pacific white shrimps (Ju et al., 2012). However, similar to microalgal biofuels, one of the obstacles faced by using microalgal protein as fishmeal replacement is the cost of mass cultivation of microalgae. Two of the solutions would be identifying protein-rich microalgae suitable for mass culture and design of a simple and effective PBR. However, before proceeding to investigate mass culture and PBR design, a characterisation and optimisation study of the chosen microalgal species would be carried out in lab scale.

### **1.1.2. The importance and hurdles of microalgal biofuels**

Given that microalgal biofuels are both sustainable and green (microalgae absorb CO<sub>2</sub> emitted from burning of biofuels for photosynthesis), they have the potential to relieve our dependence on fossil fuels in the short term and possibly replace fossil fuels in the long term. Because of this, microalgal biofuels could become one of the solutions to the global issues of energy security and climate change. Compared to oleaginous plants (like oil palm and rapeseed) and plants with high sugar content (like corn and sugar cane), microalgae grow faster, are capable of achieving higher yields of lipids and carbohydrates, require less land for cultivation, does not require arable land, and can be cultured using wastewater or brackish water (Brennan and Owende, 2010). The adaptability of microalgae to various cultivation and environmental conditions has permitted their successful cultivation in many countries. Not only can this help to produce microalgal biofuels locally, but also mitigate the concerns of food versus fuel. However, it is also well-known that

in the near-term, the mass production of microalgal biofuels is not economically viable as the various technologies involved in scaling up have yet to sufficiently bring down the cost of operation and production of microalgal biofuels industry (Davis et al., 2011). One solution to the cost issues would be to identify microalgal strains with higher biomass and lipid yields, higher adaptability to outdoor cultivation conditions, and more competitive for nutrients than other unwanted microorganisms. Another solution would be to design better performing PBRs that are cheaper to build, operate, and maintain (Chen et al., 2011).

### **1.1.3. The importance and hurdles of photobioreactor design**

Numerous research has been done in order to bring down the high cost of producing microalgal biomass. For large-scale microalgal culture to be sustainable, one of the solutions is to design an affordable and efficient PBR that can be scaled up for mass culture in outdoor conditions. The PBR can be divided into two main categories, namely open system and closed system. Open systems are bioreactors where the microalgal culture are directly exposed to the environment, such as open ponds or raceway ponds. The benefits of open systems are low cost of fabrication, simple to operate and maintain, low energy consumption, and high surface to volume ratio (Carlozzi, 2008; Fernández et al., 2013). However, the drawbacks of open systems include high risk of contamination, no control over weather conditions, high evaporative losses, low CO<sub>2</sub> mass transfer rates due to the shallow ponds (30 – 50 cm depth), and large areas of flat land required (Brennan and Owende, 2010; Carvalho et al., 2006; Fernández et al., 2013; Singh and Sharma, 2012). On the other hand, closed systems do not allow contact between the culture and the atmosphere while still allowing light to reach the culture, effectively negating the drawbacks of open systems. Some examples of closed systems include flat plate PBR, tubular PBR, air-lift PBR, and stirred tank PBR. The advantages of closed systems are full control over culture conditions, high CO<sub>2</sub> mass transfer rates, high biomass productivity, low risk of contamination, and lower land requirement. But

the disadvantages of closed systems are high fabrication cost, lower surface area to volume ratio, build-up of dissolved O<sub>2</sub>, fouling, and difficulty in scaling up (Brennan and Owende, 2010; Chisti, 2007; Masojídek et al., 2015; Posten, 2009; Ugwu et al., 2008). Given how each PBR design has their strengths and weaknesses, the commonly-used PBR systems can still be improved so that their weaknesses can be minimised.

## **1.2. Aim**

In regards to the difficulties faced by microalgal protein and biodiesel production as mentioned in Section 1.1, this thesis aims to address some of the difficulties by:

- a. Identifying new microalgal species that have high biomass and protein productivities, and proceed to optimise the selected species for maximal yield of biomass and protein in a sterile and controlled environment (laboratory scale).
- b. Identifying new microalgal species that have high biomass and lipid productivities, and proceed to optimise the selected species for maximal yield of biomass and biodiesel in a sterile and controlled environment (laboratory scale).
- c. Design a PBR that is both simple and easy to build, operate and maintain. The PBR would be designed in the hopes of catering to different microalgal strains producing different valuable metabolites.

# CHAPTER 2

## LITERATURE REVIEW

This chapter serves to review and summarise key information found in literature regarding the research scope outlined in Chapter 1. After a brief introduction of cyanobacteria and microalgae, the roles of microalgae in microalgal-derived biodiesel and protein feed were discussed. In order to culture microalgae, whether laboratory-scale or large-scale, it is important to understand the factors that play into the survival and flourishing of various microalgal species. Therefore, the factors affecting microalgal growth were broken down into six main conditions and discussed in detail. Lastly, different types of photobioreactors were examined to better understand the benefits, drawbacks, and important features of each photobioreactor.

### **2.1. A brief background of cyanobacteria and microalgae**

Cyanobacteria and microalgae are known to be one of the oldest organisms on Earth and normally found in freshwater and saltwater. They are unicellular microorganisms and can exist as single cells or clusters of cells. Unlike higher plants, cyanobacteria and microalgae do not have stems, roots, or leaves. But like higher plants, both are capable of carrying out photosynthesis and are important producers in the food chain. The simple cell structures of cyanobacteria and microalgae allows them to adapt to different environment and flourish for long periods of time (Falkowski and Raven, 2007).

Cyanobacteria are considered as prokaryotes as they lack membrane-bound organelles (such as nuclei, mitochondria, plastids, etc.) and display higher

similarities to bacteria rather than microalgae. The name “cyanobacteria” was derived from the blue-green colour of the bacteria. Meanwhile, microalgae are considered as eukaryotes due to the presence of membrane-bound organelles and are categorized based on their colour, life cycle, and basic cell composition (Khan et al., 2009). The three main classes of microalgae are green algae (*Chlorophyta*), red algae (*Rhodophyta*), and diatoms (*Bacillariophyta*). Both cyanobacteria and microalgae can perform four different metabolic mechanisms, namely photoautotrophy, heterotrophy, mixotrophy, and photoheterotrophy. Photoautotrophs undergo photosynthesis in the presence of light and inorganic carbon (CO<sub>2</sub>) to create and store chemical energy. Heterotrophs take in nutrients and organic carbon (OC) like sugars for energy. Mixotrophs have the ability to utilise both photosynthesis and organic carbon sources for energy. Photoheterotrophs, on the other hand, require light as an energy source to metabolize organic compounds. *Spirulina platensis* and *Chlorella vulgaris* are two microalgal strains that can live under photoautotrophic, heterotrophic and mixotrophic conditions. On the other hand, *Scenedesmus acutus* and *Selenastrum capricornutum* are two microalgal strains that can grow photoautotrophically, heterotrophically or photoheterotrophically (Chojnacka and Marquez-Rocha, 2004).

Although cyanobacteria and microalgae are mainly found in freshwater and saltwater, they can also grow and attach to various habitats exposed to water such as soils, rocks, glaciers, caves, and even buildings. Both cyanobacteria and microalgae are capable of synthesizing and accumulating various useful metabolites such as carbohydrates, proteins, lipids, carotenoids, vitamins, and minerals. In the past decade, cyanobacteria and microalgae have seen increasing commercial applications in various industries including biofuels, agriculture, aquaculture, pharmaceutical, nutraceutical, cosmetics, and wastewater treatment (Cardozo et al., 2007). Another benefit of cultivating cyanobacteria and microalgae is that they are estimated to absorb 1.83 kg of CO<sub>2</sub> for every 1 kg of biomass

produced (Chisti, 2007), indicating their potential for integration into carbon sequestration systems (Singh et al., 2012).

In this thesis, for the sake of brevity, both cyanobacteria and microalgae shall simply be referred to as microalgae, unless stated otherwise.

## **2.2. A brief summary of photosynthesis in cyanobacteria and microalgae**

Photosynthesis is nature's unique solution to harvest light energy from the sun and convert it into chemical energy in the form of glucose. Most life forms on Earth depend directly or indirectly on photosynthesis for food and energy. Roughly 3 billion years ago evolved the most ancient photoautotrophic microorganisms, anoxygenic photosynthetic bacteria. These bacteria utilised sunlight to release electrons and protons from different types of donor molecules (like  $\text{Fe}^{2+}$  and  $\text{H}_2\text{S}$ ), and used the free electrons and protons to reduce  $\text{CO}_2$  to produce organic molecules. Then roughly 2 billion years ago, cyanobacteria and microalgae evolved and created the oxygenous atmosphere we have today (Masojidek et al., 2013).

Photosynthesis takes place in organelles called chloroplasts for microalgae, whereas photosynthesis occurs in the thylakoid membranes in the cytoplasm of cyanobacteria. Inside the chloroplasts, the thylakoids membranes are suspended in a fluid called stroma (Razzak et al., 2013). Photosynthesis is divided into two stages, the light-dependent stage and light-independent stage. The thylakoids are the sites of the light-dependent stage. In the thylakoids are photoactive sites known as photosystem I (PS I) and photosystem II (PS II), where sunlight is harvested by antenna complexes and transferred to the chlorophyll dimer,  $\text{P}_{680}$  and  $\text{P}_{700}$ , in the reaction centres of PS II and PS I. The excitation of the  $\text{P}_{680}$  reaction centre in PS II enables splitting of water, generating oxygen ( $\text{O}_2$ ), electrons, and protons. The electrons are transferred to the  $\text{P}_{700}$  reaction centre in PS I to produce a biochemical reductant called reduced nicotinamide adenine dinucleotide phosphate (NADPH) and protons in the stroma. Protons in the stroma are pumped

into the thylakoids, and together with protons from water splitting, they flow through an enzyme embedded in the thylakoid membranes, adenosine triphosphate (ATP) synthase, back into the stroma. This flow of protons through ATP synthase triggers the production of ATP from adenosine diphosphate (ADP) and phosphate ion ( $P_i$ ). Both the ATP and NADPH are then used in the light-independent stage (also known as Calvin cycle) with carbon fixing enzyme, ribulose-1,5-bisphosphate carboxylase/oxygenase (rubisco), and  $CO_2$  to produce glucose (Masojidek et al., 2013).

### **2.3. Microalgal biodiesel synthesis**

The ever diminishing fossil fuels to cater and sustain the human population and growth as an intelligent species have propelled the search for renewable energy sources. Microalgae biofuel has become one of the most researched fields in the last few decades for its promise as a green, renewable and sustainable energy source (Halim et al., 2012). Microalgae have many advantages over conventional crops like soybean, rapeseed, sunflower, sugar cane and palm oil (Chisti, 2007). In comparison, microalgae have higher growth rate, greater lipid content and higher biomass yield, thus requiring less land area to achieve the same oil and biomass productivity as first generation energy crops (Chisti, 2007). Microalgae can also utilise water unfit for human consumption, metabolize a wide range of nutrients and prosper with little attention (Mata et al., 2010).

Microalgae can be used to generate a range of renewable fuels such as biodiesel (Tran et al., 2013), bioethanol (Ho et al., 2013), biohydrogen (Liu et al., 2013), methane (Heaven et al., 2011) and syngas (Goyal et al., 2008). Microalgal biodiesel is a popular choice due to its potential utilisation in existing diesel vehicles with little to no modifications, and compatibility with current fuel distribution infrastructure. In addition, biodiesel is also a cleaner fuel with relatively high energy density compared to diesel (Du et al., 2008). Biodiesel is acquired from the transesterification of extracted lipids from microalgal cell bodies. The catalyst

required for transesterification process can be acids (Chen et al., 2012), alkalis (Ross et al., 2010) or enzymes (Tran et al., 2012). It is common to find microalgae containing 20-50% lipids in their cell bodies (Chisti, 2007). Nitrogen starvation is the most dominant factor that resulted in lipid and carbohydrate accumulation in microalgae. The lack of nitrogen source in the medium induces stress on the growth of microalgae and in response, the microalgae accumulate lipids and carbohydrates (Breuer et al., 2012). The high oil content and biomass productivity of microalgae make them a potential producer of biodiesel.

### **2.3.1. Acid/base catalysis**

Microalgae oils are naturally more viscous than diesel oils, so transesterification process is needed to reduce the viscosity of algal oils before they can be applied to engines (Fuls et al., 1984). Direct transesterification method devised by Lepage and Roy (1984) is preferred for rapid microalgal biodiesel production (Lepage and Roy, 1984). Before transesterification, it is necessary to pre-treat the biomass by drying (oven drying, freeze-drying, sun drying) and cell disruption (ultrasonication, bead-beating, French press). In the transesterification of oils and fats, alcohols are the main substrates. Although various alcohols have been used (methanol, ethanol, propanol, butanol and amyl alcohol), the most common one is methanol due to its low cost and availability. Other than that, a catalyst (acid, alkali, enzyme) is also necessary to increase the solubility of alcohol, which is otherwise scarcely soluble in the oils and fats. Alkali catalysis is reportedly 4000 times faster than acid catalysis, but alkali catalysis is not suitable for oil mixtures with free fatty acid (FFA) content above 5% (Fukuda et al., 2001). This is because the alkali will react with the excess FFA to produce soap and water. Acid catalysis can tolerate high levels of FFA, but its conversion rate is very slow (Huang et al., 2010). An alkali-catalysed reaction normally takes 8 h depending on temperature and pressure, while an acid-catalysed conversion needs 45 h (Saka and Kusdiana, 2001). Alkali catalysis is still preferred due to its fast conversion rate. Therefore, it is essential to pre-treat oil



mixtures to reduce their FFA content to less than 5%. The commonly used alkaline catalysts are NaOH, KOH and NaMeO, while the acid catalysts are H<sub>2</sub>SO<sub>4</sub>, H<sub>3</sub>PO<sub>4</sub> and CaCO<sub>3</sub> (Karmakar et al., 2010).

On the other hand, enzymes can operate well under high FFA content, but enzyme usage is limited due to its high cost and risk of inhibition of enzymatic activity due to chemicals in the production process (Huang et al., 2010). The development of enzyme immobilization methods and multiple enzymes may provide an alternative solution in the future (Hama et al., 2006).

### **2.3.2. Direct transesterification of wet biomass**

Since dewatering and drying microalgal biomass is very costly, direct lipid from wet biomass is a good alternative method. Hence, wet lipid extraction procedure (WLEP) has been developed. The wet biomass is first hydrolysed by acid to break the cell walls. Alkali is then added to neutralize the acid. The biomass and the resulting supernatant are separated. The lipid-containing supernatant forms solid precipitates upon lowering the pH (adding sulphuric acid). Since the lipids are not soluble in the aqueous solution, the lipids aggregate with the solid precipitates. The solid precipitates are centrifuged, mixed with hexane and heated at 90°C for 15 minutes. After cooling and another centrifugation step, the top phase is lipids extracted in hexane. Hexane is evaporated to obtain homogenized lipids. For transesterification process, the lipids are mixed with 5% (v/v) sulphuric acid solution in methanol and heated at 90°C for 30 minutes. The transesterified lipids are extracted by adding hexane and heated at 90°C for another 15 minutes (Sathish and Sims, 2012). In a study, WLEP was used to extract 79% lipids from wet microalgal biomass (84% moisture content). From that, 76% lipids were transesterified to FAMES (Sathish and Sims, 2012). Although promising, WLEP still requires more research to analyse its implementation in large scale biodiesel synthesis.

### 2.3.3. Supercritical fluid method

Currently, the most developed method for biodiesel production process is alkaline catalysed method. But this method is energy intensive and presented difficulties in glycerol recovery and the need to remove the catalyst. The drawbacks from the use of alkaline catalyst led to the introduction of a new catalyst-free method to produce biodiesel, the supercritical fluid method (Saka and Kusdiana, 2001).

Upon reaching supercritical state, the hydrogen bonds in the solvents (methanol, ethanol, etc.) are greatly reduced, effectively decreasing its polarity and dielectric constant, thus allowing the molecules of the solvents to act as free monomers. Because of this phenomenon, supercritical solvents can solvate non-polar triglycerides into a homogenous liquid phase to produce FAMES and diglyceride (Saka and Kusdiana, 2001; Kasim et al., 2009). The supercritical process uses single-reactor conversion of algal biomass to biodiesel at temperatures about 250-350°C, requiring lower energy input compared to conventional lipid transesterification and extraction via co-solvent method (Patil et al., 2011).

A one-step supercritical methanol process was optimised using RSM to liquefy and convert wet algal biomass (*Nannochloropsis* sp., CCMP1776) into biodiesel, in the presence of nitrogen. The optimum conditions were: wet algae to methanol (wt/vol) ratio of 1:9 and reaction temperature of 255°C for 25 minutes. The observed FAME% ranges from 76-84% (Patil et al., 2011).

Apart from using organic solvents, supercritical carbon dioxide (SC-CO<sub>2</sub>) was also used to extract lipid from *Scenedesmus* sp. to produce biodiesel (Taher et al., 2014). A batch of experimental data from SC-CO<sub>2</sub> treatment of 3g microalgal biomass was fed into response surface methodology (RSM) for modelling. The optimum operating conditions were calculated as 53°C, 500 bar and 1.9 g/min of SC-CO<sub>2</sub>, achieving a lipid extraction yield of 7.41% (dry weight basis). The experiment was then scaled up to handle 25 g of biomass (8 times) at the optimum temperature and pressure, but 15.26 g/min of SC-CO<sub>2</sub> (8 times). It was suggested

that the lipid yield of up-scaled experiments would be similar to lab-scale, if the ratio of solvent flow rate to biomass was kept constant (Prado et al., 2014). The final yield was 6.2% after 1 hour reaction time, which was close to the value predicted by RSM (Taher et al., 2014).

## **2.4. Microalgal protein in aquaculture**

### **2.4.1. Brief summary of aquaculture**

Before the advent of the aquaculture industry, fishmeal was considered a low-cost protein feed directed towards animals. But this fact changed when aquaculture became increasingly important as a source of fish for human consumption. Farming fish requires large amounts of protein, and fishmeal is the primary protein source in fish diet. There are concerns that this may lead to overfishing and ethical issues where processed wild fish are fed to farmed fish which are then consumed by humans (Naylor et al., 2009; Tacon and Metian, 2009). However, the aquaculture industry has now become an important producer of healthy fish as well as generator of jobs and revenue for many developed and developing countries (Becker, 2007).

According to the Food and Agriculture Organization of the United Nations (FAO), the demand for fish (both seawater and freshwater fish) will continue to grow in the years to come. Not only will the global population increase, but the average per capita consumption of fish may also increase (Fisheries and Aquaculture Department (FAO), 2018). The rise in fish consumption can be attributed to strong encouragements from health authorities in developed countries to increase fish intake (Kris-Etherton et al., 2009) and rising income growth in developing countries which helps to boost the domestic fish market, especially in Asia (Rana et al., 2009). In order to satisfy the high demands for fish, the aquaculture industry must be expanded. This is because most of the world's marine fish stocks have already been fully exploited. For instance, in 2015, 59.9% of the world's marine fish stocks were maximally sustainably fished while 33.1% have been overfished. In order to practice sustainable fishing of marine fish stocks, the

global wild fish capture has been controlled at around 90 million tonnes (Mt) annually (Fisheries and Aquaculture Department (FAO), 2018). Ever since the number of overexploited and depleted wild fish stocks had significantly increased in the 1970s and 1980s, the annual global wild fish capture has been maintained around 90 Mt (Fisheries and Aquaculture Department (FAO), 2010).

#### **2.4.2. Fishmeal production and utilisation**

For more a century now, pelagic fish have been utilised to generate fish oil and fish proteins. Initially fish oil was the primary commodity which was a raw material in the manufacture of soap and paint, tanning of hides, production of lubricants, and later margarine. The remaining fish proteins (also known as press cake) were dried to form fishmeal, and utilised as fertiliser and terrestrial animal feed (Hardy and Tacon, 2002). Fishmeal is an important protein source due to its high digestibility, high content of essential amino acids, and presence of long chain omega-3 fatty acids (eicosapentaenoic acid (EPA) and docosahexaenoic acid (DHA)) as well as vitamins (such as niacin, riboflavin, vitamins A and D) and minerals (such as phosphorus, calcium, zinc, iron, iodine, and selenium) (Becker, 2007).

According to FAO, in 2016, 21.7% (19.7 Mt) of total capture fish were turned into fishmeal, and most of the fishmeal went to the aquaculture industries, generating 80.0 Mt of farmed fish (Fisheries and Aquaculture Department (FAO), 2018). This amount of farmed fish is a significant improvement compared to five years before in 2011, where the total aquaculture production was 61.8 Mt (Fisheries and Aquaculture Department (FAO), 2018). Fishmeal has become the basis for all fish diet formulas used in aquaculture. The usage of fishmeal as the main protein source in aquaculture have driven up the price of fishmeal by nearly three-fold in the last decade (Guedes et al., 2015). The price of fishmeal is expected to continue rising as global fishmeal production has remained consistent for several years now (Fisheries and Aquaculture Department (FAO), 2018). This has led to the search of alternative sources of protein that are both nutritious and sustainable for the

aquaculture industry. In this regard, microalgal protein has emerged as a potential alternative to fishmeal.

### **2.4.3. Microalgal protein as potential fishmeal replacements**

Other than carbohydrates, lipids, and carotenoids, microalgae can also be made to accumulate high amounts of protein (Becker, 2007). This can be done by varying the culture conditions of the microalgae, such as medium nitrate concentration and light intensity (Chen et al., 2015). Another important factor is the timing of harvest. Microalgal protein content and amino acid profile are strongly connected to the growth phase of the microalgae, in the sense that its protein content often declines after nitrogen depletion phase, giving rise to higher carbohydrate or lipid content. Therefore, the microalgal biomass have to be harvested before nitrogen depletion state where its protein content would be at the maximum (Ho et al., 2012; Yeh and Chang, 2011). Protein-rich microalgae biomass has been used successfully to partially replace fishmeal in the aquaculture industry. One study found that fish feed with 20% *Scenedesmus almeriensis* biomass replacement did not impact the growth of sea bream (*Sparus aurata*) juveniles negatively. Further ultrastructural study revealed that significantly enhanced the absorptive surface of intestinal mucosa in the sea bream (Vizcaíno et al., 2014). In another study, defatted microalgae meal (DMM), a by-product of astaxanthin extraction from a red microalgae *Haematococcus pluvialis*, was used to replace 12.5%, 25%, 37.5%, and 50% of fishmeal in the diet of juvenile shrimps. It was observed that the 12.5% DMM diet significantly increased the growth rate and decreased the feed conversion ratio of Pacific white shrimps (*Litopenaeus vannamei*) compared to the control diet (without DMM). The other three replacement diets did not show negative effects on the growth of the shrimps. The shrimps fed with DMM-supplemented diets were visibly redder and contained larger amounts of free and esterified astaxanthins than the control diet group (Ju et al., 2012).

## **2.5. Factors affecting microalgal growth**

Although the growth rate and maximum biomass concentration of phototrophic microorganisms vary with species, most reports agree that microalgae, like many other microorganisms, could grow much faster under favourable environmental conditions. This indicates that optimizing the cultivation condition with suitable PBRs to increase biomass productivity would definitely reduce the overall production cost. To enhance the economic feasibility of using cyanobacteria and microalgae for downstream applications, it is essential to get a better understanding of both their physiological requirements and the engineering concepts behind successful PBR design.

### **2.5.1. Light Utilisation**

The most important determinant of photosynthetic efficiency is the availability of light in the required intensity and spectral quality. Through photosynthesis, phototrophic microorganisms can convert the light energy from sunlight into chemical energy in the form of carbohydrates (Razzak et al., 2013). Cell growth of phototrophic microorganisms is often strongly affected by the level of light intensity, which can fall into one of three categories, namely light limitation, light saturation, and light inhibition (Ho et al., 2012). Below the saturated light intensity, light is one of the key limiting factors for biomass production, and photosynthesis efficiency increases with rising light intensity. Cyanobacteria and microalgae adapt to variations in light intensity by altering their cell organization and increase photosynthetic efficiency, a process called photoadaptation or photoacclimation. When light intensity is at saturation, the rate of photon absorption exceeds the rate of electron turnover and there is no further increase in the rate of photosynthesis. If the light intensity is further increased, photoinhibition occurs and causes irreversible damage to the photosynthetic sites while also inducing oxidative damage to the cells (Chisti, 2007). Given all these, the light intensity tolerance level varies across different species. For instance, Ho et al. (2012) showed that the

biomass productivity of a microalgae *Scenedesmus obliquus* CNW-N increased 3-fold with an increase in light intensity from 60 to 420  $\mu\text{mol}/\text{m}^2/\text{s}$  (Ho et al., 2012). Sun et al. (2014) also observed an increase in the biomass concentration of a microalgae *Neochloris oleoabundans* HK-129 from 1.2 to 1.7 g/L when the light intensity was increased from 50 to 200  $\mu\text{mol}/\text{m}^2/\text{s}$  (Sun et al., 2014). However, light supply is different from other environmental factors in the sense that its level cannot be kept uniform inside PBRs. For example, in outdoor cultivation, sunlight is often too intense for cells at the surface of PBRs and results in photoinhibition. On the contrary, light intensity at deeper regions of PBRs is significantly reduced because denser cultures tend to absorb and scatter light in a phenomenon called self-shading (Christenson and Sims, 2011; Kumar et al., 2011). This causes two different growth states of cyanobacteria and microalgae in PBRs, a photic zone (high light intensity) where photosynthetic growth occurs, and a dark zone (low light intensity) where fermentative growth occurs. Efficient mixing helps to ensure that the cells experience alternative light-dark cycles which increases biomass productivity and PBR efficiency (Posten, 2009). In addition, only the spectrum of sunlight from 400 to 700 nm are utilised by phototrophic microorganisms as an energy source, and this wavelength range is known as photosynthetically active radiation (PAR) (Razzak et al., 2013). Thus, increasing the utilisation of PAR is highly correlated with enhancing cell growth of phototrophic microorganisms. The utilisation of PAR can be done by designing PBR with higher surface-to-volume ratio and/or shorter light penetration path to obtain higher light receiving area for the phototrophic cells (Christenson and Sims, 2011). Ho et al. (2015) have shown that 1.4-fold greater biomass productivity of a microalgae *Chlamydomonas* sp. JSC4 was obtained by a slim-type tubular photobioreactor with high surface-to-volume ratio of 80.1  $\text{m}^2/\text{m}^3$  (Ho et al., 2015).

### 2.5.2. CO<sub>2</sub> assimilation

Carbon accounts for more than 50% of the mass of cyanobacteria and microalgae cells, and is obtained in the form of CO<sub>2</sub>. The atmospheric concentration of CO<sub>2</sub> is very low (0.03-0.04%) and not optimal for efficient photosynthesis (Ho et al., 2011). The key enzyme for CO<sub>2</sub> assimilation in the Calvin cycle, rubisco, has a relatively higher affinity for CO<sub>2</sub> than O<sub>2</sub>. But the high concentration of O<sub>2</sub> in the atmosphere (about 21%) results in O<sub>2</sub> competing with CO<sub>2</sub> for the reaction with rubisco. To counter this, photoautotrophs have developed carbon concentrating mechanisms (CCM) where the external available carbon source is actively accumulated inside the cells. This internal carbon pool feeds into the photosynthetic complexes of the cells, thereby minimising the oxygenase activity of rubisco (Raven et al., 2008). CCM is activated in low CO<sub>2</sub> environment, and suppressed in high CO<sub>2</sub> environment (Baba and Shiraiwa, 2012). As CCM is an active mechanism (requires energy input), the suppression of CCM will afford the cyanobacteria and microalgae more energy for growth. This has been demonstrated by a microalga *Nannochloropsis oceanica* mutant, whose cytosolic carbonic anhydrase (key enzyme in CCM) had been knocked down, achieved 30% higher biomass growth and 40% higher biomass productivity compared to the wild type (Wei et al., 2019). As the atmospheric CO<sub>2</sub> concentration is very low, capturing CO<sub>2</sub> from flue gas (10-20% CO<sub>2</sub> concentration) is a good solution for cultivation of cyanobacteria and microalgae (Ono and Cuello, 2003; Douskova et al., 2008). Several cyanobacteria and microalgal species have shown high CO<sub>2</sub> tolerance (14-100% CO<sub>2</sub>), indicating their potential to utilise flue gas as a carbon source (Ono and Cuello, 2003). Apart from CO<sub>2</sub> concentration, the flow rate of inlet gas also plays an important role in determining total inorganic carbon dissolved in the liquid phase. A well-designed photobioreactor should usually have larger light receiving area and advanced CO<sub>2</sub> diffuser allowing a longer CO<sub>2</sub> retention time, which can significantly enhance the penetration of light and the dissolution of CO<sub>2</sub> (Yen et al., 2015).



### 2.5.3. pH

The pH value is an important factor in the cultivation of cyanobacteria and microalgae, affecting many biological mechanisms associated with cell growth, metabolism, and uptake of ions (Khalil et al., 2010). Growth of microalgae can be significantly affected by changes in pH, as pH determines the solubility and availability of CO<sub>2</sub> and other essential nutrients, activities of intracellular and cell-wall-associated enzymes, and production of various commercially important metabolites (such as proteins and lipids). Acidic pH affects nutrient uptake capabilities, interferes with cellular processes, and induces metal toxicity. Alkaline pH lowers the affinity of cyanobacteria/microalgae for CO<sub>2</sub> and increases the flexibility of the cell wall of mother cells, which delays the completion of cell division cycles (Juneja et al., 2013). The photosynthetic assimilation of CO<sub>2</sub> from the media can increase extracellular pH and the release of CO<sub>2</sub> during dark respiration can decrease extracellular pH. Deviations from optimum pH may inhibit photosynthesis due to the sensitivity of the photosynthetic apparatus and the risk of denaturation of enzymes at extreme pH. Coleman and Colman (1980) had demonstrated that the principal carbon fixation enzyme, rubisco, in a cyanobacterium *Coccochloris peniocystis* was functional only in the pH range of 6.8 to 8.5 (Coleman and Colman, 1981). The extreme variation in external pH influences internal pH and photosynthetic efficiency of the cells. This is because the external pH determines the available species of DIC (dissolved inorganic carbon) in the media (Dodds and Whiles, 2010). There are three main species of DIC, namely aqueous CO<sub>2</sub> (CO<sub>2</sub> (aq)), bicarbonate ion (HCO<sub>3</sub><sup>-</sup>), and carbonate ion (CO<sub>3</sub><sup>2-</sup>). The concentrations of the DIC species are affected by temperature, salinity, and pressure. For instance, when microalgae are cultured in media at an average temperature of 25°C, negligible salinity (no addition of NaCl), and atmospheric pressure, CO<sub>2</sub> (aq) is the predominant form of DIC below pH around 6.3, HCO<sub>3</sub><sup>-</sup> ion predominates between pH around 6.3 – 10.3, and CO<sub>3</sub><sup>2-</sup> becomes dominant above pH around 10.3. However, when seawater or artificial seawater media are used, the increased

salinity shifts the pH range where the DIC species predominates. In this case, CO<sub>2</sub> (aq) predominates below pH around 5.8, HCO<sub>3</sub><sup>-</sup> ion predominates between pH around 5.8 – 9.0, and CO<sub>3</sub><sup>2-</sup> becomes dominant above pH around 9.0 (Zeebe and Wolf-Gladrow, 2001). The suitable pH range for cyanobacteria and microalgae is around 6 to 10. In this pH range, the cells can efficiently process HCO<sub>3</sub><sup>-</sup> in the media and absorb the resulting CO<sub>2</sub> into their cells (Hansen, 2002; Zhang et al., 2014). Freshwater cyanobacteria and microalgae have been known to tolerate a wide range of pH due to the fluctuating pH range in freshwater bodies, whereas their marine counterparts have little tolerance to changes in pH as the pH of seawater remains relatively consistent at around 8.2 (Goldman et al., 1982; Hansen, 2002). For example, Breuer et al. (2013) reported that the optimal pH for the growth of *Scenedesmus obliquus* UTEX 393 was between 6 to 8 (Breuer et al., 2013). Khalil et al. (2010) showed that the optimal pH for *Chlorella ellipsoidea* is around 10 (Khalil et al., 2010). However, in the effort to decrease cultivation cost in pilot-scale PBRs, flue gas is often utilised as the main carbon source for cell growth. Flue gas is mainly composed of CO<sub>2</sub>, NO<sub>x</sub>, and SO<sub>x</sub> (Yen et al., 2015). Increasing CO<sub>2</sub> concentration would drop the pH to 5, and if the concentration of SO<sub>x</sub> increases, the pH would decrease even lower to pH 2 to 3. This pH drop would dramatically damage the cells (Maeda et al., 1995; Westerhoff et al., 2010). This indicates that inhibition of cell growth is often caused by pH changes during cultivation, which can be prevented via preparation of buffered medium or installation of pH-stat system coupled with photobioreactors (Goldman et al., 1982).

#### **2.5.4. O<sub>2</sub> removal**

The evolution of O<sub>2</sub> from photosynthesis can quickly increase the concentration of dissolved O<sub>2</sub> in the culture media if O<sub>2</sub> removal steps or precautions are absent. Excess O<sub>2</sub> will not only increase photorespiration, but also create reactive oxygen species (ROS) in the presence of excess light, causing oxidative damage to the cells (Liu et al., 2012). High O<sub>2</sub> concentration causes rubisco to fix O<sub>2</sub> instead of CO<sub>2</sub>

with ribulose biphosphate to produce phosphoglycolate. The unwanted phosphoglycolate has to be converted, in several steps, into serine, ammonia, and CO<sub>2</sub>, expending energy of the cells. This process is called photorespiration (Masojidek et al., 2013). As a rule of thumb, the concentration of dissolved O<sub>2</sub> in the media should not exceed 400 – 500% of air saturation level. Many microalgal species cannot tolerate high levels of O<sub>2</sub> for more than 2-3 hours (Suh and Lee, 2003). Excess O<sub>2</sub> accumulation is a serious factor that decreases the efficiency of PBRs. O<sub>2</sub> removal is one of the most difficult challenges to overcome in designing effective PBRs, especially closed PBRs (e.g. tubular PBR) (Christenson and Sims, 2011). For closed systems, the problem of O<sub>2</sub> accumulation increases with an increase in the working volume of PBR (Kumar et al., 2011). Depending on the PBR design, it may be necessary to install a separate gas exchanger upon scaling up to remove the excess O<sub>2</sub> during cultivation.

#### **2.5.5. Mixing**

Mixing or agitation is a very important feature of any bioreactor. When other factors are non-limiting for microalgal growth, efficient mixing is the most important factor for high biomass yield (Suh and Lee, 2003). Mixing ensures uniform distribution of nutrients to the cells, efficient light utilisation, better heat transfer, better gas exchange, and homogenous suspension of the cells. In PBRs, mixing is also important as it moves cells between light zone and dark zone, thereby artificially providing light-dark cycles to enhance biomass productivity. In general, mixing in PBRs can be divided into non-mechanical type (e.g. airlift, bubble column, and tubular PBR) and mechanical type (stirred tank and raceway pond) (Kumar et al., 2011). However, turbulence created by these methods can cause hydrodynamic stress, resulting in cell breakage and inhibition of metabolic activity. The tolerance of microalgae to turbulence is strain dependent and needs to be evaluated individually (Mata et al., 2010). By using appropriate mixing methods, most microalgal cells and the nutrients could be uniformly distributed in the media. In

addition, an efficient gas exchange can be associated with proper mixing during cultivation, better mass transfer of CO<sub>2</sub> to cells, and efficient removal of O<sub>2</sub> and accumulated heat (Kumar et al., 2011).

#### **2.5.6. Temperature**

Temperature is one of the most important factors in the cultivation of microalgae and is highly correlated with microalgal growth rate. The effect of temperature on microalgal growth represents a typical bell-shaped curve, where growth rate increases with an increase in temperature until the optimum temperature is reached, then followed by a significant decline thereafter (Ho et al., 2013). Changes in temperature have been found to alter concentration of polyunsaturated fatty acids (PUFAs), rate of photoinhibition, protein content, starch content, and carotenoid content in microalgae. The increase in concentration of PUFAs with lower temperature is one of the most common changes observed in microalgae (Guschina and Harwood, 2009; Harwood, 1998; Thompson Jr, 1996). In one study, the concentration of PUFAs of a microalga *Dunaliella salina* increased with a decrease of temperature from 30°C to 12°C (Lynch and Thompson, 1982). At low temperatures, the fluidity of the cell membranes decreases. To compensate, cells increased the concentration of PUFAs which enhances the fluidity of cell membranes and accelerates the recovery of photosynthetic complexes from the state of photoinhibition (Nishida and Murata, 1996). On the other hand, temperatures higher than optimum resulted in lesser protein synthesis and lower starch content in the microalgal cells. One study on a microalga *Ulva pertusa* had shown that raising the temperature from 20°C to 30°C caused the intracellular free amino acid concentrations to increase from 840 to 1810 mg/100 g dry weight. Higher intracellular free amino acid concentration implies lower protein content in the cells (Kakinuma et al., 2006). As for starch, higher temperature increases the rate of degradation of starch in the microalgal cells. Nakamura and Miyachi (1982) reported 17% decline in starch and 57% rise in sucrose in *Chlorella vulgaris* when

the temperature was raised from 20°C to 38°C (Nakamura and Miyachi, 1982). Increased temperature also causes photo-oxidative damage and the microalgae respond by increasing the pigment concentration as an antioxidant measure. *Dunaliella salina* produced increased amounts of  $\beta$ -carotene when grown under high irradiance and a high temperature of 35°C (Dipak and Lele, 2005). The production of astaxanthin by *Haematococcus pluvialis* can also be induced by increasing the temperature to 30°C, whereas the optimum temperature for growth is 20°C (Tjahjono et al., 1994).

Many microalgae can adapt to a temperature drop of up to 15°C below optimum, but an increase of 2 – 4°C above optimum temperature can adversely affect cell growth and cause cell death. For instance, the specific growth rate of *Chlamydomonas reinhardtii* BAF-J5 increases with temperature over the range of 17-32°C (James et al., 2013). Xin et al. (2011) also reported that the biomass concentration of *Scenedesmus* sp. LX1 increases with an increase in temperature from 10 to 25°C but then decreases with further increase in temperature to 30°C (Xin et al., 2011). It must also be considered that under laboratory conditions, temperature is always measured and maintained, but outdoor culture systems experience seasonal and diurnal variations in temperature (Suh and Lee, 2003). The tolerance of microalgae to ambient temperature needs to be considered with regard to outdoor cultivation process, as this may significantly influence cell growth (Renaud et al., 2002). Ho et al. (2013) showed that *Scenedesmus obliquus* CNW-N can grow well on most days in subtropical areas, except for a few hot or cold days in a year (i.e., over 33°C or under 18°C) (Ho et al., 2013). In addition, some studies have reported strong inhibition of microalgal growth due to sudden heat stress from flue gas, which is often emitted from power/coal/steel plants at more than 120 – 150°C (Kao et al., 2014). Selecting a thermophilic strain with a good heat-removal photobioreactor system can be cost effective instead of an expensive heat exchanger system (Yen et al., 2015). When using the same culture conditions outdoors, the temperature of the culture media would vary with the type of PBR

used. It has also been shown that overheating can occur on especially hot days, where the internal temperature in the photobioreactor might reach as high as 55°C (Mata et al., 2010).

## 2.6. Microalgae cultivation systems

The most common cultivation condition for microalgae involves the utilisation of sunlight and CO<sub>2</sub> to produce energy and glucose via photosynthesis (Huang et al., 2010). An efficient PBR is required for mass production of microalgal biomass for different industrial applications. Normally PBRs consists of four phases, namely cells as solid phase, growth medium as liquid phase, CO<sub>2</sub>-enriched air as gaseous phase, and light radiation field (Posten, 2009). When considering the design of PBRs, issues such as gaseous exchange, mixing pattern, contamination control, light supply, building material, and geometrical configuration must be considered (Carvalho et al., 2006). Furthermore, the desired end products in the cultivated biomass and the quality of the desired products are the key factors in determining the PBR design (Fernández et al., 2013).

PBRs are classified based on their design and they can be broadly divided into two types, namely open systems (such as circular ponds and raceway ponds) and closed systems (such as tubular PBR, flat plate PBR, internally illuminated PBR, heterotrophic fermenter, etc.) (Fernández et al., 2013). The advantages and disadvantages of the open and closed PBRs are described in Table 1.

Table 1 - A comparison of the advantages and disadvantages of open and closed systems in microalgal cultivation

Culture System	Types of bioreactors	Advantages	Disadvantages
Open system	Circular pond	<ul style="list-style-type: none"> <li>• Economical</li> </ul>	<ul style="list-style-type: none"> <li>• Limited control of culture conditions</li> </ul>
	Raceway pond	<ul style="list-style-type: none"> <li>• Design is simple and flexible</li> <li>• Easy to clean</li> <li>• Easy maintenance</li> <li>• Low power consumption</li> </ul>	<ul style="list-style-type: none"> <li>• Lack of control over weather conditions</li> <li>• Poor mass transfer</li> <li>• Poor light and CO<sub>2</sub> utilisation</li> </ul>

		<ul style="list-style-type: none"> <li>• Useful for outdoor mass cultivation</li> </ul>	<ul style="list-style-type: none"> <li>• High evaporative loss</li> <li>• Easily contaminated</li> <li>• Low productivity</li> <li>• High harvesting cost</li> <li>• Limited pool of suitable microalgal strains</li> <li>• Require relatively large areas of flat land</li> <li>• Difficult to grow microalgae for long periods</li> </ul>
	Thin layer cascade	<ul style="list-style-type: none"> <li>• High surface area to volume ratio</li> <li>• High light utilisation due to thin layer of culture exposed to light (&lt;15 mm thickness)</li> <li>• Higher biomass productivity</li> <li>• Culture can be kept in retention tank during unfavourable weather</li> <li>• Lower evaporative loss than open ponds</li> <li>• Lower harvesting cost</li> </ul>	<ul style="list-style-type: none"> <li>• Lack of control over weather conditions</li> <li>• Easily contaminated</li> <li>• Require relatively large areas of flat land due to the use of very thin culture layer</li> <li>• High capital cost due to expensive construction materials</li> <li>• High operation cost due to energy requirement of pumps</li> </ul>
Closed system	Stirred tank PBR <sup>a</sup>	<ul style="list-style-type: none"> <li>• Good heat and mass transfer</li> <li>• Good light penetration</li> <li>• Less contamination concerns</li> <li>• Design is simple</li> <li>• Moderate productivity</li> </ul>	<ul style="list-style-type: none"> <li>• Relatively low surface to volume ratio</li> <li>• Mixing using stirrer may cause heating concerns</li> <li>• Mechanical mixing is costly and not scalable</li> </ul>
	Horizontal tubular PBR	<ul style="list-style-type: none"> <li>• High surface to volume ratio</li> <li>• Relatively low hydrodynamic stress</li> <li>• Moderate productivity</li> <li>• Relatively low self-shading</li> </ul>	<ul style="list-style-type: none"> <li>• Build-up of dissolved O<sub>2</sub></li> <li>• Susceptible to light inhibition</li> <li>• Susceptible to fouling</li> <li>• Relatively large space needed</li> <li>• Poor temperature regulation</li> </ul>
	Bubble column PBR	<ul style="list-style-type: none"> <li>• High mass transfer</li> <li>• No moving parts inside reactor</li> <li>• Less light inhibition</li> </ul>	<ul style="list-style-type: none"> <li>• Relatively low surface to volume ratio</li> <li>• Fabrication materials are expensive</li> <li>• Scale up is constrained by design limitations and self-shading issues</li> </ul>
	Air-lift PBR	<ul style="list-style-type: none"> <li>• High mass transfer</li> <li>• No moving parts inside reactor</li> <li>• Higher productivity than bubble column</li> </ul>	<ul style="list-style-type: none"> <li>• Relatively low surface to volume ratio</li> <li>• Fabrication materials are expensive</li> </ul>

	<ul style="list-style-type: none"><li>• More homogenous mixing than bubble column</li></ul>	<ul style="list-style-type: none"><li>• Scale up is constrained by design limitations and self-shading issues</li></ul>
Flat plate PBR	<ul style="list-style-type: none"><li>• High surface to volume ratio</li><li>• Relatively low space needed</li><li>• High photosynthetic efficiency</li><li>• Low build-up of O<sub>2</sub></li><li>• Relatively cheap</li></ul>	<ul style="list-style-type: none"><li>• Lower working volume due to lower culture thickness</li><li>• Susceptible to fouling</li><li>• Poor temperature regulation</li><li>• Not scalable as many components are needed for scale up</li></ul>

<sup>a</sup> Photobioreactor

References (Brennan and Owende, 2010; Chisti, 2007; Masojídek et al., 2015; Posten, 2009; Ugwu et al., 2008)

### 2.6.1. Open system

In open systems, the culture is directly exposed to the environment. They have been traditionally used to cultivate microalgae due to its low cost, simplicity, low energy consumption, and high availability of solar radiation (Carlozzi, 2008; Fernández et al., 2013). The most commonly used open systems are circular ponds and raceway ponds. Open systems are still widely employed in industrial processing, but has little room for further technological improvement. This is due to various constraints related to their operation for large scale applications (Carvalho et al., 2006). The major drawbacks of open ponds are limited control of culture conditions, lack of control of weather conditions, easy contamination, evaporative losses, low CO<sub>2</sub> mass transfer rates due to shallow ponds (30 – 50 cm culture depth), and requirement of large areas of relatively flat land (Brennan and Owende, 2010; Carvalho et al., 2006; Fernández et al., 2013; Singh and Sharma, 2012). Since open systems are still widely used in commercial production of microalgae as per economic concerns, it is necessary to choose an appropriate open system with suitable operating strategies based on the characteristics of the cultivated microalgal species.



### 2.6.1.1. Circular pond

With the principal advantage of using abundant sunlight as the energy source for microalgal growth, circular ponds are one of the oldest pond types used for commercial microalgal cultivation such as *Chlorella* sp. (Lee, 2001). These ponds are constructed of concrete and are equipped with a rotating arm mounted at the centre to mix the culture, as seen in Figure 1. They are also lined with materials like plastic sheets or inert membranes as a secondary containment measure. As the rotating arm travels over a greater distance, greater mixing of the culture can be attained at the periphery of the ponds (Borowitzka and Moheimani, 2013). Thus, the circular ponds are most suitable for growing cyanobacteria and microalgae that sediment easily, such as *Chlamydomonas* sp. and *Chlorella vulgaris*.

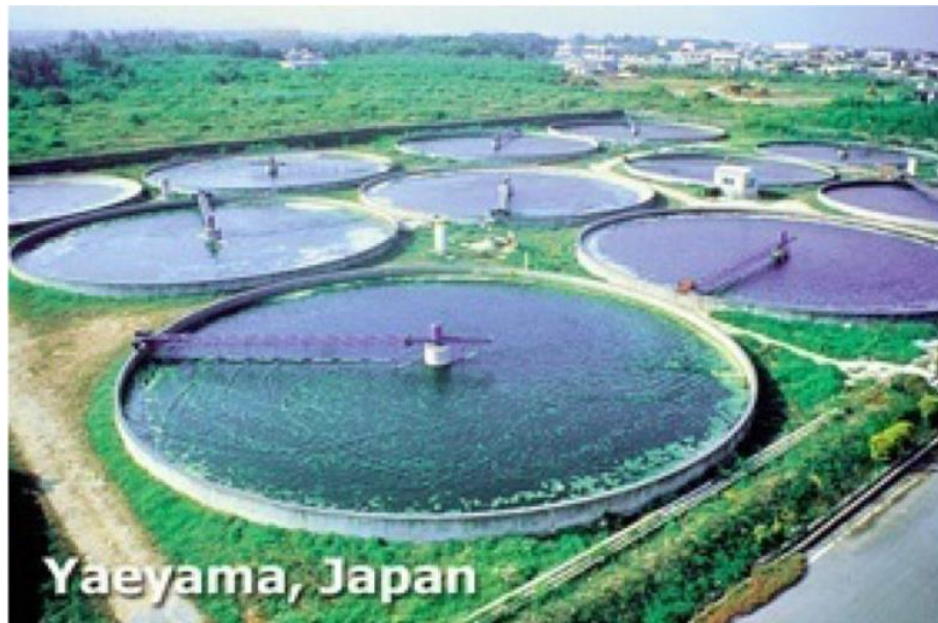


Figure 1 – Open pond with rotating arm for mixing the microalgal cultures  
(Hamed, 2016)

### 2.6.1.2. Raceway pond

Raceway ponds are the most widespread PBR used to culture microalgae commercially due to their flexibility and ease of scaling-up (Fernández et al., 2013). In raceway ponds, microalgal cells, nutrients, and water are continuously circulated

around a racetrack by using a paddlewheel, as seen in Figure 2. This provides mixing between the cells and nutrients, and also prevents sedimentation (Singh and Sharma, 2012). Usually, raceway ponds are operated in a continuous mode by adding fresh culture medium at a position before the paddlewheel. After completion of the circulation loop, microalgal culture is then harvested behind the paddlewheel. Bubbling of CO<sub>2</sub> can help to enhance aeration, CO<sub>2</sub> consumption, and mixing, thereby increasing the growth of microalgal cells (James and Boriah, 2010; Singh and Sharma, 2012).

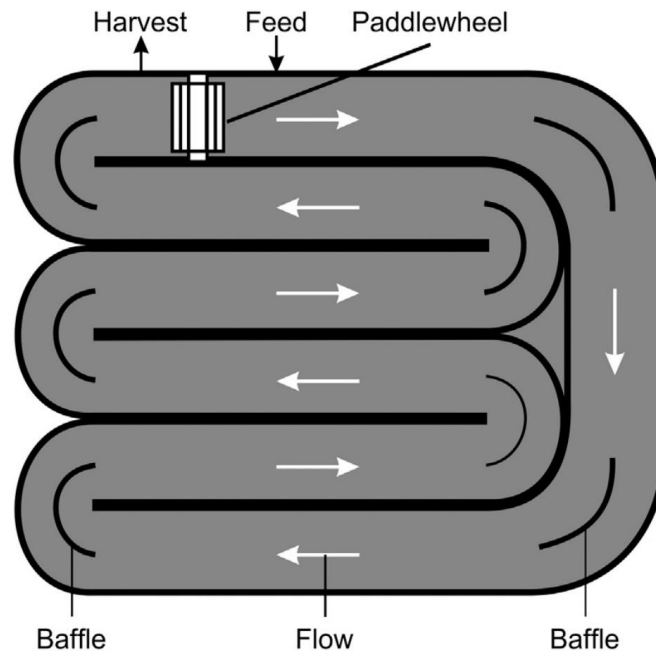


Figure 2 – Schematic diagram of raceway pond with paddlewheel to circulate the microalgal cultures (Bahadar and Bilal Khan, 2013)

Not many contaminants can survive under extreme conditions, thus contamination can be minimised by cultivating some highly resistant microalgal strains at high pH or high salinity in raceway ponds. The most successful commercial cultivation of algae in raceway ponds include *Chlorella* sp., *Spirulina* sp. and *Dunaliella* sp., which are cultivated in stringent conditions that inhibits the growth of other weed algae or pathogenic bacteria. However, pH gradients resulting

from inefficient mixing system can cause contamination in those cultures (Ugwu and Aoyagi, 2012). To overcome the problem of poor mass transfer efficiency, raceway ponds are frequently equipped with sumps or mixing columns to increase the gas and liquid contact time (Park et al., 2011; Putt et al., 2011).

### **2.6.1.3. Thin layer cascade**

There are generally 2 types of thin layer cultivation systems for microalgae, which are thin layer cascade (TLC) for open system and flat plate PBR for closed system. The TLCs are widely known as the Třeboň's or Šetlík's type (Šetlík et al., 1970). The design of TLCs involves sloping platforms where microalgal culture flows by gravity and ends in a retention tank, where the culture is pumped back to the starting point (highest point) on the sloping platforms, as shown in Figure 3. Each TLC consists of 5 components, namely sloping surface (light phase), retention tank (dark phase), pump, aeration (pure CO<sub>2</sub>), and measurement and control units. For multiple sloping platforms, the lower end of the upper platform is joined by a trough to the starting point of the lower platform. The operation of TLCs starts by filling up the retention tank with microalgal culture and turning on aeration, followed by circulation of the culture by pump to the starting point on the top-most platform. Dissolution of CO<sub>2</sub> occurs in the retention tank, and degassing of excess O<sub>2</sub> occurs on the sloping platforms. High velocity of the culture on the sloping platforms is important because the resulting high turbulence aids in mixing, reduces cell shading, and increases degassing rate. During sunny weather, the microalgal thin layer can be easily heated up by solar irradiance, and water evaporation from the culture helps in cooling down to prevent overheating. The culture flows over the sloped platforms only during sunlight hours and kept in the retention tank during night-time or unfavourable weather conditions. When the culture is kept in the retention tank, continuous aeration is provided to induce mixing and maintain biological activity. The development of special software has permitted automatic

control and data recording of the culture conditions for the duration of the experiment.

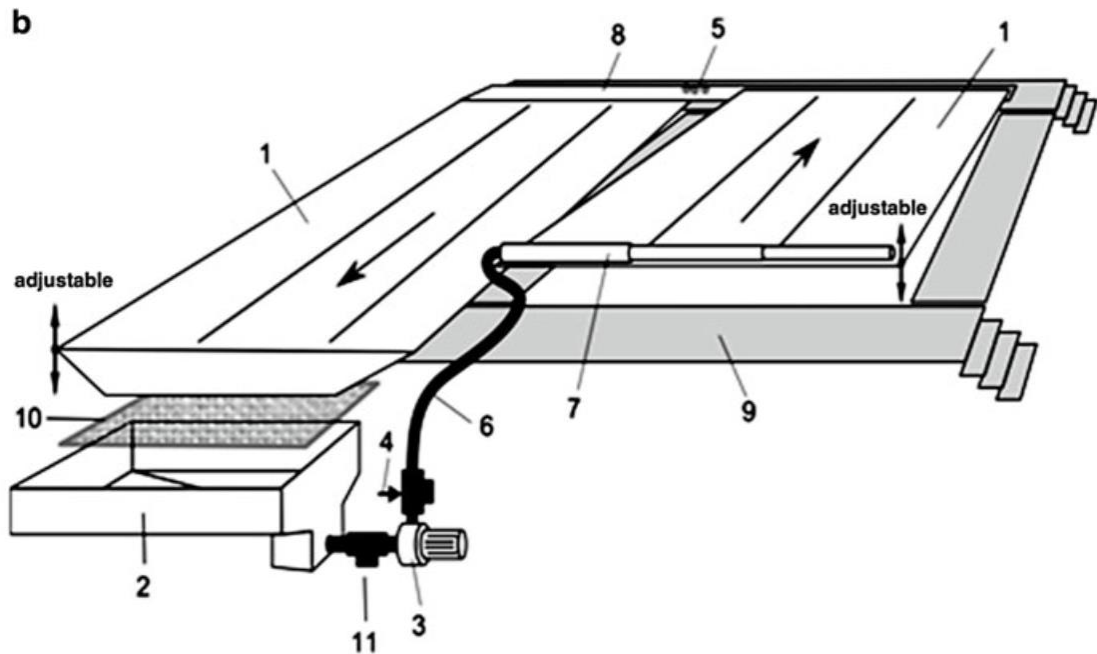


Figure 3 – Schematic diagram of thin layer cascade photobioreactor (model Dahlia), where the number represents: (1) sloping platforms, (2) retention tank, (3) pump, (4) CO<sub>2</sub> inlet, (5) measurement and control sensors (pH, dissolved O<sub>2</sub>, temperature, and liquid level), (6) return pipe to upper platform, (7) flow distributor (spreads culture flow across upper platform), (8) connecting trough, (9) elevated platform, (10) screen (helps to degas excess O<sub>2</sub> produced by the microalgae), and (11) valve for harvesting (Masojídek et al., 2015)

The concept of TLC was first established in the 1960s at the Laboratory of Algal Biotechnology of the Institute of Microbiology at Třeboň. Initially, the TLC was designed to operate with a thin layer (<50 mm) of microalgal culture in turbulent flow with the help of evenly spaced corrugated surfaces and transversal baffles. Compared to open ponds and raceway tracks where the larger depth of microalgal culture (100-300 mm) resulted in low light penetration, poor mixing, and poor gas transfer, TLCs are capable of achieving uniformly-mixed microalgae culture with higher biomass productivity (>10 g/L dry weight). The lower volume of denser

microalgal culture lessens the burden of harvesting and dewatering steps (Doucha and Lívanský, 2014).

In the 1990s, following favourable changes in the scientific atmosphere in the Czech Republic, microalgal research was resumed and an outdoor large-scale TLC unit with a surface area of 650 m<sup>2</sup> and working volume of 6,500 L was constructed at the Institute of Microbiology in Třeboň (Doucha and Lívanský, 1995; Grobbelaar et al., 1995). Compared to the TLCs employed during the 1960-1970s, this new TLC was considered the second generation TLC and focused on growing a much thinner microalgal layer (< 10 mm). To achieve higher flow velocity of 0.4 – 0.5 m/s, plastic rods with 13 mm diameter were placed 1.5 m apart, unlike the previous generation of TLCs where baffles were densely spaced. It was realized that sloping platforms could perform best when designed as a smooth inclined surface without using any baffles so the microalgal layer was only 6 – 8 mm. Using glass plates supported by steel frames as the sloping platforms had also allowed simpler cleaning and maintenance compared to the baffled TLC units. The microalgal thin layer of 6 – 8 mm coupled with high velocity of 0.4 - 0.5 m/s produced a turbulent flow (Reynolds number of roughly 4,500) which prevents self-shading. The short light path of the microalgal thin layer resulted in higher light utilisation and greater biomass concentration of 15 – 35 g/L dry weight. This new TLC unit displayed a high surface area to volume ratio of roughly 100 m<sup>-1</sup> compared to that of open ponds at around 10 m<sup>-1</sup> (Doucha and Lívanský, 1995; Grobbelaar et al., 1995). Improved design of the retention tank could lower the dark phase to roughly 20% of the total culture volume during operation. This could increase the biomass productivity as high as 50 g/m<sup>2</sup>/d (dry weight) during summer in temperate regions (Masojídek et al., 2011).

The third generation TLC, model Dahlia (Figure 3), was designed and developed in 2012 – 2013 as a modular system in the Institute of Microbiology in Třeboň (Masojídek et al., 2015). The TLC had an area of 90 m<sup>2</sup> and consisted of two identical and parallel sloping platforms placed in a north-south alignment. The

two sloping platforms were inclined in opposite directions. Compared to past generations of TLCs which used glass plates supported by metal frames as the sloping platforms, model Dahlia instead used stainless steel which were easier to clean and maintain as well as more resistant to corrosion and winter damage. The angle of each platform could be adjusted between 0.5 – 3° which would produce a varying flowrate of 20 – 60 cm/s with a microalgal thin layer of 5 – 15 mm thickness. The adjustable platforms enabled researchers to investigate the effects of different microalgal layer thickness on light utilisation and biomass concentration. The surface area to volume ratio was calculated to be 60 – 180 m<sup>-1</sup>. Apart from heating by the sun, the temperature of the culture could also be regulated by a heat exchanger in the trough and heating cables in the retention tank. Pure CO<sub>2</sub> aeration rate was regulated by a pH-stat device whereby CO<sub>2</sub> was only bubbled into the culture when pH was increased. To lower the maximum height of this TLC, the retention tank was positioned in a rectangular dugout 0.5 m below ground level. This TLC was constructed with standardized parts connected by joints which enabled easy disassembly of the entire unit. Nevertheless, the major drawbacks of TLCs are high capital cost due to expensive fabrication materials and high operation cost due to the energy-intensive nature of pumps. But these costs can be offset by high microalgal biomass productivities. For instance, in one study, when model Dahlia was tested with microalgal layer thickness of 5 mm and a mean sunlight intensity of roughly 400 μmol/m<sup>2</sup>/s, the biomass concentration of *Chlorella sorokiniana* rose from an initial concentration of 2 g/L to 18 g/L in 8 days (Masojídek et al., 2015).

### **2.6.2. Closed system**

Current researches on PBRs are primarily focused on closed systems as they are designed to overcome the constraints of open systems. In a closed system, the microalgal culture is entirely enclosed within the PBR, having no direct gaseous

exchange with the atmosphere but allow sunlight or artificial illumination to reach the culture (Borowitzka and Moheimani, 2013; Fernández et al., 2013).

### 2.6.2.1. Stirred tank photobioreactor

Stirred tank is the most conventional type of PBR, particularly for the production of high value products such as fine chemicals or pharmaceuticals (Mata et al., 2010). Stirred tank PBRs are able to ensure the precise control over processing parameters and maintain the sterility of microalgal cultures, as illustrated in Figure 4. These advantages are crucial for the production of high value products (Lee, 2001). Agitation is provided mechanically using impellers of different shapes and sizes. Vortex can be reduced by using baffles. Carbon source for microalgal growth is supplied by bubbling CO<sub>2</sub>-enriched air from the bottom of the reactor (Singh and Sharma, 2012).

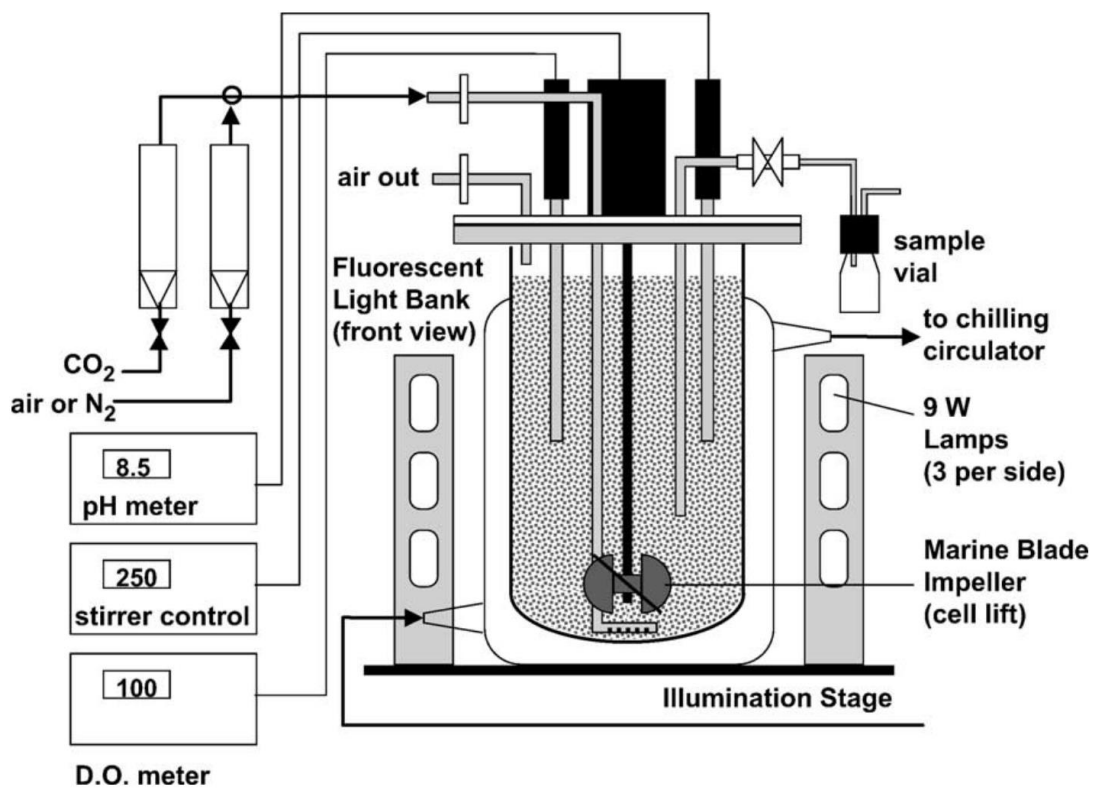


Figure 4 – Schematic diagram of stirred tank photobioreactor (Rorrer and Cheney, 2004)

However, stirred tank PBRs suffer from a few limitations. External illumination could not induce light saturation for the microalgae, so maximum photosynthetic efficiency could not be achieved. This is due to the low surface area to volume ratio of the PBR, and sufficient provision of light is ineffective in terms of cost and energy. This problem can be overcome to some extent by efficient stirring mechanisms. The unused portion of sparged gas and O<sub>2</sub> produced during photosynthesis diffuse out of the culture media and collect in the large disengagement zone at the top part of the PBR (Singh and Sharma, 2012).

#### **2.6.2.2. Horizontal tubular photobioreactor**

Tubular PBRs are broadly divided into 2 types based on their general configuration, namely horizontal tubular PBR and vertical tubular PBR. Horizontal tubular PBRs (Figure 5) are the most commonly used closed system (Gupta et al., 2015). The design of horizontal tubular PBRs involves transparent tubes organized in various arrangements such as horizontal, inclined, spiral, helicoidal, and their combinations. Apart from the layout of the tubes, other important design parameters include velocity of medium, length of tubes, type of circulation system, and configuration of the tubes to best capture light. The transparent tubes commonly measure 10 – 60 mm in diameter with total length of up to a few hundred meters. These tubes can achieve a large surface area to volume ratio (above 100/m), which is one of the primary benefits of this PBR (Posten, 2009). If the tube diameter is increased, the surface area to volume ratio will decrease, strongly affecting the photosynthetic efficiency of the culture. The tubes provide a “lens” or “focusing effect” whereby incident light normal to the surface of the tubes are being focused into the tubes, whereas incident light at other angles are diluted along the circumference of the tubes. This “focusing effect” helps to reduce self-shading and raise light intensity in the tubes (Posten, 2009). One of the major disadvantage of horizontal tubular PBRs is the accumulation dissolved O<sub>2</sub> to inhibitory concentrations in the culture media. Although horizontal tubular PBRs are widely considered as the most



practical and scalable closed system but according to Sánchez Mirón et al. (1999), horizontal tubular PBRs are not economically feasible to scale up because of the increased need for cooling and gas exchangers (Miron et al., 1999). In addition, photoinhibition caused by high dissolved O<sub>2</sub> concentration and high light intensity can decrease the biomass productivity when compared to bubble column and air-lift PBRs (Gupta et al., 2015).

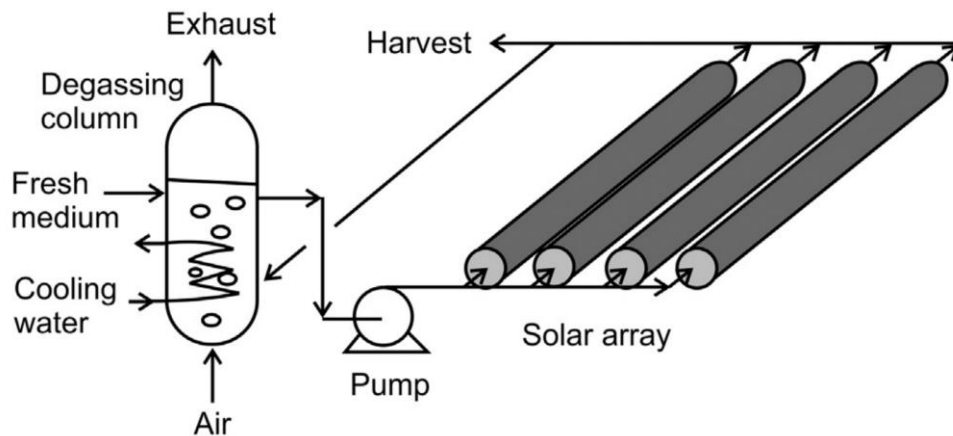


Figure 5 – Schematic diagram of horizontal tubular photobioreactor (Bahadar and Bilal Khan, 2013)

### 2.6.2.3. Vertical tubular photobioreactor

Vertical tubular PBRs have compact and user friendly designs, high surface area to volume ratio, low contamination risk, and high biomass productivity (Dasgupta et al., 2010; Mirón et al., 2002), making them suitable for large scale cultivation of microalgae. Vertical tubular PBRs consist of transparent vertical tubes to allow maximum light penetration (Kumar et al., 2011). They offer efficient mixing with high gas transfer rates and have excellent control over the growth conditions. Bubbling of gas from the bottom of the column enables efficient supply of CO<sub>2</sub> and optimal removal of excess dissolved oxygen (Dragone et al., 2010). Constant agitation of the media is generated by sparging CO<sub>2</sub>-enriched air (Dasgupta et al., 2010), causing smaller shear stress than pumps or impellers (Mirón et al., 2002). Bubble column and air-lift PBRs fall under this category and can be differentiated

based on their mode of liquid flow (Kumar et al., 2011). Air-lift PBRs possess good mixing properties whereas bubble column PBRs allow efficient aeration (Dasgupta et al., 2010).

In tubular PBR, light availability is affected by aeration rate, gas holdup and liquid velocity (Mirón et al., 2002). Both the height and diameter of a single vertical tubular PBR should not exceed a certain limit due to self-shading and the strength of the transparent materials used in fabrication (Huang et al., 2017). Sánchez Mirón et al. (1999) tested a bubble column PBR with 0.2 m diameter and variable height. The test demonstrated that volumetric biomass productivity and eicosapentaenoic acid (EPA) production declined when the column height was above 5 m. Hence, it was suggested that the optimal dimensions of a bubble column photobioreactor should be approximately 0.2 m in diameter and 4 m in height (Miron et al., 1999). Aeration rate in tubular PBR should also be adjusted within acceptable range by considering the factors like sensitivity to shear stress (Xu et al., 2009) and light penetration (Miron et al., 1999). The aeration rate should be kept at a certain minimal level to prevent cell stagnation for long periods in the dimly lit interior region of the PBR. In contrast, high aeration rates could reduce light penetration over time by generating the accumulation of persistent microbubbles (Miron et al., 1999).

#### **2.6.2.3.1. Bubble column photobioreactor**

Bubble column PBRs consist of vertical cylindrical columns and the light source is usually supplied externally, as shown in Figure 6b. It is advantageous in terms of low cost, large surface area to volume ratio, good mass and heat transfer, homogenous culture condition, and efficient O<sub>2</sub> removal. Efficiency of photosynthesis depends greatly on the gas flow rate. The increase of gas flow rate that leads to shorter light-dark cycles could significantly increase the photosynthetic efficiency of microalgae (Singh and Sharma, 2012). Separation of gas and liquid takes place at the freeboard region at the top of the PBR (Wang et

al., 2012). CO<sub>2</sub> mass transfer and mixing is done through gas bubbling from a sparger at the bottom of the PBR (Kumar et al., 2011). In a bubble column PBR, the mixing can be random and erratic due to turbulence created by the sparged gas (Halim et al., 2011; Miron et al., 1999; Wang et al., 2012). As a result, microalgal cells may be exposed to uneven light intensity for a long time and cell sedimentation are more likely to occur (Kaewpintong et al., 2007). For the purpose of scaling up, turbulence can be increased by installing perforated plates inside the column to break up and redistribute coalesced bubbles (Wang et al., 2012).

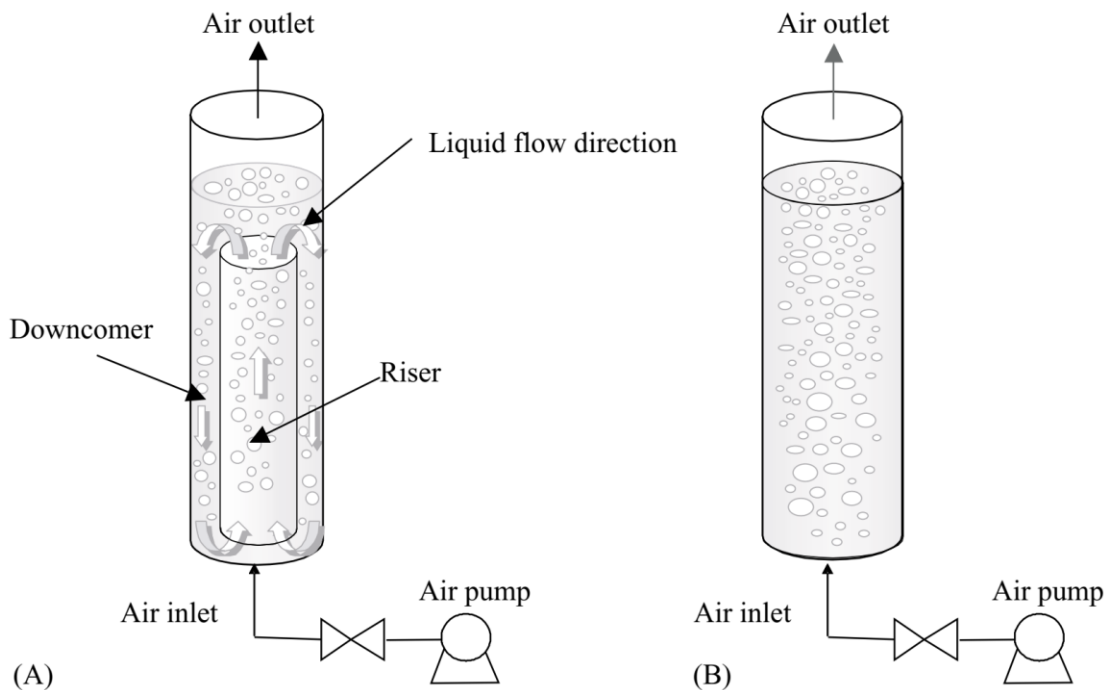


Figure 6 – Schematic diagram of (a) airlift photobioreactor and (b) bubble column photobioreactor (Krichnavaruk et al., 2005)

#### 2.6.2.3.2. Air-lift photobioreactor

Air-lift PBRs have two distinct zones called riser and downcomer, and they are separated by a cylindrical baffle, as shown in Figure 6a. The riser (inner region of the baffle) is where the sparged gas moves upwards, generating turbulence and inducing the medium within the riser to flow upwards with the gas bubbles. Whereas the downcomer (outer region of the baffle) is where the agitated medium

in the riser circulates back down to the bottom of the PBR. In the riser, mixing is done purely by gas sparging and no physical agitation is involved (Kumar et al., 2011). The fluid dynamics of air-lift PBR are influenced significantly by the gas hold-up of the downcomer. Upon reaching the maximum height of the culture, the degassed medium moves downwards through the downcomer with defined and oriented motions. The gas hold-up difference between riser and down comer is one of the most crucial parameters that should not be overlooked when designing air-lift PBRs (Barbosa et al., 2003; Kumar et al., 2011; Singh and Sharma, 2012). The common configurations used for air-lift PBRs are internal loop, internal loop concentric and external loop vessels. Of these, the external loop configuration provides better mixing because the distance between the riser and the downcomer enables efficient gas disengagement.

Air-lift PBRs enable higher microalgal growth rate compared to bubble column PBRs due to better mixing pattern (Xu et al., 2009). Air-lift PBRs are characterised by the advantage of generating circular and homogeneous mixing pattern that could provide flashing light effect to microalgal cells. This happens when the culture medium moves continuously through dark (riser) and light (downcomer) zones (Degen et al., 2001; Monkonsit et al., 2011; Xu et al., 2009). Furthermore, the residence time of the sparged gas in various zones has a significant influence on important parameters such as heat transfer, mass transfer, mixing, and turbulence (Chisti and Moo-Young, 1993).

Air-lift photobioreactors are generally recommended for microalgal cultures that are fragile and sensitive to shear stress. Efficient mixing can be achieved by increasing the aeration rates, but should be done moderately to prevent cell damage (Ugwu and Aoyagi, 2012). Oncel and Sukan (2008) observed that air-lift PBRs can sustain better biomass yields of different microalgae than bubble column PBRs. This was probably due to better mixing that can help to prevent cell sedimentation and improve the efficiency of light utilisation in air-lift PBRs (Oncel and Sukan, 2008; Wang et al., 2012). Monkonsit et al. (2011) also proved that

under the same operation conditions for both air-lift and bubble column PBRs of the same size, the cultivation of diatom *Skeletonema costatum* achieved better biomass productivity ( $6.4 \times 10^4$  cells  $s^{-1}$ ) in air-lift than in the bubble column ( $2.2 \times 10^4$  cells  $s^{-1}$ ) (Monkonsit et al., 2011). However, in large-scale production, both air-lift and bubble column PBRs suffer from light limitation. It was suggested that the installation of immersed optical fibres as internal light source could increase the light penetration efficiency in high-density cultures (Krichnavaruk et al., 2007).

#### **2.6.2.4. Flat plate photobioreactor**

As illustrated in Figure 7, flat plate PBRs are cuboid-shaped vessels with a narrow light path (Singh and Sharma, 2012) and are the most popular choice among all closed systems (Borowitzka, 1999). Flat plate PBRs are characterised by high illuminated surface area to volume ratio and open gas transfer area (Singh and Sharma, 2012; Wang et al., 2012). These two characteristics make them suitable for mass production of microalgae in both indoor and outdoor culture systems (Ugwu et al., 2008; Xu et al., 2009).

Flat plate PBRs are made of transparent materials for maximum utilisation of light energy (Ugwu et al., 2008). The thickness of each plate is the determining factor for its high surface area to volume ratio and short length of light path (Carvalho et al., 2006). Light source can be diffused and distributed effectively using thin plates which leads to higher photosynthetic efficiency and higher biomass yield (Zou and Richmond, 1999). Mixing can be provided in two ways, by bubbling air through perforated tube or rotating the plates mechanically using motors (Singh and Sharma, 2012). Baffles can be included to improve mixing efficiency (Zhang et al., 2001). The open gas disengagement system reduces the accumulation of dissolved  $O_2$  (Xu et al., 2009) and minimises the requirement for a dedicated degassing unit (Dasgupta et al., 2010). As for temperature control, water spray or internal heat exchangers can be used to cool the plates (Fernández et al., 2013). However, the thin plates are usually expensive to scale up, susceptible to fouling,

difficult to clean, and easily subjected to temperature fluctuation and light inhibition (Wang et al., 2012). Fouling occurs when cells attach to the plastic walls, causing a reduction in light availability and increment in contamination risk. Scaling up of flat plate PBR requires many components which can be expensive and difficult to maintain. Even though flat plate PBRs works well for laboratory tests and small scale purposes, their scale up for commercial production of microalgae still requires more research and efforts (Fernández et al., 2013).

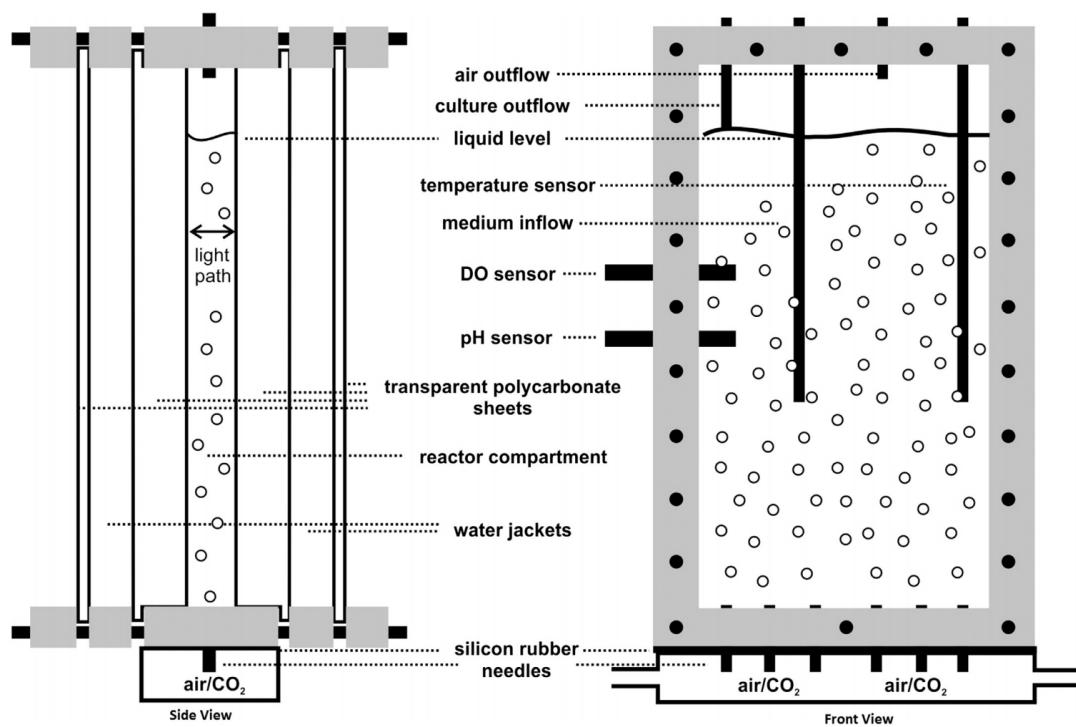


Figure 7 – Schematic diagram of flat plate photobioreactor (Bahadar and Bilal Khan, 2013)

#### 2.6.2.5. Internally illuminated photobioreactor

The usage of sunlight as the sole light source for the cultivation of photosynthetic microalgae is limited by variations in light intensity due to weather, season, and geographical location. Typically, year-round cultivation with sunlight is possible in tropical regions, whereas this type of cultivation becomes limited to only warmer months in temperate regions. Ogonna et al. (1999) showed that the microalgal

growth was stunted during prolonged period of bad weather such as cloudy or rainy days. The light source was insufficient to support microalgal growth and eventually caused a decrease in biomass productivity and biochemical composition of the microalgal cells (Ogbonna et al., 1999). Apart from that, reduction in biomass productivity can also occur when the outermost layer of cells experience photoinhibition due to exposure to excessive light, or the innermost layer of cells experience self-shading as the result of reduced light penetration due to insufficient mixing and high cell density (Xu et al., 2009).

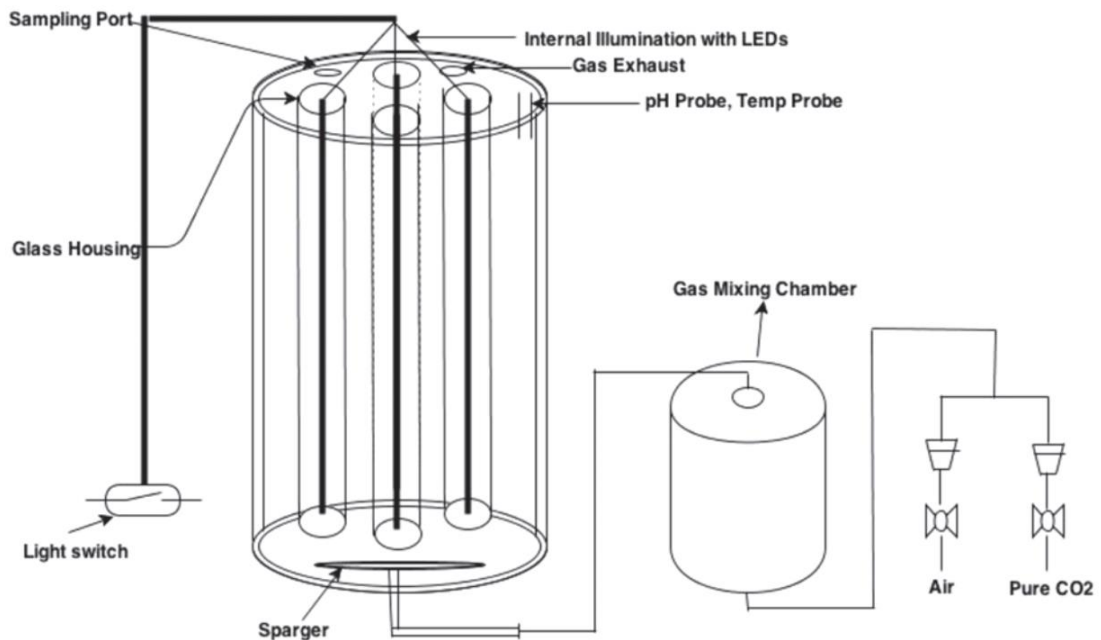


Figure 8 – Schematic diagram of internally illuminated bubble column photobioreactor (Yadavalli et al., 2014)

This impediment can be addressed by installing an internal illumination device (such as optical fibres or fluorescent lamps) inside the cultivation vessel (Ugwu et al., 2008; Xu et al., 2009). Figure 8 shows an example of internal illumination used in a bubble column PBR. Carvalho et al. (2006) also agreed that the installation of an internal illumination device like optical fibre could provide a more homogeneous distribution of light for better photosynthetic efficiency (Carvalho et al., 2006). Optical fibres are installed for solar light collection,

transmission, and distribution of light energy more efficiently and evenly inside PBRs (Ogbonna et al., 1999), increasing the average irradiance and the depth to which light reaches inside the PBRs (Javanmardian and Palsson, 1991). This type of PBR can also be modified so that light intensity of solar and artificial light systems can be controlled (Ogbonna et al., 1999). The integration of solar and artificial light devices enables continuous supply of light to the PBRs during cloudy weather or night-time (Ugwu et al., 2008). On top of that, internally-illuminated PBRs can also be heat-sterilized under pressure to reduce the risk of contamination (Ogbonna et al., 1999).

However, the use of optical fibres in PBR suffers from several limitations such as additional capital costs, difficulty in cleaning, and the loss of light energy due to attenuation inside the optical fibres. Hence, the practical feasibility for large scale application using PBRs equipped with optical fibre for internal illumination remains a challenge (Wang et al., 2012). Recently, LED has been used as an internal light source due to its lower construction cost. The LED-based internally illuminated PBR also has the advantage of emitting light at specific wavelengths (e.g. blue light or red light only). This may become beneficial to the production of specific products (e.g. carotenoids) from microalgae that are induced by light sources with specific wavelengths (Chen et al., 2010; Ho et al., 2014).

#### **2.6.2.6. Fermenter type photobioreactor**

Fermenter-type PBRs are the least expanded systems, which offer open gas exchange and are mainly used for optimization studies. The main advantage of fermenter-type PBR is the ability to monitor and control every operating parameter precisely and accurately (Carvalho et al., 2006; Dasgupta et al., 2010). However, its scale up is restricted due to low surface area to volume ratio and high capital costs. For large volume cultivation, illumination can be supplied internally and agitation can be provided using impeller or magnetic stirrer (Dasgupta et al., 2010; Heining et al., 2014). Hence, if microalgal productivity can be enhanced, fermenter-



type PBRs could become a competitive alternative for the production of high-value biochemical products from microalgae. The fermenter-type PBR is also well-suited to culturing heterotrophic microalgae, where light source is no longer a limiting factor (Carvalho et al., 2006).

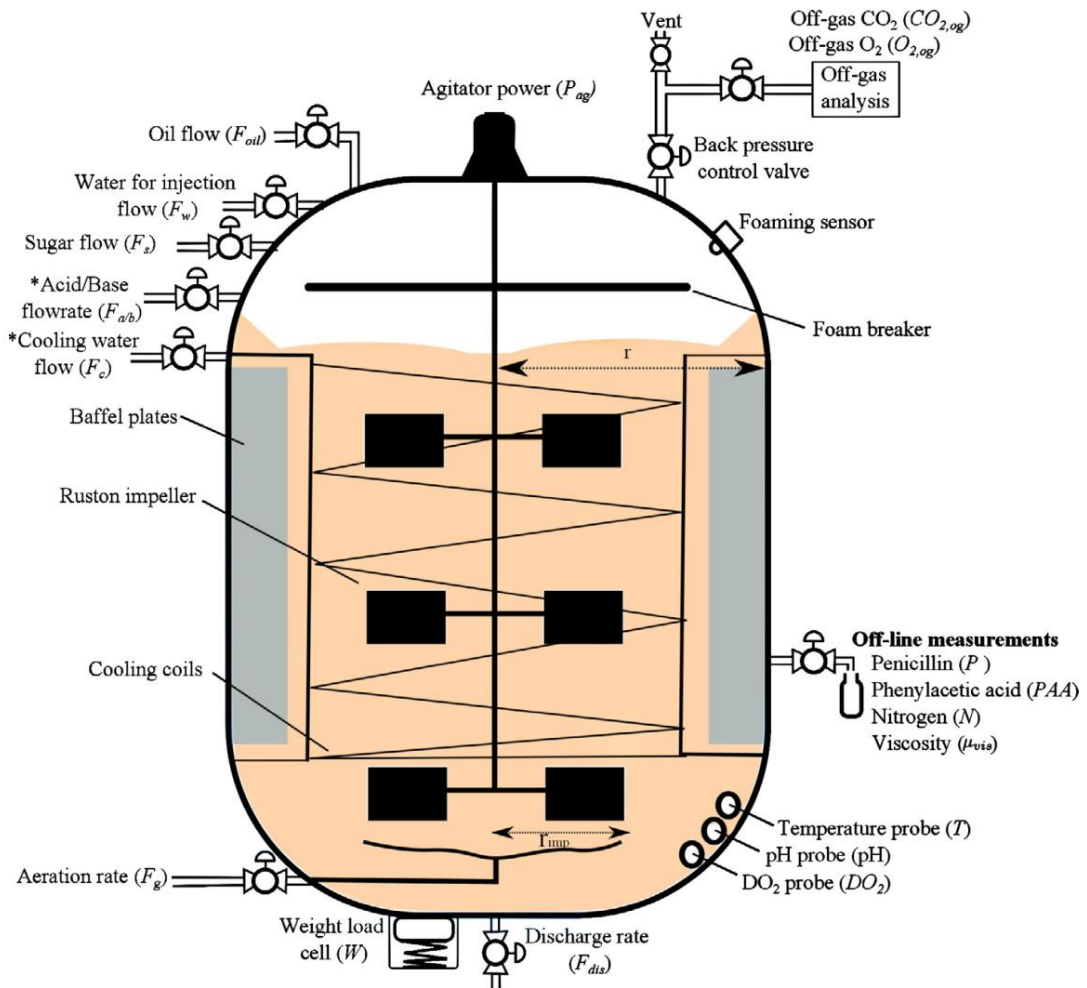


Figure 9 – Schematic diagram of fermenter type bioreactor (Goldrick et al., 2015)

# CHAPTER 3

## MATERIALS AND METHODS

In this chapter, all the materials and methods used in the experiments (explained in Chapter 4) can be found. The materials and methods are categorised into Study 1 – 4. A brief explanation on the overall protocol in each study was included in each section.

### 3.1. Study 1

Study 1 investigated the protein content and protein productivity of two microalgal species, *Chlorella sorokiniana* CY1 and *Chlorella vulgaris* ESP-31. The microalgae were cultured in 1 L laboratory bottles as described in Section 3.1.4. Three parameters were investigated and optimised for both microalgal species, which were different medium and initial nitrate concentration, CO<sub>2</sub> concentration, and light intensity. The parameters were optimised one at a time, with the most influential parameter being optimised first. The extent of the influence of each parameter were obtained from literature, which helped to choose which parameters to optimise first. The other culture conditions remained the same as the initial conditions stated in Section 3.1.1. After harvesting, the microalgal biomass was analysed for protein content using Lowry method. One-way ANOVA was also used to determine whether the investigated parameter resulted in significant improvement in the biomass and protein productivities of the microalgal species.

### 3.1.1. Microalgae strain, medium composition, and culture conditions

The microalgal species used in this study are *Chlorella sorokiniana* CY1 and *Chlorella vulgaris* ESP-31. Both species were isolated in Taiwan and obtained from National Cheng Kung University (NCKU). The medium chosen to culture the microalgae were BG-11 medium and Basal medium. The chemical composition of BG-11 medium is (g/L): NaNO<sub>3</sub>, 1.5; K<sub>2</sub>HPO<sub>4</sub>, 0.03; MgSO<sub>4</sub>·7H<sub>2</sub>O, 0.075; Citric acid anhydrous, 0.006; Na<sub>2</sub>CO<sub>3</sub>, 0.02, CaCl<sub>2</sub>·2H<sub>2</sub>O, 0.036; Ammonium iron(III) citrate, 0.006; EDTA·2Na, 0.001; H<sub>3</sub>BO<sub>3</sub>, 0.00286; MnCl<sub>2</sub>·4H<sub>2</sub>O, 0.00181; ZnSO<sub>4</sub>·7H<sub>2</sub>O, 0.000222; Na<sub>2</sub>MoO<sub>4</sub>·2H<sub>2</sub>O, 0.00039; CuSO<sub>4</sub>·5H<sub>2</sub>O, 0.000079; Co(NO<sub>3</sub>)<sub>2</sub>·6H<sub>2</sub>O, 0.000049.

The chemical composition of Basal medium is (g/L): KNO<sub>3</sub>, 1.25; KH<sub>2</sub>PO<sub>4</sub>, 1.25; MgSO<sub>4</sub>·7H<sub>2</sub>O, 1; CaCl<sub>2</sub>·2H<sub>2</sub>O, 0.1106; FeSO<sub>4</sub>·7H<sub>2</sub>O, 0.0498; EDTA·2Na, 0.5; H<sub>3</sub>BO<sub>3</sub>, 0.1142; ZnSO<sub>4</sub>·7H<sub>2</sub>O, 0.0882; MnCl<sub>2</sub>·4H<sub>2</sub>O, 0.0144; Na<sub>2</sub>MoO<sub>4</sub>·2H<sub>2</sub>O, 0.0119; CuSO<sub>4</sub>·5H<sub>2</sub>O, 0.0157; Co(NO<sub>3</sub>)<sub>2</sub>·6H<sub>2</sub>O, 0.0049 (Sorokin and Krauss, 1958).

The initial culture conditions were: 200 µmol/m<sup>2</sup>/s light intensity, 0.06 g/L initial cell concentration, 300 rpm continuous stirring, and continuous sparging of 2.5% CO<sub>2</sub> gas at a flow rate of 0.1 vvm (volume of CO<sub>2</sub> per volume of medium per minute).

### 3.1.2. Determination of microalgae cell concentration

The microalgae cell concentration in the PBR was determined daily via OD<sub>680</sub> using a spectrophotometer (UV-1800, Shimadzu, Kyoto, Japan) after appropriate dilution with distilled water. The DCW of the microalgal biomass was obtained by drying 5 ml of the culture in a weighing moisture analyser (ML-50, A&D Company, Limited, Tokyo, Japan). The dry weight of the biomass was determined using an electronic balance and converted to biomass concentration via calibration between OD<sub>680</sub> and DCW.

### **3.1.3. Determination of medium nitrate concentration**

The nitrate concentration of the culture was determined daily via optical density measurement at a wavelength of 220 nm using a spectrophotometer (UV-1800, Shimadzu, Kyoto, Japan) (Collos et al., 1999). Before measurement, the samples were centrifuged at 6000 rpm for 5 min (Centrifuge 5430, Eppendorf, Hamburg, Germany) and appropriately diluted with distilled water.

### **3.1.4. Operation of photobioreactor**

The indoor PBR was a 1 L round glass vessel which was continuously illuminated with external LED light sources mounted on two opposite sides of the PBR. The light intensity on the vessel wall of the PBR was adjusted to ca. 200  $\mu\text{mol}/\text{m}^2/\text{s}$  using LightScout quantum light meter (Spectrum Technologies, Inc., Aurora, Illinois, USA). For light intensities of 750  $\mu\text{mol}/\text{m}^2/\text{s}$  and below, 18W T5 LEDs (Ledeon, OEM, China) were used. For light intensities between 750 to 1000  $\mu\text{mol}/\text{m}^2/\text{s}$ , 36W T8 LEDs (Kwan Shing Electrical Marketing (M) Sdn. Bhd., Kepong, Kuala Lumpur, Malaysia) were used instead. The microalgae were pre-cultured and inoculated into the PBR with an inoculum size of 0.06 g/L. The microalgae were grown at room temperature of 24 – 26°C and an agitation speed of 300 rpm. Air was filtered (0.45  $\mu\text{m}$ ) and mixed with CO<sub>2</sub> to give a CO<sub>2</sub> concentration of 2.5%. The culture broth was aerated continuously at a rate of 0.1 vvm. All cultures were done in batch condition and all experiments were done in duplicates.

During cultivation, the initial pH was around 7.0 for BG-11 medium and 6.3 for Basal medium. The pH was continuously monitored during cultivation period. It was observed that the pH for both media increased steadily and became stable when the microalgae entered exponential phase (1.5 – 4.0 days). The stable pH for BG-11 medium was 7.8 – 8.0, and Basal medium was 7.6 – 7.8.

### **3.1.5. Preparation of different initial nitrate concentrations**

Four different initial nitrate concentrations (100%, 75%, 50%, and 25%) were tested to observe their effects on biomass and protein productions of *Chlorella sorokiniana* CY1 and *Chlorella vulgaris* ESP-31. The different nitrate concentrations were prepared by adding the appropriate amounts of NaNO<sub>3</sub> in BG-11 medium (100% was 1.500 g/L, 75% was 1.125 g/L, 50% was 0.750 g/L, and 25% was 0.375 g/L) and KNO<sub>3</sub> in Basal medium (100% was 1.2500 g/L, 75% was 0.9375 g/L, 50% was 0.6250 g/L, and 25% was 0.3125 g/L).

### **3.1.6. Preparation of different CO<sub>2</sub> concentrations**

Four different CO<sub>2</sub> concentrations were selected (1.25%, 2.5%, 5%, and 7.5% CO<sub>2</sub> in air) to find out their effects on the biomass and protein productions of *Chlorella sorokiniana* CY1 and *Chlorella vulgaris* ESP-31. A CO<sub>2</sub> concentration of 2.5% was taken as the initial amount as many microalgae species had shown optimum CO<sub>2</sub> concentration around or above 2% CO<sub>2</sub> (Cheah et al., 2015; Chen et al., 2015; Tan et al., 2016).

### **3.1.7. Preparation of different light intensities**

Five different light intensities were chosen for this study, 100, 200, 400, 600, and 750  $\mu\text{mol}/\text{m}^2/\text{s}$ . The light intensity on the reactor wall was measured with LightScout quantum light meter (Spectrum Technologies, Inc., Aurora, Illinois, USA). A light intensity of 200  $\mu\text{mol}/\text{m}^2/\text{s}$  was chosen as the initial amount as many microalgae species had shown optimum light intensity in the range of 30 – 400  $\mu\text{mol}/\text{m}^2/\text{s}$  (Singh and Singh, 2015; Tan et al., 2016).

### **3.1.8. Preparation of microalgal biomass for protein determination**

The protein content of the culture was determined using a modified version of a small-scale method developed by Slocombe et al. (Slocombe et al., 2013). 0.4 mL of 24% (w/v) trichloroacetic acid (TCA) was added to 10 mg of freeze-dried

microalgae biomass. The samples were vortexed, incubated at 95°C water bath for 15 min, and allowed to cool to room temperature. 1.2 mL of ultrapure water was then added to the samples in order to reduce the concentration of TCA to 6% (w/v). The samples underwent centrifugation at 6000 rpm for 20 min (Centrifuge 5430, Eppendorf, Hamburg, Germany), where the supernatants were discarded and the remaining pellets were re-suspended in 1 mL of Lowry Reagent D. After that, the samples were incubated at 55°C for 3 h, and centrifuged at 6k rpm for 20 min. The supernatants were retained and can be stored in -20°C freezer for analysis at a later time.

### **3.1.9. Determination of protein content by Lowry assay**

The protein quantification method used in this study is a modified version of Lowry assay (Lowry et al., 1951) developed by Price (Price, 1965). There are 5 reagents needed for Lowry assay. The first 3 reagents, namely Lowry Reagent A (2% (w/v) Na<sub>2</sub>CO<sub>3</sub> (anhydrous) in 0.1 N NaOH), Lowry Reagent B (1% (w/v) NaK Tartrate tetrahydrate), and Lowry Reagent C (0.5% (w/v) CuSO<sub>4</sub>.5H<sub>2</sub>O in H<sub>2</sub>O) can be stored at room temperature. Lowry Reagent D is made up daily using Lowry Reagents A, B, and C in the ratio 48:1:1. Lowry Reagent E is also made up daily using Folin-Ciocalteu phenol reagent and ultrapure H<sub>2</sub>O in the ratio 1:1.

1900 µL of Lowry Reagent D were added to 100 µL of the treated samples and mixed immediately by inversion. After incubation at room temperature for 10 min, 0.2 mL of Lowry Reagent E were added to the samples, followed by vortexing. The samples were incubated for another 30 min, and their absorbance values were measured at a wavelength of 600 nm (OD<sub>600</sub>). The absorbance values were converted into protein content via a calibration curve between OD<sub>600</sub> and protein mass (µg).

### 3.1.10. Determination of microalgal biomass and protein productivities

The biomass and protein productivities of both microalgal species were calculated using the following equation. The harvesting of microalgal biomass was divided into two types. If nitrogen starvation was achieved, the culture was harvested on the day of nitrogen starvation. If nitrogen starvation was not achieved, the culture was harvested upon reaching stationary phase.

$$Productivity = \frac{x_2 - x_1}{y_2 - y_1} \quad (1)$$

$x_1$  = biomass/protein concentration at start of exponential phase

$x_2$  = biomass/protein concentration at harvest or stationary phase

$y_1$  = time (d) at start of exponential phase

$y_2$  = time (d) at harvest or stationary phase

### 3.1.11. Statistical analysis

The experimental results presented in this study were mean values of three independent cultures for each parameter. One-way analysis of variance (ANOVA) and Tukey's test were used to determine the significance of the investigated parameters on biomass and protein production of *Chlorella sorokiniana* CY1 and *Chlorella vulgaris* ESP-31. All statistical analyses were performed using Microsoft Excel.

## 3.2. Study 2

Study 2 explored the strategies to enhance lipid production from five different microalgal species, which were *Chlamydomonas* sp. Tai-01, Tai-03, and Pin-01 as well as *Scenedesmus* sp. ESP-05 and ESP-07. The performance of all five microalgal species were evaluated by culturing in three different media. The best combination of microalgae and medium were selected and optimised for maximal lipid production under three parameters, which included initial nitrate concentration,

light intensity, and initial cell concentration. After harvesting, the microalgal biomass underwent transesterification process (Lepage and Roy method) to break up the long-chain lipid molecules inside the microalgal cells into short-chain fatty acids (also known as fatty acid methyl esters (FAME)). The FAME was analysed using gas chromatography-mass spectrophotometry (GCMS) and the lipid content was calculated. One-way ANOVA was also used to determine whether the investigated parameter resulted in significant improvement in the biomass and lipid productivities of the microalgal species.

### 3.2.1. Microalgae strain and medium composition

The 5 microalgal strains used in this study were isolated from Taiwan. The microalgae were identified as *Chlamydomonas* sp. Tai-01, Tai-03 and Pin-01, followed by *Scenedesmus* sp. ESP-05 and ESP-07. The identities of the above microalgal strains were determined via 18S rDNA sequence alignment. The 18S rDNA sequences of each strain contained 1050 base pairs and were amplified by polymerase chain reaction (PCR) using the primers NS1 (GTA GTC ATA TGC TTG TCT C) and NS4 (CTT CCG TCA ATT CCT TTA AG). The phylogenetic trees of the 5 strains were drawn using the genetics analytical software MEGA6 (Molecular Evolutionary Genetics Analysis version 6.0) and illustrated in Figure 10.

The 3 media used to culture the microalgal strains were BG-11 medium, Basal medium and Bold's Basal medium (BBM). The composition of BG-11 medium is (g/L): NaNO<sub>3</sub>, 1.5; K<sub>2</sub>HPO<sub>4</sub>, 0.03; MgSO<sub>4</sub>.7H<sub>2</sub>O, 0.075; Citric acid anhydrous, 0.006; Na<sub>2</sub>CO<sub>3</sub>, 0.02, CaCl<sub>2</sub>.2H<sub>2</sub>O, 0.036; Ammonium iron(III) citrate, 0.006; EDTA.2Na, 0.001; H<sub>3</sub>BO<sub>3</sub>, 0.00286; MnCl<sub>2</sub>.4H<sub>2</sub>O, 0.00181; ZnSO<sub>4</sub>.7H<sub>2</sub>O, 0.000222; Na<sub>2</sub>MoO<sub>4</sub>.2H<sub>2</sub>O, 0.00039; CuSO<sub>4</sub>.5H<sub>2</sub>O, 0.000079; Co(NO<sub>3</sub>)<sub>2</sub>.6H<sub>2</sub>O, 0.000049.

The composition of Basal medium is (g/L): KNO<sub>3</sub>, 1.25; KH<sub>2</sub>PO<sub>4</sub>, 1.25; MgSO<sub>4</sub>.7H<sub>2</sub>O, 1; CaCl<sub>2</sub>.2H<sub>2</sub>O, 0.1106; FeSO<sub>4</sub>.7H<sub>2</sub>O, 0.0498; EDTA.2Na, 0.5; H<sub>3</sub>BO<sub>3</sub>, 0.1142; ZnSO<sub>4</sub>.7H<sub>2</sub>O, 0.0882; MnCl<sub>2</sub>.4H<sub>2</sub>O, 0.0144; Na<sub>2</sub>MoO<sub>4</sub>.2H<sub>2</sub>O, 0.0119; CuSO<sub>4</sub>.5H<sub>2</sub>O, 0.0157; Co(NO<sub>3</sub>)<sub>2</sub>.6H<sub>2</sub>O, 0.0049.



The composition of BBM is (g/L): K<sub>2</sub>HPO<sub>4</sub>, 0.075; KH<sub>2</sub>PO<sub>4</sub>, 0.175; NaNO<sub>3</sub>, 0.25; NaCl, 0.025; MgSO<sub>4</sub>·7H<sub>2</sub>O, 0.075; CaCl<sub>2</sub>·2H<sub>2</sub>O, 0.025; EDTA, 0.05; KOH, 0.031; FeSO<sub>4</sub>·7H<sub>2</sub>O, 0.00498; H<sub>2</sub>SO<sub>4</sub>, 0.001; H<sub>3</sub>BO<sub>3</sub>, 0.01142; ZnSO<sub>4</sub>·7H<sub>2</sub>O, 0.001412; MnCl<sub>2</sub>·4H<sub>2</sub>O, 0.000232; CuSO<sub>4</sub>·5H<sub>2</sub>O, 0.000252; Co(NO<sub>3</sub>)<sub>2</sub>·6H<sub>2</sub>O, 0.00008; Na<sub>2</sub>MoO<sub>4</sub>·2H<sub>2</sub>O, 0.000192.

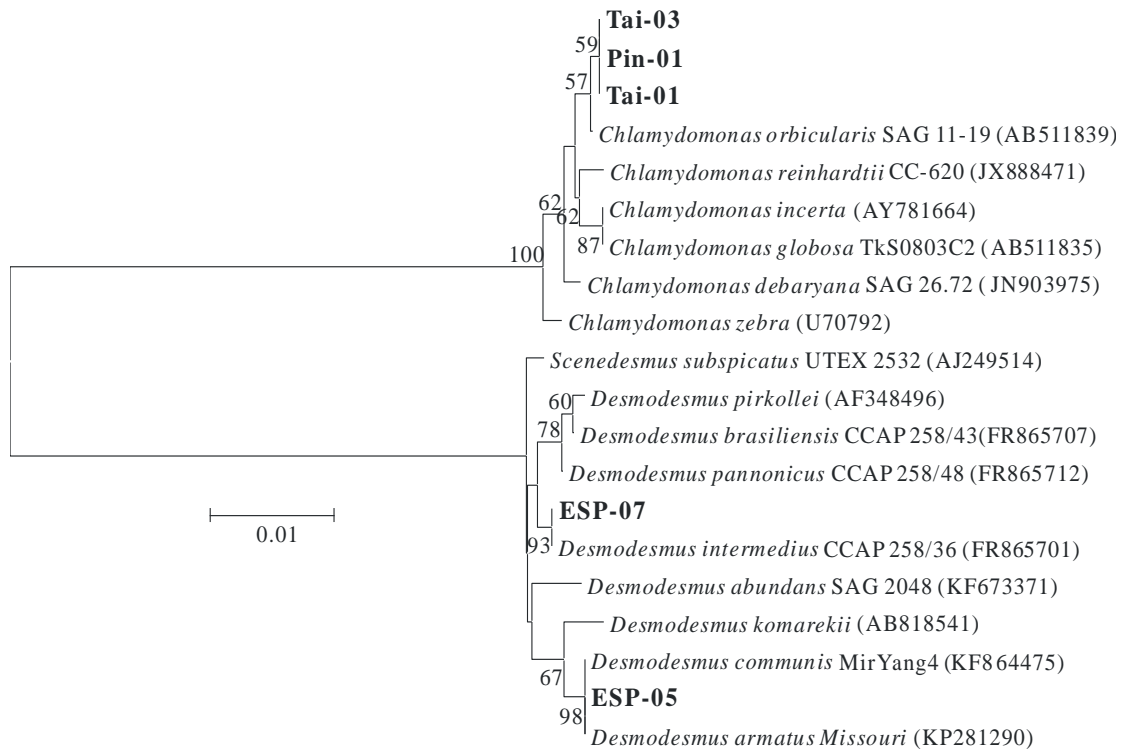


Figure 10 - The phylogenetic tree of 5 isolated microalgal strains

### 3.2.2. Determination of microalgae cell concentration

The cell concentration of the culture in the photobioreactor was determined regularly by optical density measurement at a wavelength of 688 nm (OD<sub>688</sub>) using a spectrophotometer (model U-2001, Hitachi, Tokyo, Japan) after proper dilution with deionized water. The dry cell weight of the microalgae biomass was obtained by filtering 10 ml aliquots of culture through a cellulose acetate membrane filter (0.45 µm pore size, 47 mm in diameter). Each loaded filter was dried at 105°C until the weight was invariant. The dry weight of the blank filter was subtracted from that of the loaded filter to obtain the microalgae dry cell weight (DCW). The

OD<sub>688</sub> values were converted to biomass concentration via calibration between OD<sub>688</sub> and dry cell weight.

### **3.2.3. Determination of medium nitrate concentration**

The medium nitrate concentration of the culture in the photobioreactor was determined regularly by optical density measurement at a wavelength of 220 nm (OD<sub>220</sub>) using a spectrophotometer (model U-2001, Hitachi, Tokyo, Japan) after proper dilution with deionized water (Collos et al., 1999). The microalgae samples were centrifuged and the supernatant was tested in the spectrophotometer. The OD<sub>220</sub> values were converted to nitrate concentration via calibration between OD<sub>220</sub> and nitrate concentration.

### **3.2.4. Determination of light intensity**

The light intensity on the reactor wall was measured with an LI-250 light meter with a LI-190SA quantum sensor (LI-COR, Inc., Lincoln, Nebraska, USA). This light meter gives a unit of  $\mu\text{mol}/\text{m}^2/\text{s}$  for the measured light intensity.

### **3.2.5. Determination of oil/lipid content**

After appropriate cell growth, the microalgae cells were harvested from the culture broth by centrifugation (9000 rpm for 10 min). The cells were washed twice with deionized water, lyophilized, and weighed. The lipid composition was determined as fatty acid methyl esters (FAMES) through the direct transesterification method described by Lepage and Roy (Lepage and Roy, 1984). The sample was analysed by gas chromatography (GC-2014, Shimadzu, Kyoto, Japan) equipped with a flame ionization detector (FID). Samples were injected into a 30 m long capillary column (Type no. 260M143P, Thermo Fisher Scientific, Waltham, MA, USA) with an internal diameter of 0.32 mm. Helium was used as the carrier gas, with a flow rate of 1.3 ml/min. The temperatures of the injector and detector were set at 250 and 280°C, respectively. The oven temperature was initially set at 110°C, increased from 150

to 180°C at a rate of 10°C/min, 180 to 220°C at a rate of 1.5°C/min, 220 to 260°C at a rate of 30°C/min and held at 260°C for 5 min.

### **3.2.6. Operation of photobioreactor**

The indoor PBR was a 1L round glass vessel which was continuously illuminated with external LED light sources (DanceLight, Jan Cheng Lighting Co. Ltd., Taiwan) mounted on two opposite sides of the PBR. The microalgae were grown at room temperature of 24–26°C and an agitation speed of 300 rpm. The light intensity on the vessel wall of the PBR was adjusted to ca. 200  $\mu\text{mol}/\text{m}^2/\text{s}$  using a LI-250 light meter with a LI-190SA pyranometer sensor (LI-COR, Inc., Lincoln, Nebraska, USA). The microalgae were pre-cultured and inoculated into the PBR with an inoculum size of 0.06 g/L. Air was filtered (0.22  $\mu\text{m}$ ) and mixed with CO<sub>2</sub> to give a CO<sub>2</sub> concentration of 2.0%. The culture broth was aerated continuously at a rate of 200 mL min<sup>-1</sup> (0.2 vvm, volume gas per volume media per min). LED was chosen as the external light source because LED consumes less electricity and has uniform light intensity across the length of the light tube compared to fluorescent lamps (Chen et al., 2011). CO<sub>2</sub> gas was chosen to imitate the utilisation of flue gases from industries for mass culture of microalgae. All cultures were done in batch condition and all experiments were done in duplicates.

During cultivation, the initial pH for BG-11 medium was 7.0, Basal medium was 6.3, and BBM was 6.40. The pH was continuously monitored during cultivation period. It was observed that the pH for all 3 media increased steadily and became stable when the microalgae entered exponential phase (1.5 – 4.0 days). The stable pH for BG-11 medium was 8.0–8.2, Basal medium was 7.6 – 7.8, and BBM was 7.3 – 7.5.

All the microalgal biomass was harvested for analysis after entering nitrogen starvation for 2, 4, 6, and 8 days. The highest lipid content occurred at 4 or 6 days after nitrogen starvation for all species. If nitrogen starvation did not occur, all the biomass was harvested when the microalgae enters stationary phase (9 – 14 days).

### **3.2.7. Adjustment of initial nitrate concentration**

The initial nitrate concentrations of BG-11 medium and Basal medium were adjusted to improve the microalgal cell growth and lipid production. 5 different initial nitrate concentrations were used for BG-11 medium (100%, 75%, 50%, 25%, and 12.5%), and they were prepared by adding 1.5000, 1.125, 0.7500, 0.3750, and 0.1875 g/L of NaNO<sub>3</sub>). On the other hand, 4 different initial nitrate concentrations were used for Basal medium (100%, 75%, 50%, and 25%), which were prepared by adding (1.2500, 0.9375, 0.6250, and 0.3125 g/L of KNO<sub>3</sub>).

### **3.2.8. Statistical analysis**

Design Expert 7.0 software (Stat-Ease, Inc., Minneapolis, MN, USA) was used to analyse the experimental results. In this study, one factor response surface methodology was used to evaluate the results. The effects of different parameters on the results were determined by analysis of variance (ANOVA) study. In the case where the difference between specific data points was unclear, Student's t-test was also used to distinguish between the data points.

## **3.3. Study 3**

Study 3 continued to optimise the selected microalgal species from Study 2, which was *Chlamydomonas* sp. Tai-03, using three new parameters. They were CO<sub>2</sub> concentration, organic carbon concentration, and medium replacement ratio. After harvesting, the microalgal biomass underwent transesterification process (Lepage and Roy method) to break up the long-chain lipid molecules inside the microalgal cells into short-chain fatty acids (also known as fatty acid methyl esters (FAME)). The FAME was analysed using gas chromatography-mass spectrophotometry (GCMS) and the lipid content was calculated. One-way ANOVA was also used to determine whether the investigated parameter resulted in significant improvement in the biomass and lipid productivities of the microalgal species.

### **3.3.1. Microalga strain, medium composition, and culture conditions**

The microalgal species used in this study is *Chlamydomonas* sp. Tai-03, identical to the strain used in Study 2. This species was isolated in Taiwan, and was obtained from National Cheng Kung University (NCKU). The medium chosen to culture the microalga was BG-11 medium, which has a chemical composition (in g/L) of: NaNO<sub>3</sub>, 1.5; K<sub>2</sub>HPO<sub>4</sub>, 0.03; MgSO<sub>4</sub>·7H<sub>2</sub>O, 0.075; Citric acid anhydrous, 0.006; Na<sub>2</sub>CO<sub>3</sub>, 0.02, CaCl<sub>2</sub>·2H<sub>2</sub>O, 0.036; Ammonium iron(III) citrate, 0.006; EDTA·2Na, 0.001; H<sub>3</sub>BO<sub>3</sub>, 0.00286; MnCl<sub>2</sub>·4H<sub>2</sub>O, 0.00181; ZnSO<sub>4</sub>·7H<sub>2</sub>O, 0.000222; Na<sub>2</sub>MoO<sub>4</sub>·2H<sub>2</sub>O, 0.00039; CuSO<sub>4</sub>·5H<sub>2</sub>O, 0.000079; Co(NO<sub>3</sub>)<sub>2</sub>·6H<sub>2</sub>O, 0.000049.

The optimal culture conditions for maximal lipid production in *Chlamydomonas* sp. Tai-03 had been determined by Study 2, and the conditions were: BG-11 medium with 25% initial nitrate concentration (0.375 g/L NaNO<sub>3</sub>), 200 μmol/m<sup>2</sup>/s light intensity, 0.12 g/L initial cell concentration, 300 rpm continuous stirring, and continuous sparging of 2.5% CO<sub>2</sub> gas at a flow rate of 0.2 vvm.

### **3.3.2. Determination of microalgae cell concentration**

The microalgae cell concentration in the PBR was determined daily via OD<sub>680</sub> using a spectrophotometer (UV-1800, Shimadzu, Kyoto, Japan) after appropriate dilution with distilled water. The DCW of the microalgal biomass was obtained by drying 5 ml of the culture in a weighing moisture analyser (ML-50, A&D Company, Limited, Tokyo, Japan). The dry weight of the biomass was determined using an electronic balance and converted to biomass concentration via calibration between OD<sub>680</sub> and DCW.

### **3.3.3. Determination of medium nitrate concentration**

The nitrate concentration of the culture was determined daily via optical density measurement at a wavelength of 220 nm using a spectrophotometer (UV-1800, Shimadzu, Kyoto, Japan) (Collos et al., 1999). Before measurement, the samples

were centrifuged at 6000 rpm for 5 min (Centrifuge 5430, Eppendorf, Hamburg, Germany) and appropriately diluted with distilled water.

#### **3.3.4. Determination of light intensity**

The light intensity on the reactor wall was measured with LightScout quantum light meter (Spectrum Technologies, Inc., Aurora, Illinois, USA). This light meter gives a unit of  $\mu\text{mol}/\text{m}^2/\text{s}$  for the measured light intensity.

#### **3.3.5. Determination of oil/lipid content**

After appropriate cell growth, the microalgae cells were harvested from the culture broth by centrifugation (9000 rpm for 10 min). The cells were washed twice with deionized water, lyophilized, and weighed. The lipid composition was determined as fatty acid methyl esters (FAMES) through the direct transesterification method described by Lepage and Roy (Lepage and Roy, 1984). The sample was analysed by gas chromatography (GC-2014, Shimadzu, Kyoto, Japan) equipped with a flame ionization detector (FID). Samples were injected into a 30 m long capillary column (Type no. 260M143P, Thermo Fisher Scientific, Waltham, MA, USA) with an internal diameter of 0.32 mm. Helium was used as the carrier gas, with a flow rate of 1.3 ml/min. The temperatures of the injector and detector were set at 250 and 280°C, respectively. The oven temperature was initially set at 110°C, increased from 150 to 180°C at a rate of 10°C/min, 180 to 220°C at a rate of 1.5°C/min, 220 to 260°C at a rate of 30°C/min and held at 260°C for 5 min.

#### **3.3.6. Operation of photobioreactor**

The indoor PBR was a 1 L round glass vessel which was continuously illuminated with external LED light sources mounted on two opposite sides of the PBR. The light intensity on the vessel wall of the PBR was adjusted to ca. 200  $\mu\text{mol}/\text{m}^2/\text{s}$  using LightScout quantum light meter (Spectrum Technologies, Inc., Aurora, Illinois, USA). For light intensities of 750  $\mu\text{mol}/\text{m}^2/\text{s}$  and below, 18W T5 LEDs (Ledeon, OEM,

China) were used. For light intensities between 750 to 1000  $\mu\text{mol}/\text{m}^2/\text{s}$ , 36W T8 LEDs (Kwan Shing Electrical Marketing (M) Sdn. Bhd., Kepong, Kuala Lumpur, Malaysia) were used instead. The microalgae were pre-cultured and inoculated into the PBR with an inoculum size of 0.06 g/L. The microalgae were grown at room temperature of 24 – 26°C and an agitation speed of 300 rpm. Air was filtered (0.45  $\mu\text{m}$ ) and mixed with  $\text{CO}_2$  to give a  $\text{CO}_2$  concentration of 2.5%. The culture broth was aerated continuously at a rate of 0.1 vvm. All cultures were done in batch condition and all experiments were done in duplicates.

During cultivation, the initial pH was around 7.0 for BG-11 medium and 6.3 for Basal medium. The pH was continuously monitored during cultivation period. It was observed that the pH for both media increased steadily and became stable when the microalgae entered exponential phase (1.5 – 4.0 days). The stable pH for BG-11 medium was 7.8 – 8.0, and Basal medium was 7.6 – 7.8.

### 3.3.7. Addition of organic carbon sources

The five OCs used in this study were glucose (Glu), sucrose (Su), glycerol (Gly), acetate (Ac) from sodium acetate, and fructose (Fru). The initial OC concentrations were calculated based on the molecular weight (MW) ratio of each OC molecule to their respective carbon molecules, and the unit was gram(s) of carbon per litre of culture (g C/L), as shown in Table 2.

Table 2 - The concentrations of different organic carbons (OCs) used in Study 2

OC	MW <sup>a</sup> (g/mol)	Mass of OC (g) for 1 g C/L <sup>b</sup>
Glu	180	2.500
Su	342	2.375
Gly	180	2.500
Ac	92	2.556
Fru	82	3.417

<sup>a</sup> = Molecular weight, <sup>b</sup> = gram(s) of carbon equivalent per litre of culture

### **3.3.8. Operation of semi-batch culture with medium replacement**

Upon reaching the intended day of harvest, the photobioreactors and fresh media were put into a horizontal laminar flow cabinet equipped with ultraviolet (UV) light (AHC-5A1, Esco Micro Pte. Ltd., Singapore), and a medium replacement was carried out. A portion (in this case 25%, 50%, or 75%) of the cultures were harvested, and the remaining cultures were topped up to the starting volume (1 L) with fresh media.

### **3.3.9. Statistical analysis**

All experimental results presented in this study were mean values of two independent cultures for each parameter together with sample standard deviation calculated using Microsoft Excel. Analysis of variance (ANOVA) was used to determine the significance of the effects of different parameters on biomass and lipid production of *Chlamydomonas* sp. Tai-03. Design Expert 7.0 software (Stat-Ease, Inc., Minneapolis, MN, USA) was used to perform the ANOVA studies.

## **3.4. Study 4**

Study 4 focused on designing a new semi-closed thin layer cascade PBR that would be suitable for the culture of all three microalgal species tested in Studies 1 – 3. The dimensions of the basic PBR design was calculated in Microsoft Excel. The computational fluid dynamics (CFD) software (ANSYS CFX) was then used to more properly visualise the fluid flow patterns in the initial concept of the PBR.

### **3.4.1. Design of photobioreactor**

The calculations involved in the design of semi-closed TLC PBR was carried out in Microsoft Excel. The drawings of the design were done in Microsoft Visio.



### 3.4.2. Simulation of photobioreactor

The design of semi-closed TLC PBR was simulated in a computational fluid dynamics program to study the behaviours of fluid flow and mixing patterns of the microalgal culture. The CFD program used was ANSYS CFX version 18.1 software (ANSYS, Inc., Canonsburg, Pennsylvania, USA).

### 3.4.3. Governing equations in ANSYS CFX

#### 3.4.3.1. Transport Equations

ANSYS CFX uses a series of mathematical equations to model fluid flow, heat, and mass transfer for single-phase, multiphase, and multi-component flow without combustion or radiation. One of the most important set of equations in CFD are transport equations. There are four transport equations, as shown below.

##### a. The Continuity Equation

$$\frac{\partial \rho}{\partial t} + \nabla \cdot (\rho U) = 0 \quad (2)$$

Where  $\rho$  is density,  $t$  is time, and  $U$  is velocity vector

##### b. The Momentum Equations

$$\frac{\partial(\rho U)}{\partial t} + \nabla \cdot (\rho U \otimes U) = -\nabla p + \nabla \cdot \tau + S_M \quad (3)$$

Where  $\otimes$  is tensor product,  $\tau$  is stress tensor, and  $S_M$  is the sum of body forces

The stress tensor,  $\tau$ , is related to the strain rate by:

$$\tau = \mu(\nabla U + (\nabla U)^T - \frac{2}{3}\delta \nabla \cdot U) \quad (4)$$

Where  $\mu$  is viscosity,  $T$  is temperature

c. The Total Energy Equation

$$\frac{\partial(\rho h_{tot})}{\partial t} - \frac{\partial p}{\partial t} + \nabla \cdot (\rho U h_{tot}) = \nabla \cdot (\lambda \nabla T) + \nabla \cdot (U \cdot \tau) + U \cdot S_M + S_E \quad (5)$$

Where  $\lambda$  is thermal conductivity,  $S_E$  is energy source,

And  $h_{tot}$  is the total enthalpy, related to the static enthalpy  $h(T, p)$  by:

$$h_{tot} = h + \frac{1}{2} U^2 \quad (6)$$

d. The Thermal Energy Equation

$$\frac{\partial(\rho h)}{\partial t} - \frac{\partial p}{\partial t} + \nabla \cdot (\rho U h) = \nabla \cdot (\lambda \nabla T) + U \cdot \nabla p + \tau : \nabla U + S_E \quad (7)$$

**3.4.3.2. Buoyancy**

When calculating buoyancy, the following source term is added to the momentum equation.

$$S_{M,buoy} = (\rho - \rho_{ref})g \quad (8)$$

Where  $\rho_{ref}$  is reference density and  $g$  is gravitational constant

**3.4.3.3. The Homogeneous Model**

When selecting the homogeneous model for multiphase flow, all fluids share a common flow field and other relevant fields like temperature and turbulence. This simplifies some parts of the multi-fluid model which results in the homogeneous model. The bulk transport equation in the homogeneous model can be represented:

$$\frac{\partial}{\partial t}(\rho \varphi) + \nabla \cdot (\rho U \varphi - \Gamma \nabla \varphi) = S \quad (9)$$

Where:

$$\rho = \sum_{\alpha=1}^{N_p} r_{\alpha} \rho_{\alpha} \quad (10)$$

$$U = \frac{1}{\rho} \sum_{\alpha=1}^{N_p} r_{\alpha} \rho_{\alpha} U_{\alpha}$$

$$\Gamma = \sum_{\alpha=1}^{N_p} r_{\alpha} \Gamma_{\alpha}$$

Where  $\varphi$  is general scalar variable,  $\Gamma$  is diffusivity,  $r$  is location vector,  $S$  is mass flow rate, and  $\alpha$  is a subscript to denote that the quantity applies to phase  $\alpha$

#### 3.4.3.4. The $k$ -epsilon Turbulence Model

The term  $k$  refers to the turbulence kinetic energy and is represented as the variance of the fluctuations in velocity.  $k$  has units of (Length<sup>2</sup> Time<sup>-2</sup>) The term epsilon ( $\varepsilon$ ) refers to the turbulence eddy dissipation or the rate at which the velocity fluctuations dissipate.  $\varepsilon$  has units of  $k$  per unit time (Length<sup>2</sup> Time<sup>-3</sup>). The  $k$ - $\varepsilon$  model presents two new variables into the system, which then changes the continuity equation to:

$$\frac{\partial \rho}{\partial t} + \frac{\partial}{\partial x_j} (\rho U_j) = 0 \quad (11)$$

Which then changes the momentum equation to:

$$\frac{\partial \rho U_i}{\partial t} + \frac{\partial}{\partial x_j} (\rho U_i U_j) = -\frac{\partial p'}{\partial x_i} + \frac{\partial}{\partial x_j} \left[ \mu_{eff} \left( \frac{\partial U_i}{\partial x_j} + \frac{\partial U_j}{\partial x_i} \right) \right] + S_M \quad (12)$$

Where  $\mu_{eff}$  is effective viscosity causing the turbulence and represented by:

$$\mu_{eff} = \mu + \mu_t \quad (13)$$

Where  $\mu_t$  is turbulence viscosity and assumed to be linked to the turbulence kinetic energy and dissipation by:

$$\mu_t = C_{\mu} \rho \frac{k^2}{\varepsilon} \quad (14)$$

Where  $C_{\mu}$  is a constant

And  $p'$  is modified pressure as defined by:

$$p' = p + \frac{2}{3}\rho k + \frac{2}{3}\mu_{eff} \frac{\partial U_k}{\partial x_k} \quad (15)$$

### 3.4.3.5. Mesh Adaption

In ANSYS CFX, the mesh adaption function selectively refines the mesh in regions that depend on the adaption criteria specified. The mesh adaption process can occur up to the number of times specified by the user in a single run. As the solution is being calculated, the mesh can be automatically refined in regions where the solution variables are changing most rapidly, in order to resolve the characteristics of the flow those regions. When the adaption criteria method is set as "Solution Variation", then the adaption criteria ( $A_i$ ) for a particular mesh edge  $i$  of length  $l_i$  is defined by:

$$A_i = \sum_j \frac{|\Delta\varphi_{ji}|}{N_{\varphi_j} |\Delta\varphi_j|} \quad (16)$$

Where  $\Delta\varphi_j$  is the global range of the scalar variable  $\varphi_j$  over all of the nodes (except those on wall boundary conditions in turbulent flow),  $\Delta\varphi_{ji}$  is the difference between  $\varphi_j$  at one end of the edge and the other end, and  $N_{\varphi_j}$  is a scalar for adaption variable  $j$  to scale all the  $A_i$  to obtain values between 0 and 1

# CHAPTER 4

## RESULTS AND DISCUSSION

In this chapter, the experimental results of four different studies (presented as Study 1 – 4) were analysed and elaborated in detail. The four studies were performed in the hopes of fulfilling the aims of this research as outlined in Section 1.2 above. In each study, the aim and objectives were clarified before continuing with the representation and explanation of the experimental data. Section 4.1 (Study 1) investigated the protein content and protein productivity of two microalgal species, *Chlorella sorokiniana* CY1 and *Chlorella vulgaris* ESP-31. Three parameters were investigated and optimised for both microalgal species, which were different medium and initial nitrate concentration, CO<sub>2</sub> concentration, and light intensity. Apart from testing the protein production capabilities of microalgae, the second microalgae-derived metabolite chosen for investigation was lipid. Hence, Section 4.2 (Study 2) explored the strategies to enhance lipid production from five different microalgal species, which were *Chlamydomonas* sp. Tai-01, Tai-03, and Pin-01 as well as *Scenedesmus* sp. ESP-05 and ESP-07. The performance of all five microalgal species were evaluated by culturing in three different media. The best combination of microalgae and medium were selected and optimised for maximal lipid production under three parameters, which included initial nitrate concentration, light intensity, and initial cell concentration. Section 4.3 (Study 3) continued to optimise the selected microalgal species from Study 2, which was *Chlamydomonas* sp. Tai-03, using three new parameters. They were CO<sub>2</sub> concentration, organic carbon concentration, and medium replacement ratio. Section 4.4 (Study 4) focused on designing a new semi-closed thin layer cascade PBR that would be

suitable for the culture of all three microalgal species tested in Studies 1 – 3. The basic design of the PBR was first explained, followed by the use of computational fluid dynamics software (ANSYS CFX) to more properly visualise the fluid flow patterns in the upper and lower cascade portion of the PBR.

#### **4.1. Study 1 - Investigation of the performance of *Chlorella sorokiniana* CY1 and *Chlorella vulgaris* ESP-31 in protein production**

##### **4.1.1. Aim and objectives of study**

In this study, our aim is to optimise 2 microalgal species, *Chlorella sorokiniana* CY1 and *Chlorella vulgaris* ESP-31, for protein production. An investigation will be performed to find the suitable combination of culture medium and initial medium nitrate concentration, followed by the effects of different concentrations of CO<sub>2</sub> gas and different levels of light intensity on the biomass and protein growths of both microalgal species.

##### **4.1.2. Growth curves of microalgal species**

Figure 11 shows the growth curves of *Chlorella sorokiniana* CY1 and *Chlorella vulgaris* ESP-31 under increasingly optimized conditions investigated in this study. Only the growth curves of both species under the three increasingly optimized conditions were shown in Figure 11 because the overlapping nature of the growth curves in each experiment group would give a confusing graphical representation. In Figure 11, it was found that the lag phase for both species in all three culture conditions were 0.5 d. The protein contents in all cases were also observed to increase until the day nitrogen starvation began, and then decreased as the culture remained in nitrogen starvation phase. This phenomenon coincided with other studies, where proteins were diverted into the creation and storage of

carbohydrates and lipids in microalgae during nitrogen starvation phase (Chen et al., 2015; Ho et al., 2012).

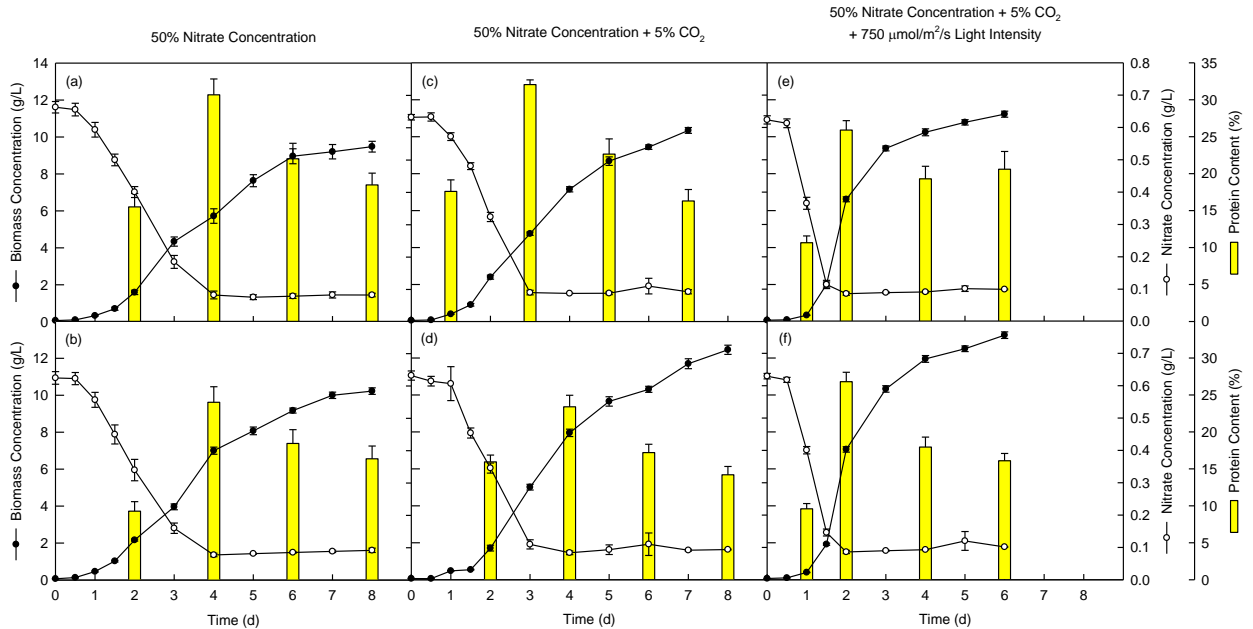


Figure 11 - Biomass concentration, nitrate concentration, and protein content evolution of *Chlorella sorokiniana* CY1 (a, c, e) and *Chlorella vulgaris* ESP-31 (b, d, f). All growth graphs were from optimized conditions in each optimization step. Both species become increasingly optimized when viewed vertically from left to right.

#### 4.1.3. Effects of different medium and initial nitrate concentrations on microalgal biomass and protein productions

The element nitrogen is one of the basic building blocks necessary for microalgal cells to live and function. Nitrogen is involved in the synthesis of nucleic acids, amino acids, proteins, enzymes, and chlorophyll in the microalgal cells. Despite the importance of nitrogen, it is still essential to optimize the nitrate concentration of culture media in order to be cost-effective and to achieve a balance between high-biomass-concentration and high-protein-content in the harvested biomass (Pancha et al., 2014).

In Figure 12, there are five parameters with their cultivation time marked red, signifying cultures that did not reach nitrogen starvation phase. These cultures

were harvested during stationary phase. The cultivation time marked black represented cultures that were harvested on the day nitrogen starvation began. In Figure 12a, the biomass concentrations of both *Chlorella sorokiniana* CY1 and *Chlorella vulgaris* ESP-31 followed a general trend where the harvested biomass reduced with decreasing initial nitrate concentration. This was because reducing the initial nitrate concentration shortened the cultivation time required for the cultures to enter nitrogen starvation phase. The shorter cultivation time yielded lower biomass concentrations but higher biomass productivities. In Figure 12b, the protein contents for all parameters in both microalgal species vary between 20 – 27% DCW. There were no significant differences in the protein contents of both *Chlorella sorokiniana* CY1 and *Chlorella vulgaris* ESP-31 when cultured in BG-11 medium ( $p > 0.05$ ) or Basal medium ( $p > 0.05$ ). Despite this, the protein contents of *Chlorella sorokiniana* CY1 in 50% and 25% Basal medium demonstrated an increase of 11.8% and 9.6% compared to 75% Basal medium. This increment could be due to the shorter cultivation times in 50% and 25% Basal medium, where the biomass was harvested before the microalgal cells could perform further multiply. Through the study of *Nannochloropsis gaditana*, Fábregas et al. (2002) showed that cell division in *Nannochloropsis gaditana* occurred during dark cycles, with lipids being preferentially converted to energy followed by carbohydrates via respiration. Its protein content dropped from 3 to 1.6 pg cell<sup>-1</sup> (46.7% decrease) after cell division (Fábregas et al., 2002). In our study, both microalgal species followed a general trend of increasing protein contents with increasing initial nitrate concentrations, as observed by other researchers (Chen et al., 2016; Pancha et al., 2014; Xie et al., 2017). The optimum protein content for *Chlorella sorokiniana* CY1 was found at 50% BG-11 and 50% Basal medium, while the optimum for *Chlorella vulgaris* ESP-31 was located at 75% Basal medium.



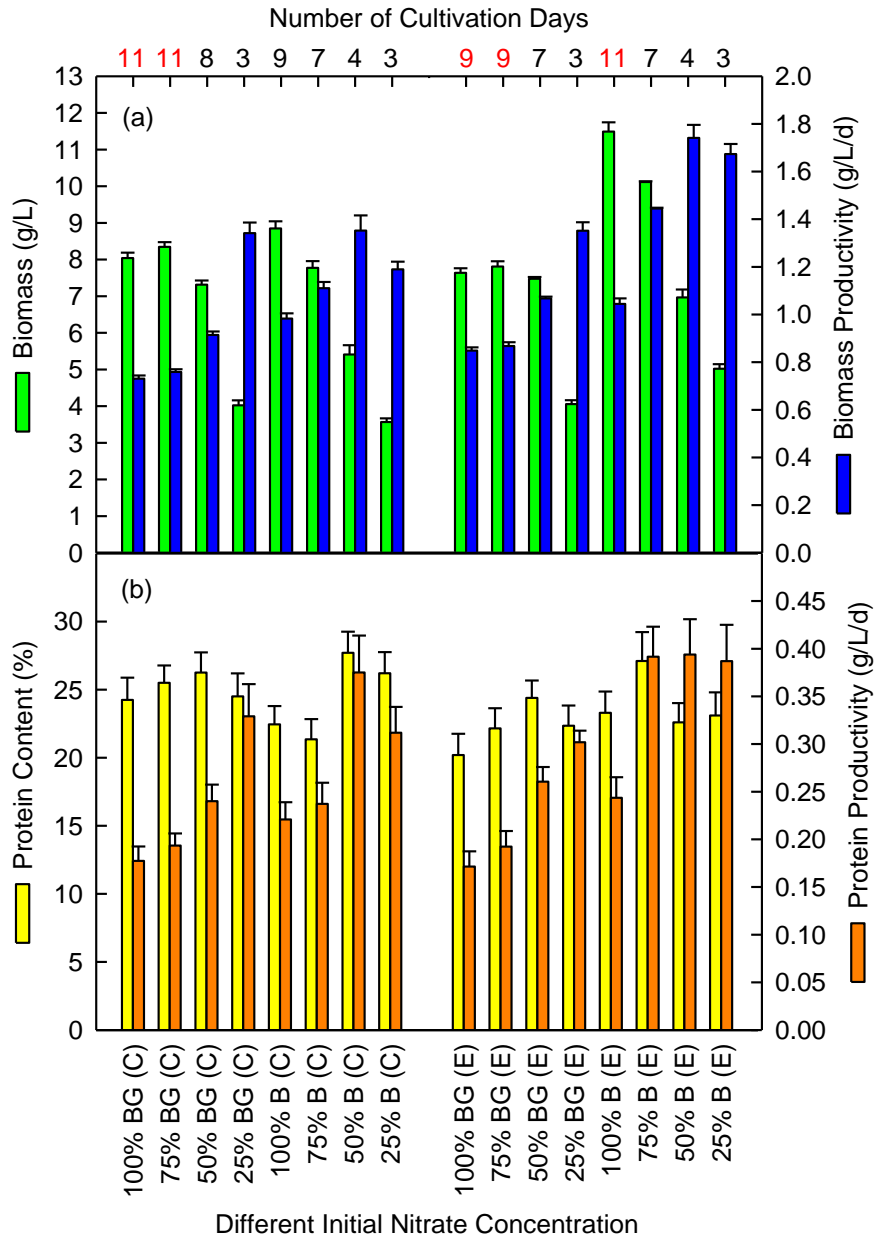


Figure 12 - Effects of different initial nitrate concentration on biomass and protein productions of *Chlorella sorokiniana* CY1 (C) and *Chlorella vulgaris* ESP-31 (E) using BG-11 medium (BG) and Basal medium (B). The number of cultivation days marked in red are parameters where the microalgal strains did not reach nitrogen starvation and were harvested during stationary phase.

Since productivity is a metric that ties microalgal growth to cultivation time, the productivities of biomass and protein were used as the criteria for choosing the best performing medium. In Figure 12, the best medium for *Chlorella sorokiniana* CY1 was 50% Basal medium, giving the highest biomass and protein productivities

( $1.61 \pm 0.11$  and  $0.422 \pm 0.026$  g/L/d) with second highest protein content ( $26.3 \pm 1.84\%$ ) and moderate biomass concentration ( $5.72 \pm 0.39$  g/L). When compared with the second best medium of 25% BG-11 medium, the biomass concentration under 50% Basal medium was enhanced by 38.2% ( $p < 0.01$ ). On the other hand, the best medium for *Chlorella vulgaris* ESP-31 was also 50% Basal medium, achieving second highest biomass and protein productivities ( $1.96 \pm 0.06$  and  $0.472 \pm 0.044$  g/L/d) with moderate biomass ( $7.00 \pm 0.20$  g/L) and protein content ( $24.1 \pm 2.1\%$ ). Upon comparing with the second best medium of 25% Basal medium, the biomass concentration under 50% Basal medium was enhanced by 37.7% ( $p < 0.01$ ).

#### **4.1.4. Effects of different CO<sub>2</sub> concentrations on microalgal biomass and protein productions**

Apart from nitrogen, CO<sub>2</sub> is another primary nutrient needed for the survival of microalgal cells. CO<sub>2</sub> is the main carbon source involved in photosynthesis, providing the microalgal cells with food in the form of glucose. The energy obtained from glucose enables synthesis of proteins essential for cell growth and cell division (Cheah et al., 2015). The range of CO<sub>2</sub> concentrations suitable for microalgal growth was found to be 1 – 50% (Cheah et al., 2015; Maeda et al., 1995). Therefore, it is economically important to determine the optimum CO<sub>2</sub> concentration for *Chlorella sorokiniana* CY1 and *Chlorella vulgaris* ESP-31. The medium used for both species was 50% Basal medium.

In Figure 13a, the biomass concentrations and cultivation days of *Chlorella sorokiniana* CY1 decreased with increasing CO<sub>2</sub> concentration, allowing the biomass productivities to rise with increasing CO<sub>2</sub> concentration up to 5% CO<sub>2</sub>. For *Chlorella vulgaris* ESP-31, both the biomass concentration and productivity increased with increasing CO<sub>2</sub> concentration up to 5% CO<sub>2</sub>. At 7.5% CO<sub>2</sub>, both microalgal species require one more day to reach nitrogen starvation phase when compared to 5% CO<sub>2</sub>. The biomass concentration of *Chlorella sorokiniana* CY1 under 7.5% CO<sub>2</sub> could

not reach the same level as 2.5% CO<sub>2</sub> despite having the same cultivation time, whereas the biomass concentration of *Chlorella vulgaris* ESP-31 decreased under 7.5% CO<sub>2</sub> compared to 5% CO<sub>2</sub>. This observation indicated that the biomass growth rate of both species were negatively impacted by 7.5% CO<sub>2</sub> aeration. In Figure 14, the pH of 7.5% CO<sub>2</sub> in both species was observed to drop to the lowest pH value starting on day 6. Compared to 5% CO<sub>2</sub>, the acidic condition created by 7.5% CO<sub>2</sub> might have decreased the activity of extracellular carbonic anhydrase. This would reduce the uptake of surrounding CO<sub>2</sub> by the microalgal cells and lowers growth rate (Cheah et al., 2015; Maeda et al., 1995; Tang et al., 2011a).

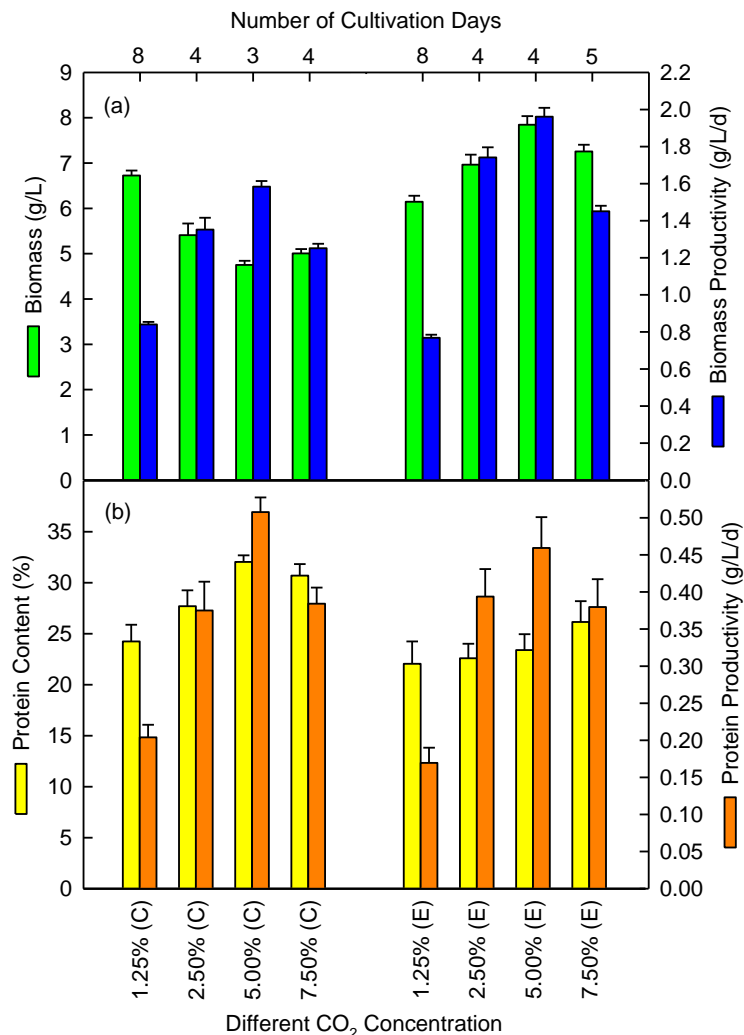


Figure 13 - Effects of different CO<sub>2</sub> concentration on biomass and protein productions of *Chlorella sorokiniana* CY1 (C) and *Chlorella vulgaris* ESP-31 (E) using Basal medium with 50% initial nitrate concentration.

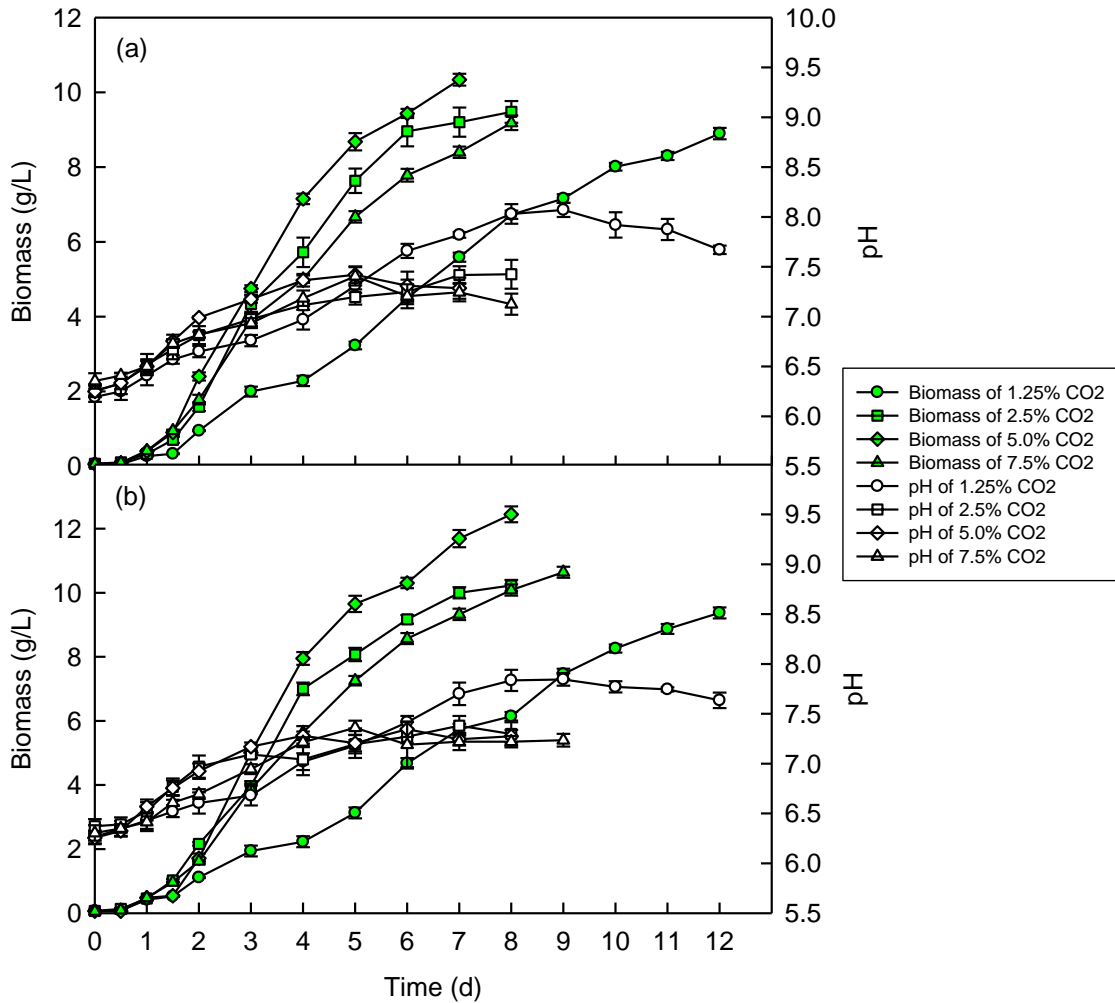


Figure 14 - Effect of different CO<sub>2</sub> concentrations on the biomass and pH of (a) *Chlorella sorokiniana* CY1 and (b) *Chlorella vulgaris* ESP-31.

In Figure 13b, the protein content of *Chlorella sorokiniana* CY1 increased with increasing CO<sub>2</sub> concentration ( $p < 0.01$ ), whereas CO<sub>2</sub> concentration did not influence the protein contents of *Chlorella vulgaris* ESP-31 (22 – 26% DCW) ( $p > 0.05$ ). The increase in protein contents of *Chlorella sorokiniana* CY1 at higher CO<sub>2</sub> concentrations of 5% and 7.5% was also been observed in other studies. For instance, Brown et al. (1997) had demonstrated that the protein contents of 17 microalgae species were enhanced when aerated with 1% CO<sub>2</sub> compared to atmospheric CO<sub>2</sub> level (Brown et al., 1997). In contrast, Chu et al. (1996) shown that the protein content of *Nitzschia inconspicua* Grunow were reduced in favour for higher lipid and carbohydrate content when the CO<sub>2</sub> concentration was

increased to 5% (Chu et al., 1996). In Figure 13, it could be inferred that at 5% CO<sub>2</sub> concentration, *Chlorella sorokiniana* CY1 accumulated proteins preferentially whereas *Chlorella vulgaris* ESP-31 accumulated biomass while keeping protein at stable levels. The effect of CO<sub>2</sub> concentration was species-dependent in our study.

After comparing biomass and protein productivities, it was clear that 5% CO<sub>2</sub> was the optimum for both species. At 5% CO<sub>2</sub>, the biomass productivity ( $p < 0.05$ ), protein content ( $p < 0.05$ ), and protein productivity ( $p < 0.01$ ) of *Chlorella sorokiniana* CY1 were significantly enhanced compared to 2.5% CO<sub>2</sub>. In the case of *Chlorella vulgaris* ESP-31, the biomass ( $p < 0.01$ ) and biomass productivity ( $p < 0.01$ ) under 5% CO<sub>2</sub> were significantly improved compared to 2.5% CO<sub>2</sub>.

#### **4.1.5. Effects of different light intensity on microalgal biomass and protein productions**

Light is one of the three components for photosynthesis in microalgal cells, other than CO<sub>2</sub> and water. The photons in visible light are captured by photosystem I (PS I) and photosystem II (PS II) in the chloroplasts of microalgal cells. The energy from the photons are used to convert adenosine diphosphate (ADP) and nicotinamide adenine dinucleotide phosphate (NADP<sup>+</sup>) into energy-carrying molecules of adenosine triphosphate (ATP) and reduced nicotinamide adenine dinucleotide phosphate (NADPH). This process is known as light dependent stage, which is the first stage of photosynthesis. The second stage of photosynthesis is known as light independent stage, whereby the ATP and NADPH generated are used to fix CO<sub>2</sub> to produce glucose (Zhao and Su, 2014). The chosen light intensity to culture microalgal cells should be high enough to penetrate through dense cultures but does not reach the light threshold of the cells. Above the light threshold, excessive light damages the light absorbing systems, primarily PS II. This causes photoinhibition and restricts the photosynthetic capability of the microalgal cells (Takahashi and Badger, 2011). Therefore, the effects of light intensity on the

biomass and protein productions of *Chlorella sorokiniana* CY1 and *Chlorella vulgaris* ESP-31 were investigated.

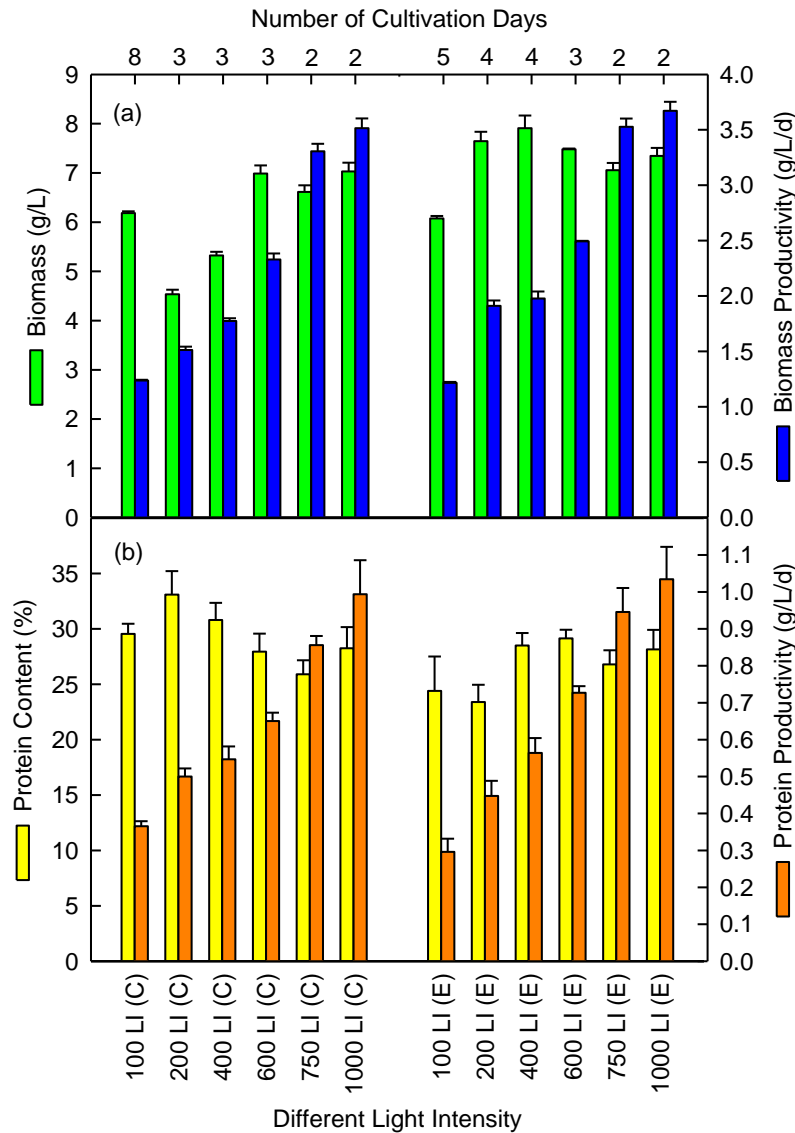


Figure 15 - Effects of different light intensity (LI) on biomass and protein productions of *Chlorella sorokiniana* CY1 (C) and *Chlorella vulgaris* ESP-31 (E) using Basal medium with 50% initial nitrate concentration.

In Figure 15a, the biomass concentration of *Chlorella sorokiniana* CY1 saw an increasing trend when the light intensity was increased from 200 to 600  $\mu\text{mol}/\text{m}^2/\text{s}$ , before levelling off at 600 to 1000  $\mu\text{mol}/\text{m}^2/\text{s}$ . For *Chlorella vulgaris* ESP-31, its biomass concentration increased to peak value when the light intensity was increased from 100 to 200 and 400  $\mu\text{mol}/\text{m}^2/\text{s}$ , before decreasing and levelling

off at 600 to 1000  $\mu\text{mol}/\text{m}^2/\text{s}$ . At 750 and 1000  $\mu\text{mol}/\text{m}^2/\text{s}$ , the cultivation time of both species decreased to 2 days, giving rise to high biomass productivities. In Figure 15b, the lowest protein content of *Chlorella sorokiniana* CY1 at 750  $\mu\text{mol}/\text{m}^2/\text{s}$  was significantly less than at 200  $\mu\text{mol}/\text{m}^2/\text{s}$  ( $p < 0.05$ ), while the protein contents at other light intensities did not show any meaningful differences ( $p > 0.05$ ). In the case of *Chlorella vulgaris* ESP-31, its protein content was not impacted by changes in light intensities ( $p > 0.05$ ). Increasing light intensity enhances light penetration into the culture, which in turn raised the biomass growth rate of both species. Any effects of photoinhibition were also indistinct as the biomass concentrations of both species were high and protein contents were stable at high light intensities of 750 and 1000  $\mu\text{mol}/\text{m}^2/\text{s}$ . The one exception (protein content at 750  $\mu\text{mol}/\text{m}^2/\text{s}$  of *Chlorella sorokiniana* CY1) could be due the accumulation of biomass at the expense of protein (Fábregas et al., 2002). This phenomenon had also been illustrated by Seyfabadi et al. (2010) (Seyfabadi et al., 2011). Increasing the light intensity from 37.5 to 62.5  $\mu\text{mol}/\text{m}^2/\text{s}$  markedly improved the cell numbers and protein contents of *Chlorella vulgaris*. But when the light intensity was further increased to 100  $\mu\text{mol}/\text{m}^2/\text{s}$ , the cell numbers dropped but protein contents were increased (Seyfabadi et al., 2011). The greater biomass growth rates at higher light intensities were also observed by Qiang et al. (1998), who reported that the volumetric biomass productivity ( $\text{mg dry wt L}^{-1} \text{ h}^{-1}$ ) of *Spirulina platensis* (Norstedt) Geitler (strain M2) was enhanced with increasing light intensity from 270 to 8000  $\mu\text{mol}/\text{m}^2/\text{s}$ . Photoinhibition effects on the growth rate of *Spirulina platensis* were not observed even at light intensity of 8000  $\mu\text{mol}/\text{m}^2/\text{s}$  (4-fold light intensity of full sunlight) (Qiang et al., 1998). This was in contrast with another study, where photoinhibition occurred during noon in two *Spirulina platensis* strains grown outdoors in open ponds (Vonshak and Guy, 1992).

Table 3 - Comparison of biomass and protein productions of *Chlorella sorokiniana* CY1 and *Chlorella vulgaris* ESP-31 with other studies

Microalgae	Culture Medium	Culture Type	Culture Time <sup>b</sup> (d)	Biomass		Protein		Reference
				Conc. <sup>c</sup> (g/L)	Pr. <sup>d</sup> (g/L/d)	Content (% w/w)	Pr. (g/L/d)	
<i>Chlorella</i> sp. CH2	F	B (10 L)	5	~3.00 <sup>a</sup>	0.60	38.9	0.233 <sup>a</sup>	(Guccione et al., 2014)
<i>Chlorella</i> sp. F&M-M49	BG-11	B (10 L)	5	~2.15 <sup>a</sup>	0.43	40.5	0.174 <sup>a</sup>	(Guccione et al., 2014)
<i>Chlorella</i> sp. PROD1	BG-11	B (10 L)	5	~1.60 <sup>a</sup>	0.32	41.3	0.132 <sup>a</sup>	(Guccione et al., 2014)
<i>Chlorella sorokiniana</i> IAM C-212	BG-11	B (10 L)	5	~2.05 <sup>a</sup>	0.41	39.8	0.163 <sup>a</sup>	(Guccione et al., 2014)
<i>Chlorella vulgaris</i> C9-JN2010	MWW <sup>h</sup>	B (7.5 L)	-	0.76	-	55.0	-	(Li et al., 2013)
<i>Chlorella vulgaris</i> FSP-E	Modified Basal	B <sup>e</sup> (1 L)	4.5	3.17	0.699	52.3	0.365	(Chen et al., 2015)
<i>Chlorella vulgaris</i> FSP-E	Modified Basal	B (50 L)	10	~3.25 <sup>a</sup>	0.268	~52	0.155	(Chen et al., 2016)
<i>Chlorella vulgaris</i> FSP-E	Modified Basal	SB <sup>f</sup> (50 L) w/ 50% MRR <sup>g</sup>	(3 Repl) 6	~3.25 <sup>a</sup>	~0.269 <sup>a</sup>	52.2	0.125	(Chen et al., 2016)
<i>Chlorella sorokiniana</i> CY1	Modified Basal	B (1 L)	2	6.61 ± 0.13	4.35 ± 0.09	25.9 ± 1.3	1.126 ± 0.035	This study
<i>Chlorella vulgaris</i> ESP-31	Modified Basal	B (1 L)	2	7.06 ± 0.15	4.64 ± 0.10	26.8 ± 1.3	1.243 ± 0.084	This study

Considering the combination of high biomass and protein productivities, the light intensity of 750  $\mu\text{mol}/\text{m}^2/\text{s}$  was chosen as the optimum. This was because the biomass and protein productivities at light intensity of 750  $\mu\text{mol}/\text{m}^2/\text{s}$  were significantly enhanced compared to light intensities of 100 to 600  $\mu\text{mol}/\text{m}^2/\text{s}$  ( $p > 0.01$ ), while insignificantly different compared to light intensity of 1000  $\mu\text{mol}/\text{m}^2/\text{s}$  ( $p > 0.05$ ). The lower light intensity of 750  $\mu\text{mol}/\text{m}^2/\text{s}$  was also easier to implement for experiments and consume less electricity to operate when compared with 1000



$\mu\text{mol}/\text{m}^2/\text{s}$ . The growth values of both *Chlorella sorokiniana* CY1 and *Chlorella vulgaris* ESP-31 can be found in Table 1, together with a comparison of the performance of different microalgal species in literature. Although the biomass concentration, biomass productivity, and protein productivity of both *Chlorella sorokiniana* CY1 and *Chlorella vulgaris* ESP-31 were greater than the other species in Table 3, the protein contents of both species were lacking. This disparity could be due to difference in culture media, cultivation time, choice of optimization parameters, and priority of chosen parameters. For instance, in the case of *Chlorella vulgaris* FSP-E, the selected medium was modified Basal medium with urea as the nitrate source rather than potassium nitrate ( $\text{KNO}_3$ ). The performance of different photobioreactors, light intensity, and urea concentration were investigated for 1 L indoor culture, whereas the urea concentration, inoculum size, aeration rate, and partial medium replacement were optimized for 50 L outdoor culture with sunlight as the light source. Optimizing these parameters resulted in high protein contents of around 52%, but the trade-off would be longer cultivation time as well as lower biomass and protein productivities. Despite this, it is undeniable that the protein contents of *Chlorella sorokiniana* CY1 and *Chlorella vulgaris* ESP-31 were mediocre and should be improved before they could be considered as potential producers of microalgal protein.

## 4.2. Study 2 – Strategies for enhancing lipid production from indigenous microalgae isolates

### 4.2.1. Aim and objective of study

In this study, five different indigenous microalgal strains from Taiwan were characterised in terms of their lipid contents and productivities. The strain with the highest oil productivity was chosen for optimization strategies, which included altering the initial nitrate concentrations, LED light intensity and initial cell concentrations. The information obtained from this study would be useful for evaluating the potential of using the strain as feedstock for the production of biodiesel. The performance of recent research on microalgal biodiesel production is listed in Table 4.

Table 4 - Comparison of oil productivity with recent research in lab-scale cultures

Strain	Medium	Oil Content (% dry wt)	Oil Pr. <sup>a</sup> (mg/L/d)	CT <sup>b</sup> (d)	Reference
<i>Ankistrodesmus falcatus</i> (UTEX 242)	3N BBM <sup>c</sup>	12.0	55.0	14	(Griffiths et al., 2012)
<i>Chlamydomonas</i> sp. JSC4	3.5% sea salt HSM <sup>d</sup>	33.1	169.1	7	(Nakanishi et al., 2014)
<i>Chlorella sorokiniana</i> CY1	20% DSW <sup>e</sup> -amended medium	61.0	189.3	12	(Chen et al., 2013)
<i>Chlorella vulgaris</i> UTEX 395	3N BBM	57.0	67.0	14	(Griffiths et al., 2012)
<i>Dunaliella tertiolecta</i> UTEX LB 999	Erdschreiber's medium	23.4	11.4	8	(Tang et al., 2011b)
<i>Nannochloropsis</i> sp.	f/2 medium	35.0	63.0	14	(Griffiths et al., 2012)
<i>Scenedesmus</i> sp.	3N BBM	43.0	106.0	14	(Griffiths et al., 2012)
<i>Scenedesmus rubescens</i>	Seawater	31.6	107.8	10	(Lin et al., 2012)
<i>Thalassiosira</i> sp.	Enriched SW <sup>f</sup> medium	-	248.5	6	(Nurachman et al., 2012)
<i>Chlamydomonas</i> sp. Tai-03	BG-11 medium	28.6	124.1	8	This study

<sup>a</sup> = Productivity, <sup>b</sup> = Cultivation time, <sup>c</sup> = Bold's basal medium, <sup>d</sup> = High salt medium, <sup>e</sup> = Deep seawater, <sup>f</sup> = Seawater

#### 4.2.2. Microalgae selection

The five microalgal strains were cultured using BG-11 medium, Basal medium and BBM. Their resulting lipid content and productivity were compared (Table 5). This step served to eliminate the strains with low lipid content and productivity, so the best strain can be selected for further lipid optimization. First the microalgae were pre-cultured at 24 – 26°C for 4 – 7 days. Upon reaching the appropriate cell concentration, the microalgae were inoculated into 1 L PBRs.

From Table 5, it can be seen that among all five microalgal strains, *Chlamydomonas* sp. Tai-03 had a high biomass growth and the highest oil productivity in both BG-11 and Basal medium. *Chlamydomonas* sp. Tai-03 achieved a biomass and oil productivity of  $3.08 \pm 0.09$  g/L and  $82.4 \pm 6.0$  mg/L/d respectively in BG-11 medium, compared to  $5.52 \pm 0.01$  g/L and  $66.8 \pm 5.9$  mg/L/d in Basal medium. In both BG-11 and Basal medium, *Chlamydomonas* sp. Pin-01 and Tai-01 ranked second and third in terms of biomass production and oil productivity. Although the biomass growth of Pin-01 and Tai-01 were significantly higher in Basal medium compared to BG-11 medium, the lower oil contents in Basal medium resulted in overall lower oil productivity. On the other hand, both the *Scenedesmus* sp. ESP-05 and ESP-07 achieved similar biomass growth in BG-11 and Basal medium. ESP-05 had higher oil productivity ( $56.7 \pm 5.9$  mg/L/d) in BG-11 medium compared to ESP-07 ( $39.7 \pm 6.3$  mg/L/d).

Upon culturing in BBM all five strains showed a low biomass accumulation compared to BG-11 and Basal medium (Table 5). The oil contents for all strains were also low (9 – 17%) except for ESP-05, which accumulated an oil content of  $35.29 \pm 1.61\%$ . But due to the low biomass production of ESP-05 ( $1.36 \pm 0.04$  g/L), its oil productivity ( $59.7 \pm 1.0$  mg/L/d) was similar to Pin-01 ( $60.1 \pm 1.0$  mg/L/d). In BBM, Pin-01 had the highest biomass production ( $2.61 \pm 0.18$  g/L) and highest oil productivity, but the second lowest oil content of  $11.6 \pm 0.6\%$ .

Table 5 - Biomass and oil analysis of five microalgae in BG-11, Basal and BBM

Medium	Species	Biomass (g/L)	Biomass Pr. <sup>a</sup> (g/L/d)	Oil	
				Oil Content (%)	Oil Pr. (mg/L/d)
BG-11	Tai-01	1.80 ± 0.11	0.238 ± 0.015	27.62 ± 1.27	65.93 ± 7.66
	Tai-03	3.08 ± 0.09	0.282 ± 0.008	29.20 ± 1.05	82.44 ± 5.97
	Pin-01	3.25 ± 0.07	0.298 ± 0.006	25.85 ± 0.71	76.97 ± 1.07
	ESP-05	2.61 ± 0.04	0.187 ± 0.003	30.35 ± 3.56	56.68 ± 5.94
	ESP-07	2.43 ± 0.07	0.187 ± 0.006	23.41 ± 3.57	39.68 ± 6.28
Basal	Tai-01	4.28 ± 0.09	0.425 ± 0.009	11.27 ± 0.41	47.97 ± 2.72
	Tai-03	5.52 ± 0.01	0.499 ± 0.001	13.38 ± 1.08	66.78 ± 5.88
	Pin-01	5.43 ± 0.11	0.543 ± 0.011	11.15 ± 0.55	60.41 ± 1.91
	ESP-05	2.75 ± 0.08	0.196 ± 0.006	12.19 ± 0.86	24.55 ± 1.84
	ESP-07	2.83 ± 0.25	0.177 ± 0.015	13.82 ± 1.85	24.16 ± 1.24
BBM	Tai-01	1.07 ± 0.01	0.268 ± 0.003	9.03 ± 0.53	24.17 ± 1.71
	Tai-03	2.45 ± 0.08	0.350 ± 0.012	14.39 ± 1.50	50.58 ± 6.92
	Pin-01	2.61 ± 0.18	0.521 ± 0.036	11.57 ± 0.59	60.10 ± 1.03
	ESP-05	1.36 ± 0.04	0.170 ± 0.005	35.29 ± 1.61	59.73 ± 0.96
	ESP-07	0.92 ± 0.05	0.154 ± 0.009	16.93 ± 1.30	25.96 ± 0.53

<sup>a</sup> = Productivity

Overall all five strains accrued higher oil contents in BG-11 medium compared to both Basal medium and BBM, except for the case of ESP-05 in BBM. All five microalgal strains achieved the highest biomass production in Basal medium, but the resulting low oil content led to low oil productivity. When cultured in BG-11 medium, the moderate biomass production and high oil contents gave the highest lipid productivities. This might be due to the presence of salt stress (Na<sup>+</sup>) in BG-11 medium, dampening the biomass growth but increasing the accumulation of lipids. Freshwater isolates can generally withstand up to about 2% NaCl concentration, compared to 8 – 10% NaCl in marine isolates. Meanwhile, the Na<sup>+</sup> concentration for essential growth in freshwater microalgae is typically 1 mg NaCl/L, whereas that of marine microalgae ranges from 10 – 100 mg NaCl/L (Batterton and Van Baalen, 1971). High concentrations of Na<sup>+</sup> ions dampen microalgae growth more by ionic stress than osmotic stress. The ionic stress causes a direct reduction in photosynthesis, but instead promotes the accumulation of metabolites (such as lipids, carbohydrates and pigments) in microalgal cells (Takagi and Yoshida, 2006; Pal et al., 2011). The lower lipid productivities in Basal medium were due to the

very low concentration of Na<sup>+</sup> in the medium. The lower lipid productivities in BBM were because of a low nitrate concentration available in the medium. The best performance was obtained by culturing *Chlamydomonas* sp. Tai-03 in BG-11 medium. Therefore, *Chlamydomonas* sp. Tai-03 and BG-11 medium were selected for the next experiment.

#### **4.2.3. Effects of initial nitrate concentration on the cell growth and lipids production of *Chlamydomonas* sp. Tai-03**

It is well known that the availability of nitrogen source in microalgae culture strongly affects the accumulation of lipids in microalgae (Fidalgo et al., 1998; Mata et al., 2010). Lipid accumulation is usually triggered when nitrogen starvation in the microalgae culture occurs (Roessler, 1990; Breuer et al., 2012) However, when the nitrogen source is depleted, the cell growth rate significantly decreases. The stunted cell growth will also lead to a decrease in the lipid productivity of microalgae. Therefore, adjusting the initial nitrogen concentration of the culture medium was shown to be an effective way to control and optimise the lipid content and lipid productivity of microalgae (Chen et al., 2010; Ho et al., 2012; Ho et al., 2014). In this study, the effects of different initial nitrate concentration on the growth and lipid production of the *Chlamydomonas* sp. Tai-03 strain were explored. The initial nitrate concentration was set as 100%, 75%, 50%, 25%, and 12.5% of the original nitrate concentration (1.5 g/L) in BG-11 medium.

From Figure 16, when the nitrate concentration was decreased from 100% to 75% and 50%, the biomass production increased from  $3.08 \pm 0.09$  g/L to  $3.48 \pm 0.04$  g/L and  $3.57 \pm 0.04$  g/L respectively. However, the resulting oil productivities at 100%, 75%, and 50% nitrate concentration were similar due to slight decreases in oil contents. At 25% nitrate concentration, the biomass production declined to  $2.73 \pm 0.03$  g/L but its oil content reached  $30.2 \pm 1.5\%$ . Because *Chlamydomonas* sp. Tai-03 at 25% nitrate concentration only needed 8 days to reach maximum oil content (compared to 11 days for 75% and 50% nitrate

concentration), its oil productivity increased to  $110.0 \pm 4.6$  mg/L/d. Further reducing the nitrate concentration to 12.5% resulted in a sharp decrease in biomass production to  $2.05 \pm 0.15$  g/L. The highest oil content and oil productivity were also reduced sharply to  $19.5 \pm 0.9\%$  and  $57.3 \pm 6.8$  mg/L/d. After performing a one-way analysis of variance (ANOVA), it was found that the biomass productivity ( $p < 0.0254$ ) and oil productivity ( $p < 0.0336$ ) were significantly influenced by initial nitrate concentration.

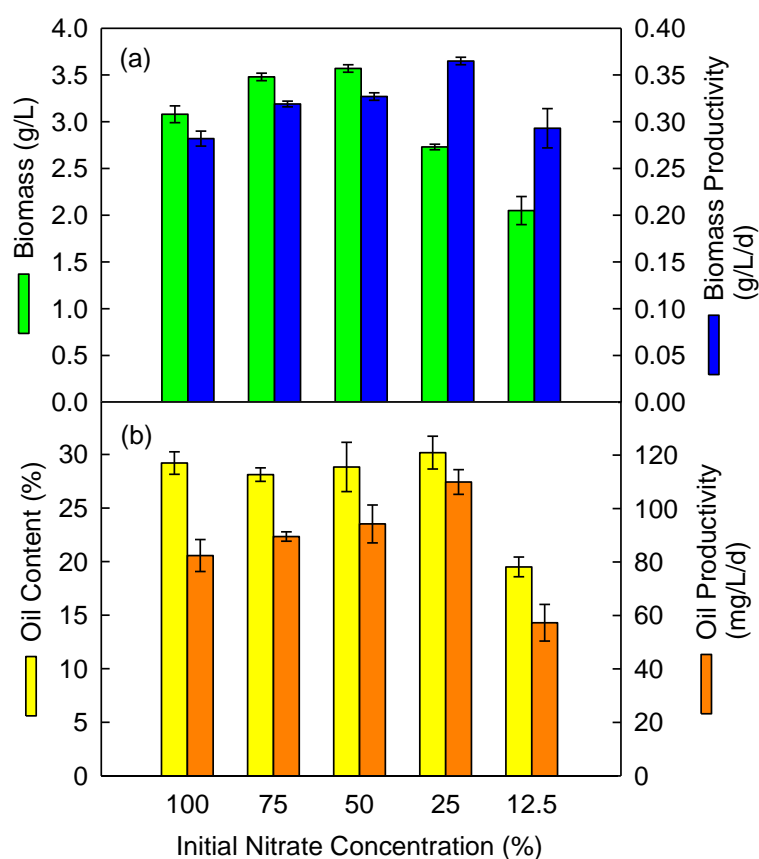


Figure 16 - Influence of differing initial nitrate concentration on (a) biomass and biomass productivity; (b) oil content and oil productivity of *Chlamydomonas* sp. Tai-03.

The lower initial nitrate concentration of 25% caused *Chlamydomonas* sp. Tai-03 to enter nitrogen starvation stage faster, thus allowing a more rapid accumulation of lipids. The ionic stress caused by  $\text{Na}^+$  ions in BG-11 medium also further enhanced its lipid content (Takagi and Yoshida, 2006; Pal et al., 2011). The

reason for continual accumulation of lipids might be because lipids do not contain nitrogen; hence they continued to be synthesized in the absence of nitrogen source. The synthesis of nucleic acids and proteins would have stopped, minimising further biomass growth (Roessler, 1990). Since *Chlamydomonas* sp. Tai-03 achieved the highest oil productivity at 25% nitrate concentration, this combination was chosen for the next study.

#### **4.2.4. Effects of light intensity on the cell growth and lipids production of *Chlamydomonas* sp. Tai-03**

Light intensity play a pivotal role in the growth of phototrophic microalgae since light energy is the major energy source required for the microalgal growth and lipid synthesis (Napolitano, 1994). Literature also shows that there exists an optimal light intensity for the microalgae to exhibit the best lipid accumulation and productivity (Cheirsilp and Torpee, 2012). Therefore, the effects of different light intensity (100, 200, 400 and 600  $\mu\text{mol}/\text{m}^2/\text{s}$ ) on the biomass and lipid productivity of *Chlamydomonas* sp. Tai-03 were investigated.

As seen in Figure 17, the harvested biomass, biomass productivity and oil productivity increased with increasing light intensity. The oil content was  $11.3 \pm 0.05\%$  at a light intensity of 100  $\mu\text{mol}/\text{m}^2/\text{s}$ ; but increased to  $30.2 \pm 1.5\%$  above 200  $\mu\text{mol}/\text{m}^2/\text{s}$ . Due to the low biomass ( $2.61 \pm 0.07$  g/L) at 100  $\mu\text{mol}/\text{m}^2/\text{s}$ , the biomass productivity ( $0.326 \pm 0.008$  g/L/d) and oil productivity ( $36.8 \pm 0.68$  mg/L/d) suffered. Although the biomass at 200  $\mu\text{mol}/\text{m}^2/\text{s}$  ( $2.73 \pm 0.03$  g/L) was lower than that of 400  $\mu\text{mol}/\text{m}^2/\text{s}$  ( $2.90 \pm 0.13$  g/L) and 600  $\mu\text{mol}/\text{m}^2/\text{s}$  ( $2.91 \pm 0.07$  g/L), the respective oil productivities did not vary significantly. The oil productivities at 200, 400, and 600  $\mu\text{mol}/\text{m}^2/\text{s}$  were  $110.0 \pm 4.6$ ,  $117.4 \pm 15.2$ , and  $124.1 \pm 5.8$  mg/L/d respectively. An analysis using ANOVA revealed that the harvested biomass ( $p < 0.0401$ ) and biomass productivity ( $p < 0.0168$ ) were significantly affected by light intensity. Higher light intensity allowed the microalga to grow more rapidly, hence reaching nitrogen starvation in a shorter time. As the

biomass concentration increased, the light penetration of the PBRs reduced. Little light could travel into the dense medium, which led to a relatively small increase in biomass and oil content (Chen and Johns, 1991). Since the focus is on high oil productivity, the initial light intensity of 200  $\mu\text{mol}/\text{m}^2/\text{s}$  offered the best oil productivity against electrical energy consumed. Hence, the light intensity of 200  $\mu\text{mol}/\text{m}^2/\text{s}$  was chosen for the next experiment.

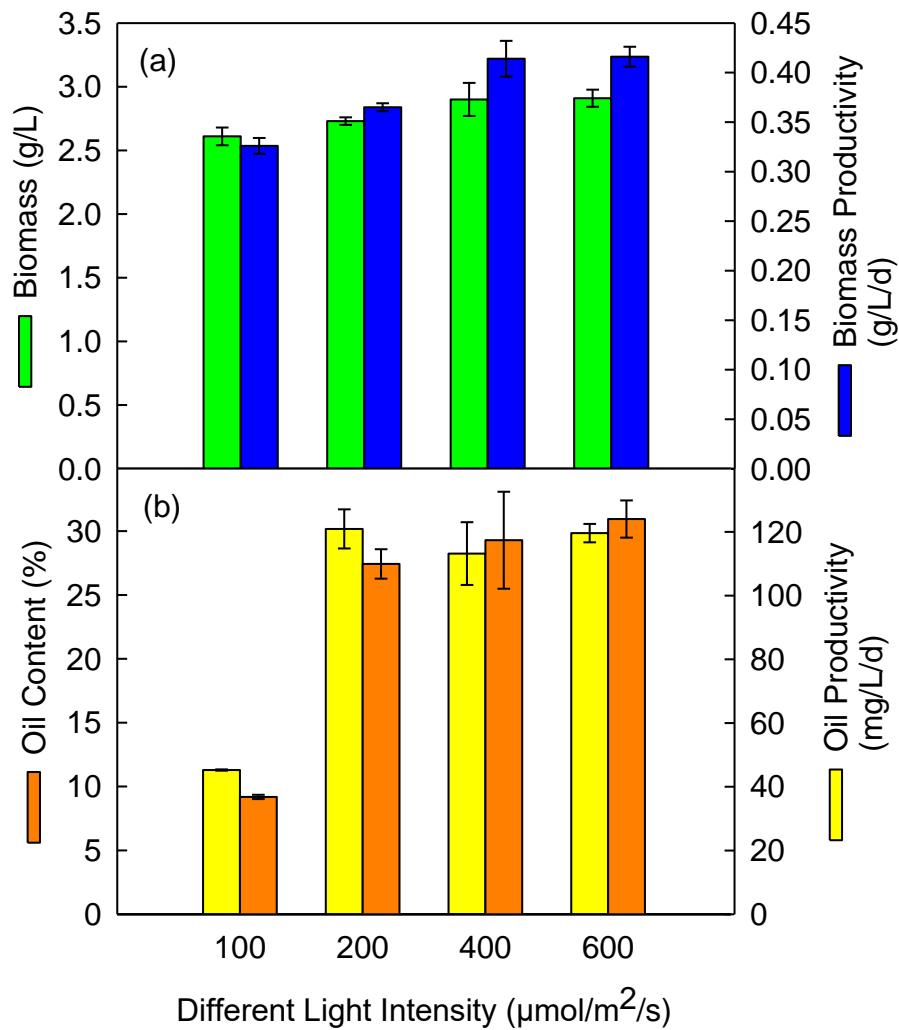


Figure 17 - Influence of differing light intensity on (a) biomass and biomass productivity; (b) oil content and oil productivity of *Chlamydomonas* sp. Tai-03.



#### 4.2.5. Effects of initial cell concentration on the cell growth and lipids production of *Chlamydomonas* sp. Tai-03

Initial cell concentration (or inoculum size) of the microalgae culture is considered as an effective factor influencing microalgal cell growth, especially for outdoor cultivation. Using an appropriate inoculum size is critical in promoting cell growth when the culture is exposed to full sunlight with very high light intensity (Hallenbeck et al., 2015). Higher initial cell concentration also increased the microalga growth rate and nutrient uptake efficiency (Lau et al., 1995). The microalga *Chlamydomonas* sp. Tai-03 was selected to examine the effects of different initial amounts of inoculation (i.e., 0.03, 0.06, 0.09, 0.12, and 0.15 g/L).

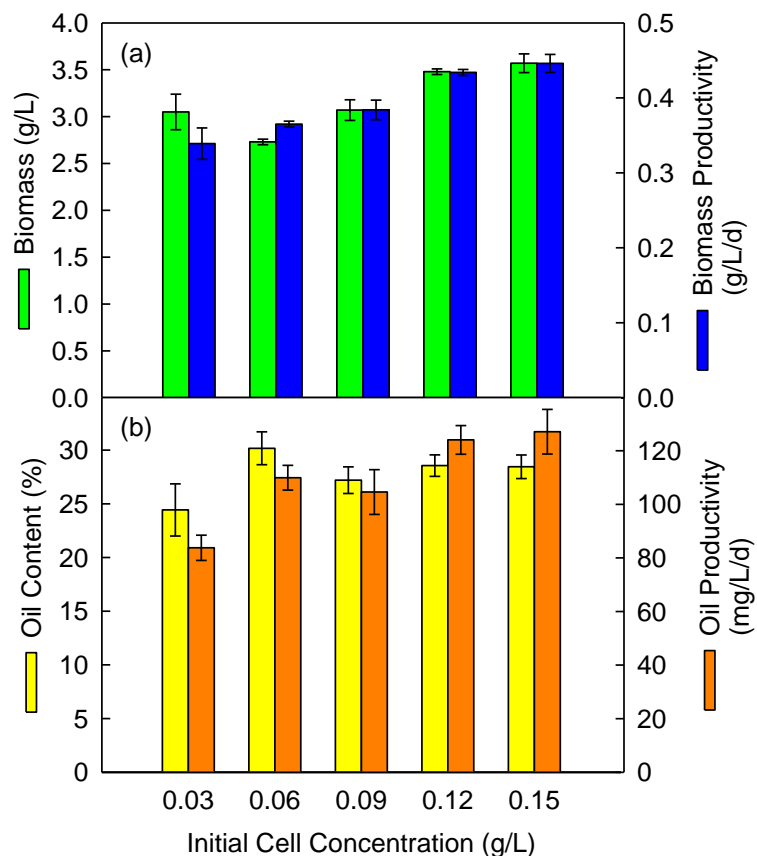


Figure 18 - Influence of differing initial cell concentration on (a) biomass and biomass productivity; (b) oil content and oil productivity of *Chlamydomonas* sp. Tai-03.

According to Figure 18, as the initial cell concentration increased, the biomass also increased. However, at an initial cell concentration of 0.06 g/L, the biomass saw a slight decrease to  $2.73 \pm 0.03$  g/L; whereas the biomass of 0.03 and 0.09 g/L initial cell concentration were  $3.05 \pm 0.19$  and  $3.07 \pm 0.11$  g/L. The biomass further rose to  $3.48 \pm 0.03$  and  $3.57 \pm 0.10$  g/L at initial cell concentrations of 0.12 and 0.15 g/L. According to Student's t-test, there was no significant difference between the biomass values for initial cell concentration of 0.03 and 0.06 g/L. The variance for the biomass of 0.03 g/L (0.013) was higher than that of 0.06 g/L (0.0014). This shows that the higher biomass for 0.03 g/L was due to experimental errors. Apart from experimental errors, biological systems may still exhibit varying growth in isolated environments even though all five experiments were conducted using identical medium composition and the same pre-culture. However, the biomass productivity increased steadily from initial cell concentration of 0.03 to 0.15 g/L. The oil content for the 0.03 g/L was low ( $24.4 \pm 2.4\%$ ), but the oil contents for 0.06, 0.09, 0.12, and 0.15 g/L were in  $30.2 \pm 1.5\%$ ,  $27.2 \pm 1.2\%$ ,  $28.6 \pm 1.0\%$ , and  $28.5 \pm 1.1\%$  respectively. As a result, 0.03 g/L had the lowest oil productivity of  $83.8 \pm 4.7$  mg/L/d; followed by 0.06 and 0.09 g/L at  $110.0 \pm 4.6$  and  $104.6 \pm 8.4$  mg/L/d; and finally 0.12 and 0.15 g/L at  $124.1 \pm 5.4$  and  $127.1 \pm 8.3$  mg/L/d respectively. The oil productivities saw significant improvements at initial cell concentrations of 0.06 g/L (29% increase compared to 0.03 g/L) and 0.12 g/L (13% increase compared to 0.06 g/L). Since the oil content was in the range of 27 – 30%, an initial cell concentration of 0.12 g/L was considered the optimum due to its higher oil productivity. A one-way ANOVA study showed that the harvested biomass ( $p < 0.0442$ ), biomass productivity ( $p < 0.0024$ ), and oil productivity ( $p < 0.0282$ ) were significantly influenced by initial cell concentration.

The FAME profile of *Chlamydomonas* sp. Tai-03 was shown in Table 6, and the FAMES were composed mainly of palmitic acid, oleic acid and linoleic acid. These fatty acids are suitable for biodiesel production (Knothe, 2008). The oil productivity

of *Chlamydomonas* sp. Tai-03 is relatively high compared to the results of most other research (Table 4), making it a potential strain for large-scale outdoor cultivation to generate biodiesel. The future prospect for this research will be to investigate the performance of *Chlamydomonas* sp. Tai-03 in outdoor mass culture systems. A detailed economic analysis will shed light on the financial feasibility of large-scale operations, while a life cycle assessment (LCA) will evaluate the self-sustainability of biodiesel synthesis from *Chlamydomonas* sp. Tai-03.

Table 6 - Fatty acid methyl ester (FAME) profile of *Chlamydomonas* sp. Tai-03

<b>Type of FAME</b>	<b>Percentage per dry cell weight</b>
Palmitic acid (C16:0)	12.56%
Palmitoleic acid (C16:1)	1.59%
Margaric acid (C17:0)	0.97%
Oleic acid (C18:1)	6.87%
Linoleic acid (C18:2)	4.58%
Alpha Linoleic acid (C18:3)	1.99%

### **4.3. Study 3 – Exploring the potency of integrating semi-batch operation into lipid yield performance of *Chlamydomonas* sp. Tai-03**

#### **4.3.1. Aim and objective of study**

The aim of this study is to further optimise the culture conditions of a microalgal strain *Chlamydomonas* sp. Tai-03 to enhance lipid production compared to our previous optimization study (Study 1). In this study, investigation on further optimization parameters will be carried out, including the effects of different concentrations of organic carbon (OC) sources and CO<sub>2</sub> gas on the microalgal biomass and lipid productions. Then, semi-batch operations with different medium replacement ratios (MRRs) was conducted to enhance the biomass and lipid productivities.

#### **4.3.2. Effects of organic and inorganic carbon on microalgal biomass and lipid production of *Chlamydomonas* sp. Tai-03**

Based on the uptake and assimilation of carbon by microalgae, their metabolism can be of three types, namely photoautotrophic, heterotrophic, and mixotrophic modes. In photoautotrophic culture, microalgae use light and inorganic carbon source (CO<sub>2</sub> or soluble carbonates) for growth via photosynthesis (Huang et al., 2010). In heterotrophic culture, microalgae consume OC (like glucose and acetate) for growth in the absence of light via aerobic respiration (Xiong et al., 2008). In mixotrophic culture, microalgae utilise both organic and inorganic carbon sources for growth in the presence of low light intensities (Heredia-Arroyo et al., 2011). Many studies have demonstrated that mixotrophic cultivation of microalgae, using appropriate amounts of OCs, could yield higher biomass and lipid production. The growth rate of microalgal cells in mixotrophic mode is known to be the sum of autotrophic and heterotrophic modes combining their advantages and overcoming

light limitations of autotrophic mode (Zhan et al., 2017). For instance, Cheirsilp and Torpee found that the biomass of *Chlorella* sp. and *Nannochloropsis* sp. increased with increasing initial glucose concentration. The maximum lipid production for *Chlorella* sp. and *Nannochloropsis* sp. were observed when glucose concentration was increased to 10 g/L and 15 g/L respectively (Cheirsilp and Torpee, 2012). Therefore, the effects of mixotrophic (2.5% CO<sub>2</sub> and different concentrations of OC) and autotrophic (1.25, 2.5, 5, and 7.5% CO<sub>2</sub> in air) cultivation on the biomass and lipid production of *Chlamydomonas* sp. Tai-03 were investigated. The selected OCs were glucose (Gly), sucrose (Su), glycerol (Gly), acetate (Ac), and fructose (Fru). The OCs were normalized based on their molecular weight to obtain 2 g carbon equivalent and 4 g carbon equivalent OCs for all the tests, and they are denoted as 2-OC and 4-OC. The other culture conditions were identical to the optimal conditions (stated in Section 3.1.2) determined in our previous study (PS), which is Study 1.

As shown in Figure 19a, the highest biomass productions were achieved by 7.5% and 5% CO<sub>2</sub> ( $4.26 \pm 0.07$  and  $4.14 \pm 0.08$  g/L/d), which were improvements of 23% and 19% compared to the biomass production of PS ( $3.48 \pm 0.04$  g/L/d). The addition of OC did not show a significant effect on biomass production, but the addition of an appropriate type and amount of OC significantly increased biomass productivity. This is because the addition of OC reduced the number of cultivation days needed for *Chlamydomonas* sp. Tai-03 to reach maximum lipid productivity compared with PS (shown at the top axis of Figure 19a). From Figure 19a, the biomass productivities of 4-Glu, 4-Su, 2-Gly, and 4-Gly were the highest ( $0.66 \pm 0.02$ ,  $0.64 \pm 0.02$ ,  $0.64 \pm 0.01$ , and  $0.64 \pm 0.01$  g/L/d), showing enhancements of 52%, 47%, 48%, and 48% compared to PS. This was followed by 2-Glu and 2-Ac ( $0.56 \pm 0.01$  and  $0.58 \pm 0.02$  g/L/d) which show an increase of 28% and 33%. The biomass productivities of 2-Su, 4-Ac, 4-Fru, and 1.25% CO<sub>2</sub> ( $0.47 \pm .01$ ,  $0.49 \pm 0.01$ ,  $0.48 \pm 0.02$ , and  $0.45 \pm 0.01$  g/L/d) were similar to PS ( $0.43 \pm 0.01$  g/L/d), whereas 2-Fru had the lowest biomass productivity ( $0.31 \pm 0.01$  g/L/d). In the

case of inorganic carbon source, an increase of CO<sub>2</sub> concentration to 5% and 7.5% enhanced the biomass productivities by 19% and 23% compared to PS (which was 2.5% CO<sub>2</sub>).

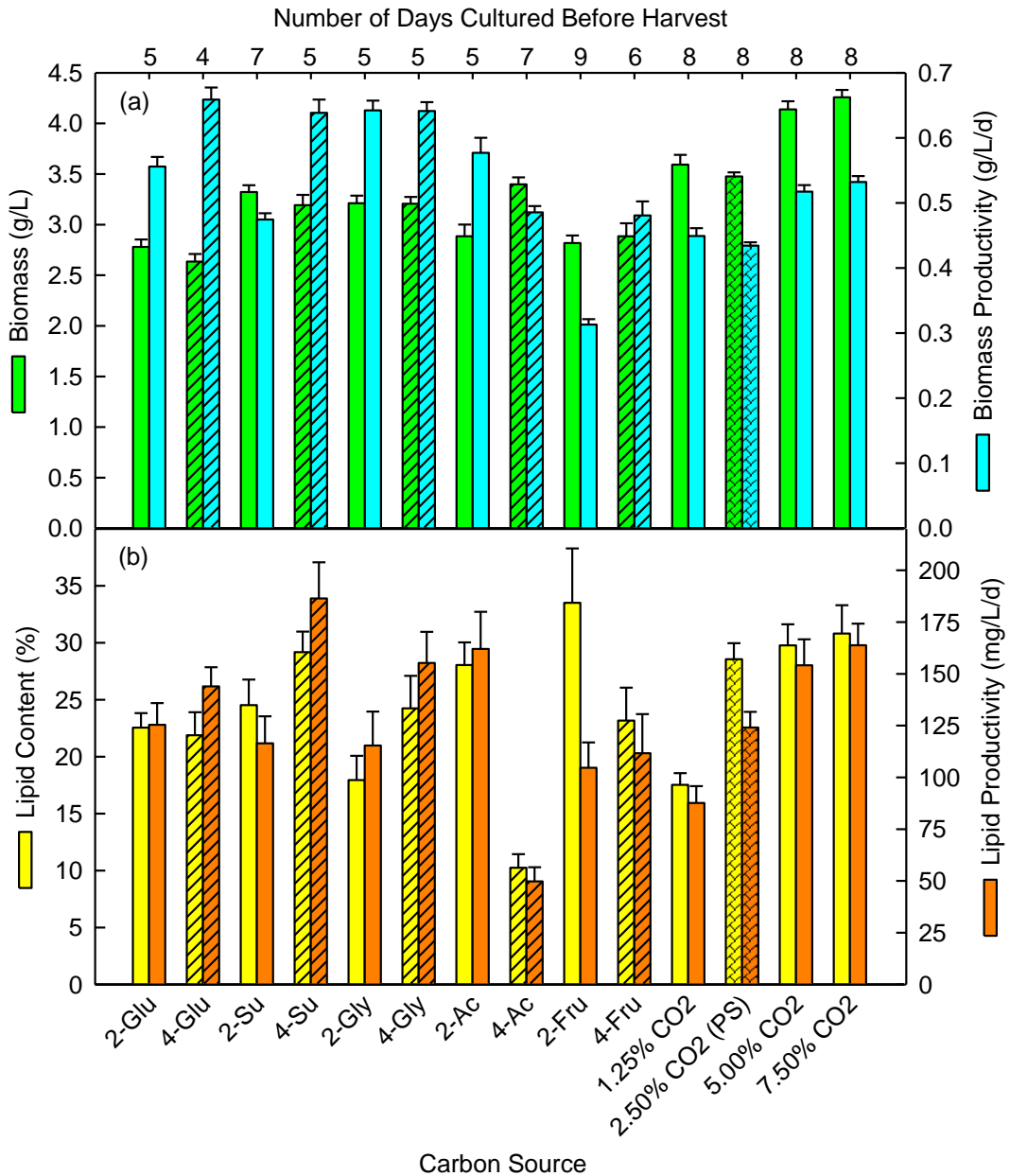


Figure 19 - Comparison of *Chlamydomonas* sp. Tai-03 biomass and lipid production when supplemented with different concentrations of organic carbons (OCs) and inorganic CO<sub>2</sub> gas, where 2 and 4 = OC concentrations in g C/L (grams of carbon equivalent per litre of culture) (PS = Previous study, Glu = Glucose, Su = Sucrose, Gly = Glycerol, Ac = Acetate, Fru = Fructose)

Figure 19b shows that the highest lipid content was achieved by adding 2-Fru ( $33.5 \pm 4.8\%$ ), an increase of 17% compared to PS ( $28.6 \pm 1.4\%$ ). The lipid content of 4-Su, 2-Ac, 5% CO<sub>2</sub>, and 7.5% CO<sub>2</sub> were similar to PS ( $29.2 \pm 1.8\%$ ,  $28.0 \pm 2.0\%$ ,  $29.8 \pm 1.8\%$ , and  $30.8 \pm 2.5\%$ ). On the other hand, from Figure 19b, the highest lipid productivity was obtained by adding 4-Su ( $186.4 \pm 17.5$  mg/L/d), an increment of 50% compared to PS ( $124.1 \pm 7.6$  mg/L/d). The lipid productivity of 2-Ac, 4-Gly, 5% CO<sub>2</sub>, and 7.5% CO<sub>2</sub> were similar to one another ( $162.0 \pm 17.9$ ,  $155.3 \pm 15.0$ ,  $154.1 \pm 12.5$ , and  $163.8 \pm 10.4$  mg/L/d), and represent an improvement of 31%, 25%, 24%, and 32% compared to PS. The tests using 2-Glu, 2-Su, 2-Gly, and 4-Fru showed similar lipid productivities as PS ( $125.4 \pm 10.5$ ,  $116.5 \pm 13.0$ ,  $115.4 \pm 16.3$ , and  $111.7 \pm 18.9$  mg/L/d). The lowest lipid content and productivity were produced by 4-Ac ( $10.2 \pm 1.2\%$  and  $49.8 \pm 6.8$  mg/L/d), although biomass concentration and productivities were not affected by the increased concentration of acetate. During cultivation of *Chlamydomonas* sp. Tai-03 with 4-Ac, the microalgae did not reach nitrogen depletion state, which is defined as the state where the medium nitrate concentration is less than 10% of the initial amount. In this case, the 4-Ac culture was harvested after the biomass growth reached stationary phase (data not shown). The use of 4-Ac also increased the amount of Na<sup>+</sup> ions (due to the sodium acetate salt) in the culture, causing greater osmotic stress to the microalgal cells. Higher osmotic stress could induce the build-up of ROS which could degrade the thylakoid lipids and PS II complex in the microalgal cells, decreasing the cells' photosynthetic efficiency (Liu et al., 2012). This could be the reason for the lower absorption of nitrate and less accumulation of lipids (Panacha et al., 2015).

In the case of inorganic carbon source, from Figure 19b, even though the highest lipid productivity was obtained using 7.5% CO<sub>2</sub>, the increment in lipid productivity from 5% CO<sub>2</sub> was only 6%. Meanwhile, the lowest CO<sub>2</sub> concentration of 1.25% gave the lowest lipid content and productivity of  $17.5 \pm 1.0\%$  and  $87.6 \pm 8.1$  mg/L/d. The low CO<sub>2</sub> concentration in the aeration stream could have

restricted the availability of inorganic carbon in the culture medium, thereby minimising the ability of microalgal cells to accumulate lipids (Gardner et al., 2013). But when the CO<sub>2</sub> concentration was increased to 5% and 7.5%, the lipid content was maintained while biomass growth was increased. This shows that a higher dosage of CO<sub>2</sub> assisted *Chlamydomonas* sp. Tai-03 in higher cell growth rather than higher lipid content. This growth pattern is similar to a study done by Ji et al. (2015), where *Scenedesmus obliquus* was cultured in municipal wastewater supplemented with 0.5% food wastewater (Ji et al., 2015). When the CO<sub>2</sub> concentration was increased from 5% to 10% and 14.1%, the biomass production increased from about 0.39 g/L to 0.43 and 0.44 g/L, whereas the lipid contents were similar (18.4%, 19.7%, and 20.0%) (Ji et al., 2015). However, in another study, Sun et al. (2015) had shown that both the biomass and lipid content of *Chlorella sorokiniana* CS-1 increased from about 2.5 g/L and 17.5% under 1% CO<sub>2</sub> to 3.3 g/L and 28.0% under 10% CO<sub>2</sub> (Sun et al., 2015). This implies that the enhancement of biomass and lipid productions under a higher dosage of CO<sub>2</sub> varies among different microalgal strains.

In this section, the best mixotrophic cultivation condition is the addition of 4 g C/L equivalent of sucrose, demonstrating high biomass and lipid productivities and lipid content ( $0.64 \pm 0.02$  g/L/d,  $186.4 \pm 17.5$  mg/L/d, and  $29.2 \pm 1.8\%$ ), with moderate biomass growth ( $3.19 \pm 0.10$  g/L). ANOVA study between PS and 4-Su shows that the addition of 4-Su significantly affected biomass productivity ( $p < 0.005$ ) and lipid productivity ( $p < 0.044$ ). Meanwhile, the best autotrophic condition is 5% CO<sub>2</sub> in terms of high biomass growth, lipid productivity, and lipid content ( $4.14 \pm 0.08$  g/L,  $154.1 \pm 12.5$  mg/L/d, and  $29.8 \pm 1.85\%$ ), with moderate biomass productivity ( $0.52 \pm 0.01$  g/L/d). ANOVA test between PS and 5% CO<sub>2</sub> reveals that increasing CO<sub>2</sub> dosage to 5% significantly increased biomass concentration ( $p < 0.009$ ) and biomass productivity ( $p < 0.009$ ). These results have shown that *Chlamydomonas* sp. Tai-03 can flourish under both autotrophic and mixotrophic cultivation without the need for any conditioning steps.



### **4.3.3. Cost analysis of the use of different organic carbon and CO<sub>2</sub> concentrations on microalgal biomass and lipid production of *Chlamydomonas* sp. Tai-03**

In Table 7, the cost of the five OCs and CO<sub>2</sub> gas cylinder used in this study as acquired from local chemical and gas suppliers are presented and the cost analysis of carbon for a single run of a 1L PBR is given. The cost of using CO<sub>2</sub> gas only at 5% concentration was higher than mixotrophic cultivation with most OCs, with the exception of fructose. Out of the four cheaper OCs, 4-Su was the best performing but the most expensive option. On the other hand, 4-Gly was the second best performing yet cheapest OC. When compared to 4-Gly, 4-Su had 21% better lipid content yield and 20% better lipid productivity yield despite a 19% increased cost. Looking at 4-Su and 5% CO<sub>2</sub>, the biomass and lipid productivities of 4-Su were higher because the cultivation time with 4-Su was 5 days, whereas with 5% CO<sub>2</sub> it was 8 days. But the lower cultivation time of 4-Su also translated to lesser biomass growth compared to 5% CO<sub>2</sub>. Although using 4-Su was cheaper than 5% CO<sub>2</sub>, the use of OC may escalate the extent of culture contamination by bacteria when scaling up, especially into an open pond system. Upon exposure to air, contamination of microalgal culture with heterotrophic bacteria is unavoidable (Erkelens et al., 2014). Although the bacteria species may not be harmful, this co-existence may lead to a need for additional preventive measures and purification processes depending on the intended application of the microalgal biomass (Chisti, 2016). Even though 5% CO<sub>2</sub> system was more expensive than 4-Su system, CO<sub>2</sub> can be sourced from fermentation off-gas or flue gas, which are free. Flue gas normally contains about 10-20% CO<sub>2</sub> concentration (Ono and Cuello, 2003; Douskova et al., 2008) and comes out at high temperatures. In this case, as *Chlamydomonas* sp. Tai-03 is not a thermotolerant strain, the temperature of the flue gas will need to be reduced first. If large-scale cultivation is involved, the hot flue gas can be cooled by heat exchangers before passing through the culture medium. This method serves to conserve operational heat energy in the process

chain and provide high CO<sub>2</sub> gas stream for the culture. In consideration of large scale microalgae cultivation for biodiesel production, most facilities employ open ponds or raceway tracks due to their easy installation and low cost (Borowitzka and Moheimani, 2013). In open systems, CO<sub>2</sub> gas is more suitable as the carbon source, but if closed systems are used, mixotrophic cultivation using sucrose becomes the better choice. In light of the fact that most biodiesel-related cultures are open systems, 5% CO<sub>2</sub> was chosen to be used in the next study.

Table 7 - Analysis of cost for organic carbons (OCs) and CO<sub>2</sub> in 1 L batch operation (as of July 2018), and comparison of biomass and lipid production yields using 5% CO<sub>2</sub> condition as a reference

Carbon Source	Cost (RM/kg)	Best Operating Condition	Cost of Carbon Input (RM/L) <sup>b</sup>	Biomass Growth Yield	Biomass Pr. <sup>a</sup> Yield	Lipid Content Yield	Lipid Pr. Yield
Glucose	50.00	4-Glu	0.91	0.64	1.27	0.73	0.93
Sucrose	48.00	4-Su	0.96	0.77	1.23	0.98	1.21
Glycerol	30.00	4-Gly	0.81	0.77	1.24	0.81	1.01
Sodium Acetate	70.00	2-Ac	0.86	0.70	1.12	0.94	1.05
Fructose	100.00	4-Fru	1.97	0.70	0.93	0.78	0.72
CO <sub>2</sub> Gas Cylinder	4.50	5% CO <sub>2</sub>	1.62	1.00	1.00	1.00	1.00

<sup>a</sup> Pr. = Productivity

<sup>b</sup> Cost of carbon input for all OCs include the cost of continuous sparging of 2.5% CO<sub>2</sub> (mixotrophic cultivation), calculated from the start of culture to day of harvest

#### 4.3.4. Effects of different medium replacement ratio on microalgal biomass and lipid production of *Chlamydomonas* sp. Tai-03

In order to assess the economic feasibility of culturing *Chlamydomonas* sp. Tai-03, a semi-batch system mode with partial culture harvest was performed for the same 1L cultivation system. Three different medium replacement ratios (MRRs) of the culture were tested, as shown in Figure 20. Continuous sparging was carried out using 5% CO<sub>2</sub> concentration at a flow rate of 0.2 vvm. When *Chlamydomonas* sp. Tai-03 was grown using 25% MRR, the biomass returned to peak value after 1 day (Figure 20a), whereas under 50% and 75% MRRs, the biomass took 5 days to reach the peak value (Figure 20b and Figure 20c). The mean peak biomass

concentration in both replacement cycles of 25%, 50%, and 75% MRR were  $4.15 \pm 0.12$ ,  $4.18 \pm 0.08$ , and  $4.27 \pm 0.14$  g/L. Meanwhile, the average biomass concentration after medium replacement in both replacement cycles of 25%, 50%, and 75% MRR were  $4.36 \pm 0.13$ ,  $3.81 \pm 0.48$ , and  $3.73 \pm 0.78$  g/L. From the observations of biomass concentration, 25% MRR had the lowest mean peak biomass but the highest average biomass after replacement. During each replacement cycle in all three MRRs, the cultures returned to nitrogen depletion state after 1 day. The rapid absorption of newly added nitrogen by the microalgal cells was reflected by high biomass productivities after 1 day, and the mean biomass productivities of 25%, 50%, and 75% MRR were  $1.23 \pm 0.02$ ,  $0.96 \pm 0.03$ , and  $1.21 \pm 0.08$  g/L/d. From Table 8, it can be seen that 25% MRR yielded the highest biomass and lipid productivities ( $1.23 \pm 0.15$  g/L/d and  $239.6 \pm 24.8$  mg/L/d). In contrast, the biomass and lipid productivities of 50% and 75% MRR were relatively low. This was because, in 25% MRR, the microalgal biomass bounced back to maximum growth in one day after the replacement was done. Since 75% of the culture was still retained after intermittent harvest, 25% MRR provided a higher initial biomass loading which promoted maximal growth. For 50% and 75% MRR, the microalgal biomass and lipid productivities reached their respective maximum five days after replacement. Since there were more nutrients available in 50% and 75% MRR compared to 25% MRR, the mean peak biomass of 50% and 75% MRR were higher than 25% MRR. Even though *Chlamydomonas* sp. Tai-03 was capable of reaching maximum biomass growth regardless of different MRRs and replacement cycles (Fig 2a, 2b, and 2c), the lipid contents could not return to the maximum amounts (28 – 31% obtained before replacement starts) after each replacement cycles (as shown in Table 8). This phenomenon may be due to nutrient limitation caused by partial medium replacements. The available nutrients were mostly utilised for biomass growth, and insufficient nutrients remained for the microalgal cells to synthesize and accumulate lipids. Therefore, 25% of MRR was chosen as the best medium replacement treatment for

*Chlamydomonas* sp. Tai-03. Upon performing ANOVA analysis of 25% MRR and 5% CO<sub>2</sub> batch culture, it was found out that biomass productivity ( $p < 4.47 \times 10^{-7}$ ), lipid content ( $p < 0.003$ ), and lipid productivity ( $p < 0.012$ ) were significantly affected under 25% MRR operation.

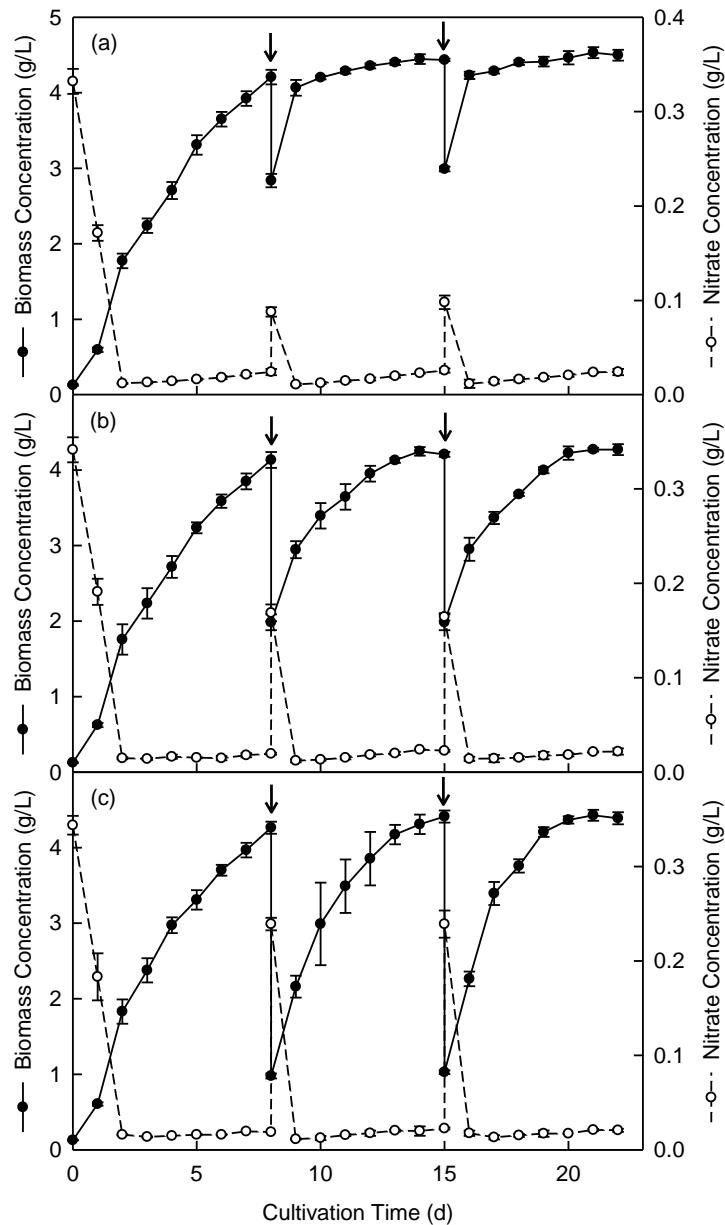


Figure 20 - Biomass growth and medium nitrate profile of *Chlamydomonas* sp. Tai-03 under semi-batch operation with medium replacement ratios of (a) 25%, (b) 50%, and (c) 75% (Arrows show the days of medium replacements)

In one study, *Desmodesmus* sp. F2 was cultivated using modified bold 3N medium in semi-batch cultivation with 50% MRR. *Desmodesmus* sp. F2 achieved a high biomass concentration and lipid content of 3.99 g/L and 45.6%, with biomass and lipid productivities of 0.67 g/L/d and 302 mg/L/d (Ho et al., 2014). In another study, *Chlorella* sp. was cultured using modified f/2 medium supplemented with artificial seawater in semi-batch mode with 50% MRR. A six-parallel photobioreactor design was used, and the growth rates of *Chlorella* sp. were the sum of six photobioreactors. *Chlorella* sp. attained a moderate lipid content of 32 – 34% with high biomass and lipid productivities of 3.20 g/L/d and 1065 mg/L/d (Chiu et al., 2008). In comparison, when *Chlamydomonas* sp. Tai-03 was switched to semi-batch mode, its biomass concentration ( $4.15 \pm 0.12$  g/L) was comparable to *Desmodesmus* sp. F2, whereas biomass productivity ( $1.23 \pm 0.02$  g/L/d) was higher than *Desmodesmus* sp. F2 (Ho et al., 2014). Looking at lipid production, the lipid content of *Chlamydomonas* sp. Tai-03 is lower than both species ( $19.4 \pm 2.0\%$ ). However, due to the rapid biomass growth of *Chlamydomonas* sp. Tai-03 after medium replacements, its lipid productivity rose to  $239.6 \pm 24.8$  mg/L/d and is comparable to *Desmodesmus* sp. F2 (Ho et al., 2014) but lower than *Chlorella* sp. (Chiu et al., 2008).

Table 8 - Comparison of different medium replacement ratio (MRR) on biomass and lipid production of *Chlamydomonas* sp. Tai-03

MRR (%)	Culture Time <sup>b</sup> (d)	Biomass		Lipid	
		Growth (g/L)	Pr. <sup>a</sup> (g/L/d)	Content (%)	Pr. (mg/L/d)
25	8	$4.21 \pm 0.10$	$0.53 \pm 0.01$	$27.6 \pm 2.1$	$145.2 \pm 14.4$
	(2 Repl) 1	$4.15 \pm 0.11$	$1.23 \pm 0.15$	$19.4 \pm 2.0$	$239.6 \pm 24.8$
50	8	$4.13 \pm 0.11$	$0.52 \pm 0.01$	$31.1 \pm 2.3$	$160.5 \pm 7.7$
	(2 Repl) 5	$4.18 \pm 0.08$	$0.44 \pm 0.02$	$21.9 \pm 2.4$	$95.6 \pm 9.9$
75	8	$4.26 \pm 0.08$	$0.53 \pm 0.01$	$28.3 \pm 2.5$	$150.9 \pm 16.0$
	(2 Repl) 5	$4.27 \pm 0.14$	$0.65 \pm 0.02$	$13.4 \pm 2.7$	$87.5 \pm 15.6$

<sup>a</sup> = Productivity

<sup>b</sup> Culture time of replacement cycles follows (X Repl) Y, where X = total number of replacements, and Y = the number of days after replacement

In Table 9, the FAME profile of *Chlamydomonas* sp. Tai-03 under different culture conditions are listed. Under all four culture conditions, the three major FAMES (palmitic acid (C16:0), oleic acid (C18:1), and linoleic acid (C18:2)) were the same. When *Chlamydomonas* sp. Tai-03 was cultured under 4-Su, the three minor FAMES (palmitoleic acid (C16:1), heptadecanoic acid (C17:0), and  $\alpha$ -linoleic acid (C18:3)) were also the same as PS. But when *Chlamydomonas* sp. Tai-03 was cultured using 5% CO<sub>2</sub> and 25% MRR, the minor FAMES shifted to  $\alpha$ -linoleic acid (C18:3) and eicosanoic acid (C20:0). The high biomass and lipid productivities of *Chlamydomonas* sp. Tai-03, coupled with the availability of three short-chain major FAMES (C16:0, C18:1, and C18:2), makes this microalgal strain a suitable candidate for biodiesel production (Nascimento et al., 2013).

Table 9 - FAME (fatty acid methyl ester) profile of *Chlamydomonas* sp. Tai-03

Condition	FAME (% weight per biomass dry weight)							
	C16:0	C16:1	C17:0	C18:0	C18:1	C18:2	C18:3	C20:0
PS <sup>a</sup>	12.56	1.59	0.97	-	6.87	4.58	1.99	-
4-Su <sup>b</sup>	9.76	1.22	1.04	-	8.64	6.68	1.86	-
5.00% CO <sub>2</sub>	11.53	-	-	-	9.34	5.08	1.80	2.04
25% MRR <sup>c</sup>	8.31	-	-	-	5.37	3.96	1.07	1.08

<sup>a</sup> = Previous study, <sup>b</sup> = 4 grams of carbon equivalent of Sucrose per liter of culture, <sup>c</sup> = Medium replacement ratio

## **4.4. Study 4 – Design of semi-closed thin layer cascade photobioreactor for microalgal culture**

### **4.4.1. Aim and objective of study**

In this study, the aim is to design a PBR suitable for different microalgal strains that can be easily fabricated, operated, cleaned, and maintained. For these purposes, a design that integrates the open TLC system with a semi-closed setup is proposed. The advantages of this semi-closed TLC PBR are:

- High surface to volume ratio of TLC system
- Reduced risk of contamination and water evaporative loss due to semi-closed setup
- Better control of growth parameters
- Using a semi-closed cover on the retention tank can protect the microalgal culture from environmental conditions while providing gas exchange via natural purging

To better understand the workings of the proposed PBR system, the benefits of using a computational fluid dynamics (CFD) program was considered. Therefore, CFD analysis was conducted to simulate the behaviours of culture flow and mixing in the proposed PBR system. The information from CFD was used to improve mixing in the semi-closed TLC PBR.

### **4.4.2. Initial design concept of semi-closed thin layer cascade photobioreactor**

Figure 21 shows the initial design concept of the semi-closed TLC PBR. The design is divided into three parts, the upper platform, the lower platform, and the retention tank. The transition basin highlighted in both upper and lower platforms is actually one unit (there is no wall in between). The function of the transition basin is to direct fluid flow from the upper platform towards the lower platform. The lower

basin is used to reduce the culture thickness from 5 cm to 3 cm. This is achieved by placing a 3 cm baffle on the far side of the lower basin (shown in Figure 23) before releasing the culture into the retention tank. The presence of the lower basin helps to ensure culture thickness of 5 cm is maintained in the sloping region of lower platform. The cascade outlet cover is attached onto the empty space on the retention tank, allowing fluid flow into the retention tank and providing shelter from the environment. During operation, the culture is pumped from the retention tank to the upper platform, where it travels down to the lower platform and back into the retention tank. When the culture returns to the tank, this cycle repeats again. Mixing is done passively via the movement of the culture through the PBR. Rubber pipes are inserted into the retention tank via openings (shown in Figure 24) for aeration with air and CO<sub>2</sub> gas.

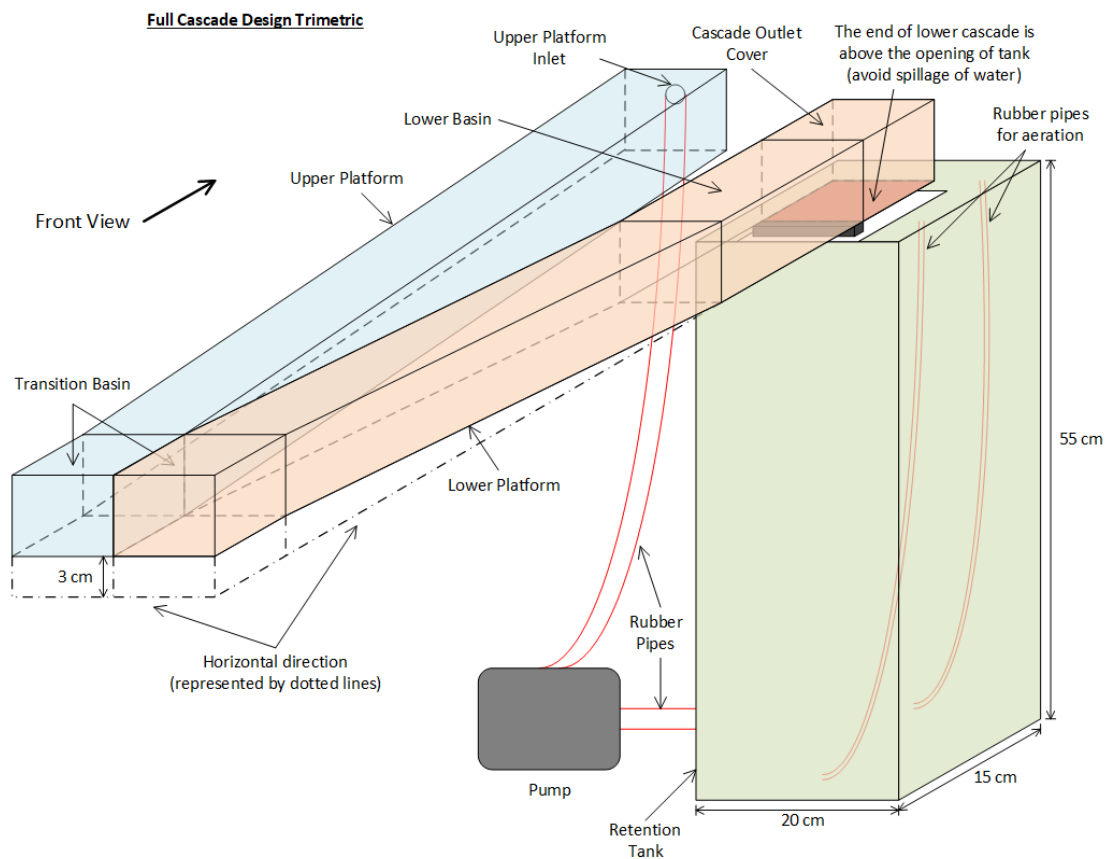


Figure 21 – Trimetric view of semi-closed thin layer cascade photobioreactor design



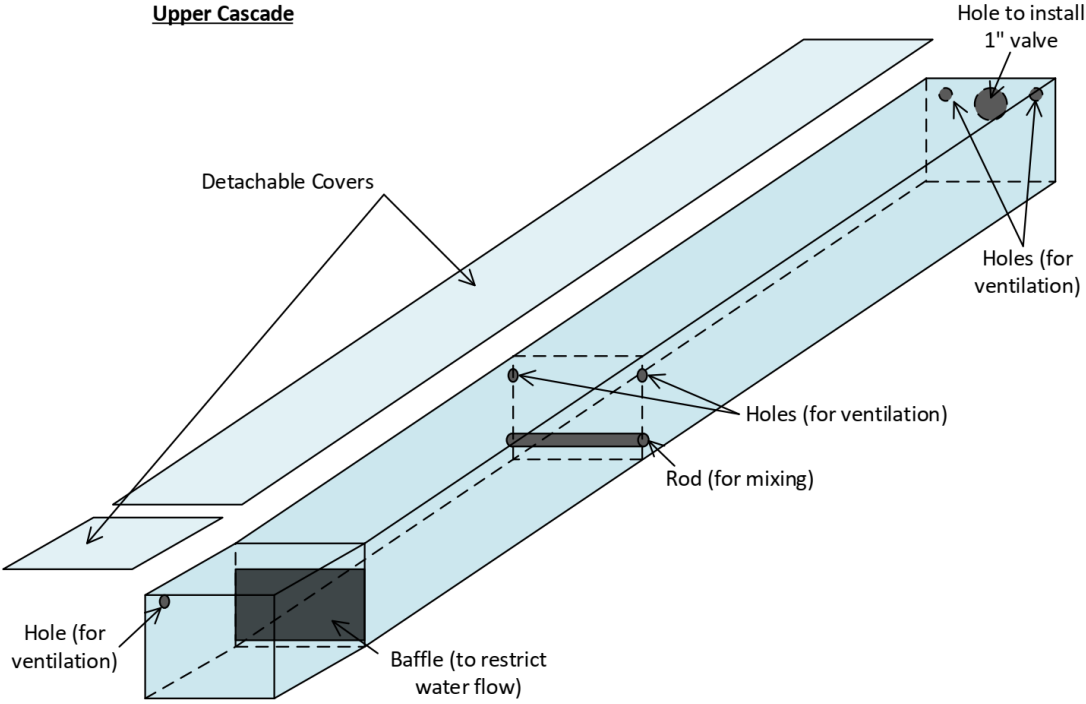


Figure 22 – Trimetric view of upper platform

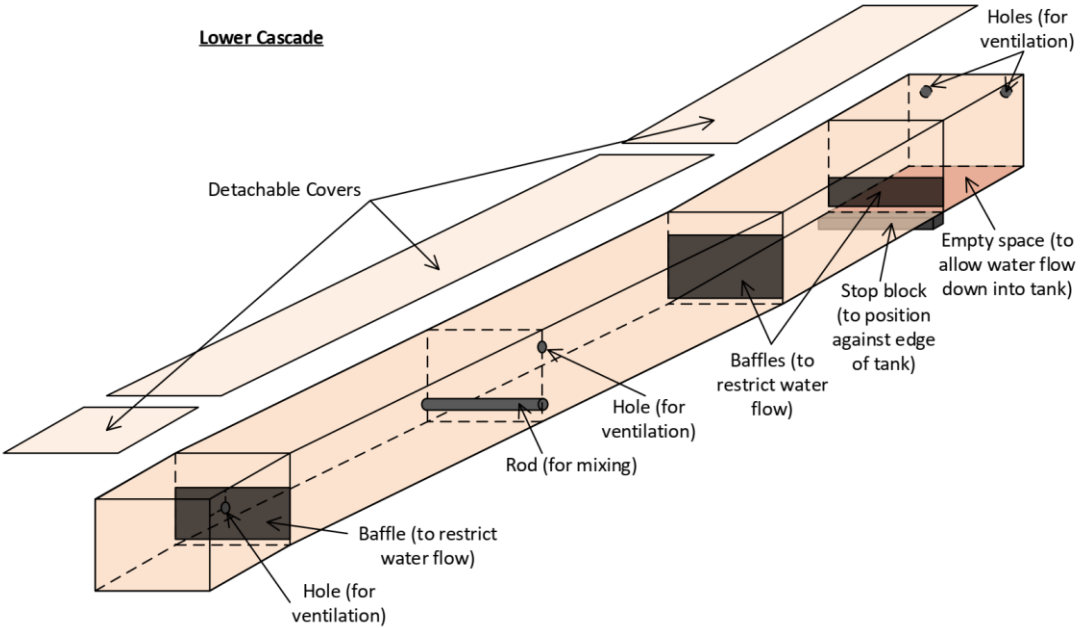


Figure 23 – Trimetric view of lower platform

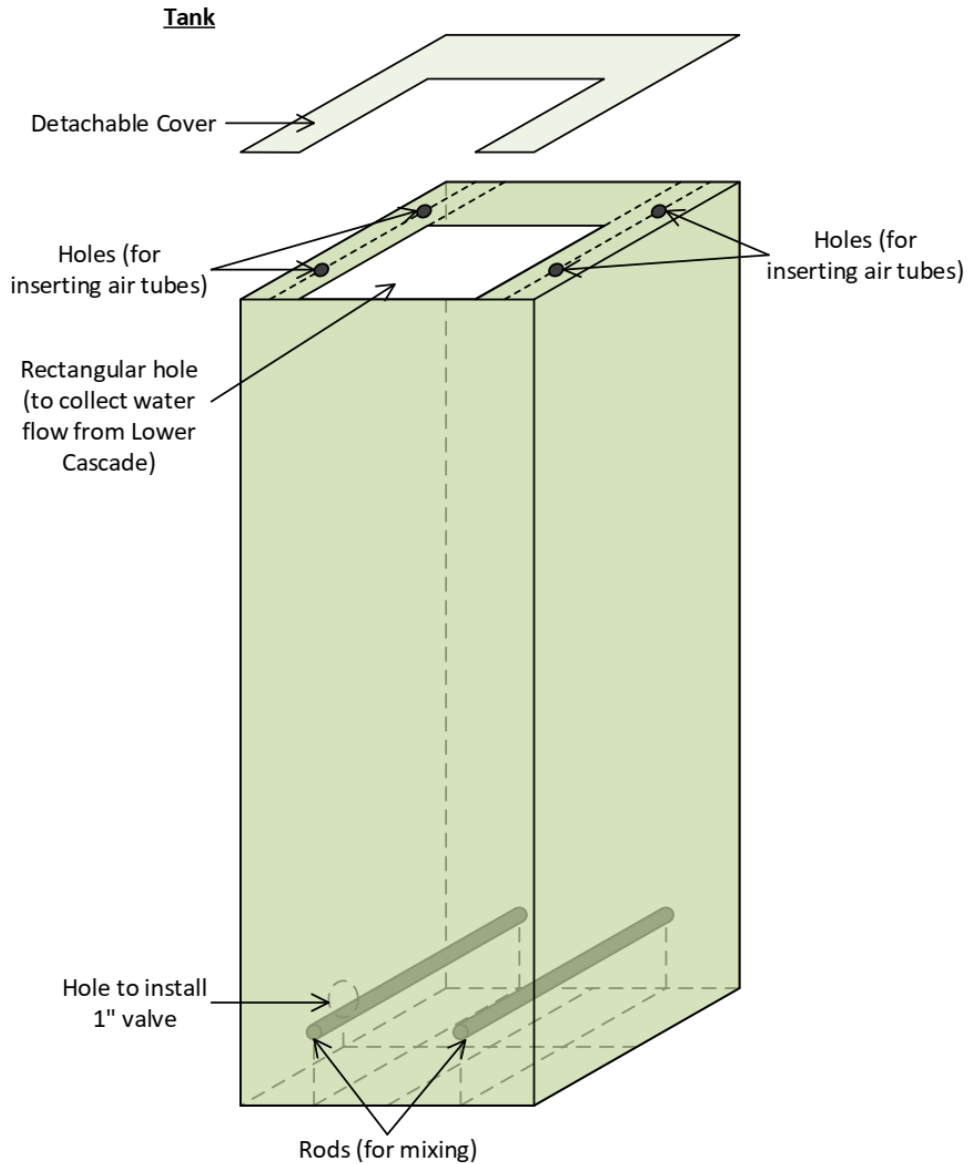


Figure 24 – Trimetric view of retention tank

In Figure 22, Figure 23, and Figure 24, the different fittings within each part of the PBR have been labelled and their functions briefly described. Apart from utilising detachable transparent covers (made from acrylic), another feature of this design is the use of rectangular baffles which allow fluid flow below and above the baffles. In both the upper and lower platforms, all the baffles have a clearance height of 0.5 cm below them. This baffle feature may aid in mixing when the culture thickness is maintained at 3 – 6 cm. This culture thickness range was chosen

because there would still be sufficient light penetration in cultures less than 5 cm thickness (Masojídek and Prášil, 2010).

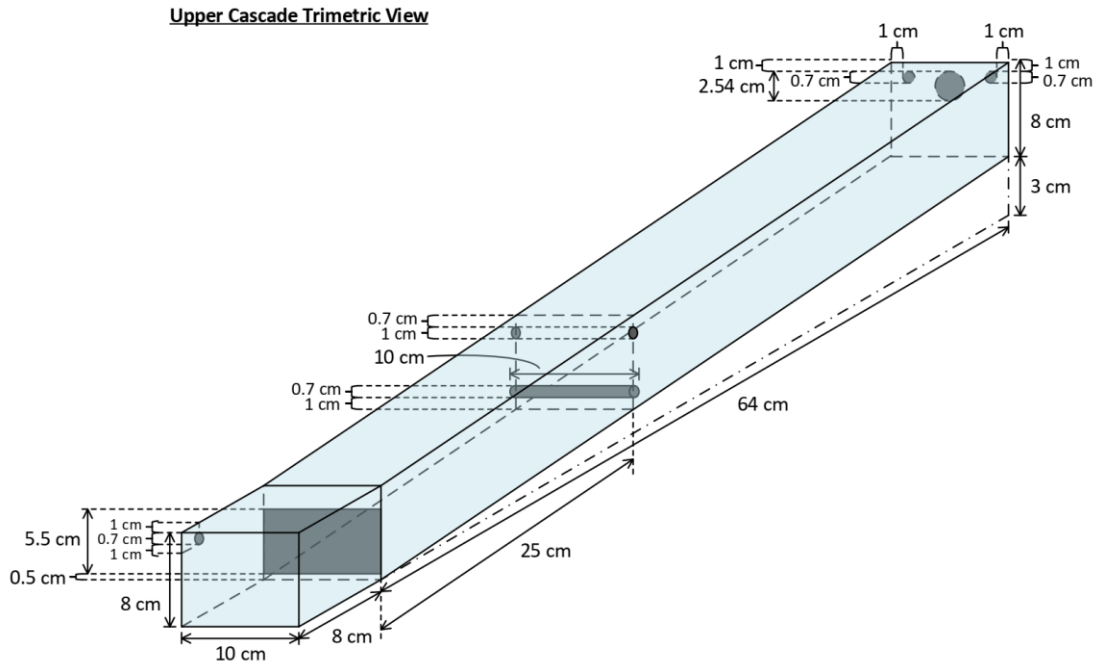


Figure 25 – Dimensions of upper platform

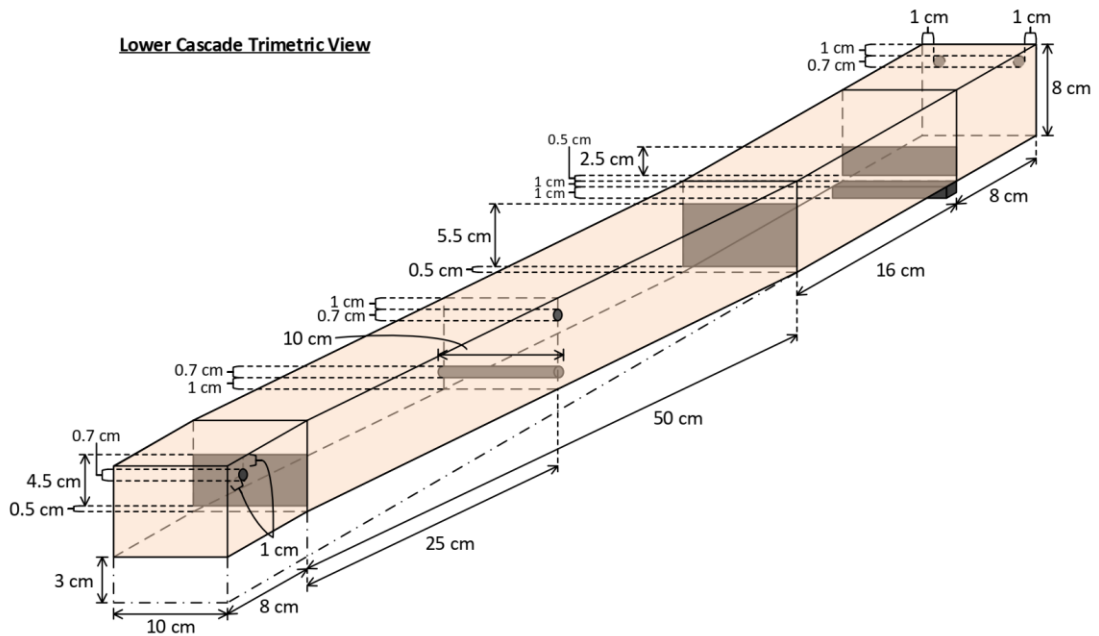


Figure 26 – Dimensions of lower platform

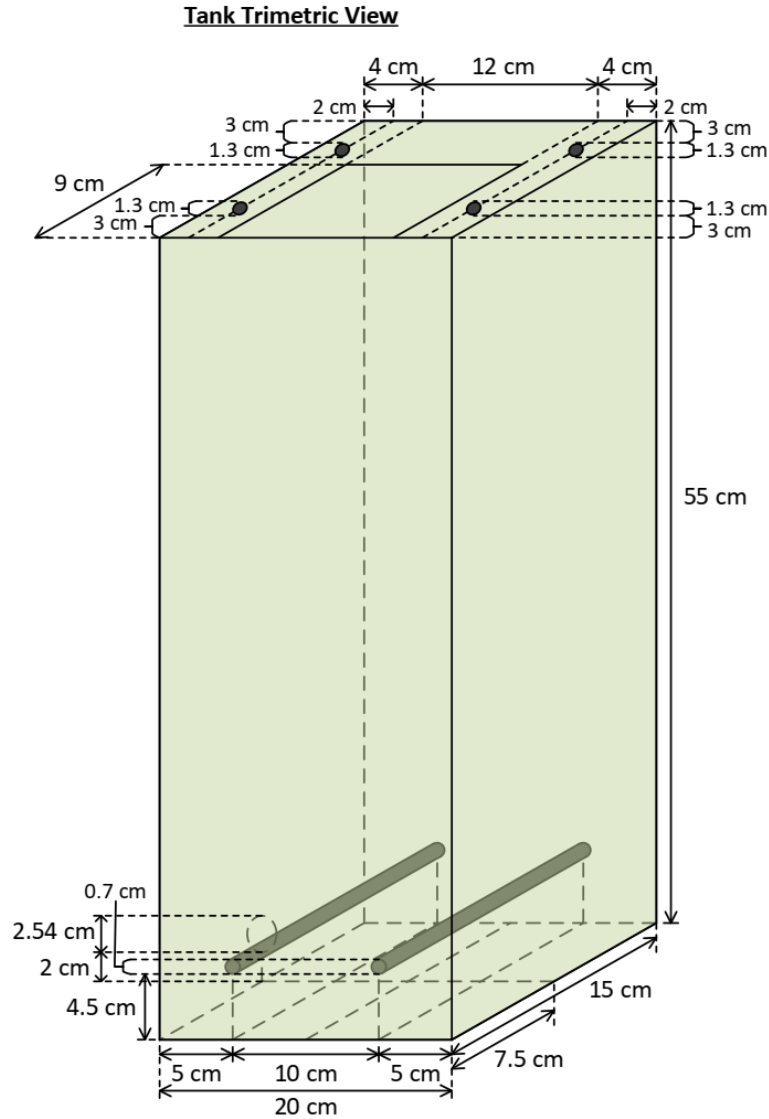


Figure 27 – Dimensions of retention tank

Figure 25, Figure 26, and Figure 27 shows the dimensions of the upper platform, lower platform, and retention tank respectively. In Figure 25, the upper platform is divided into two regions, where the sloping part has a chosen length of 64 cm and an incline of 3 cm (2.7°). The main sloping portion of both the upper and lower platforms were arbitrarily chosen as 50 cm as a starting point. However, on the upper platform, and additional 14 cm was added to its length. This 14 cm would give more room to install an additional pipe to direct the culture flow at the upper platform inlet. Since the culture velocity was calculated as 0.99 m/s, the installed pipe would aid in slowing down and directing the culture flow. Another

reason for the 14 cm extension was to provide room for the installation of a support stand to hold the PBR in place. The degree of inclination of both platforms were recommended to be around  $0.5 - 3^\circ$  so that the culture flows down the platforms at a moderate speed, increasing the amount of time the culture was exposed to light (Masojídek et al., 2015). Taking this into consideration, the degree of inclination was chosen to be close to  $3^\circ$ . In this case, the incline was taken to be 3 cm ( $2.7^\circ$ ) because whole numbers are easier to deal with during fabrication process.

In Figure 26, the lower platform is divided into 4 regions, and the sloping region has a chosen length of 50 cm with an incline of 3 cm ( $3.4^\circ$ ). Small holes of diameter 0.7 cm are located on both the upper and lower platforms as a means of ventilation. The diameter of the holes was chosen as 0.7 cm because  $1/8''$  rubber tubes (with total diameter of about 0.63 cm) can be fitted properly for pressure relieve purposes. Another function of the rubber tubes would be to minimise the amount of external contaminants (such as rain water, atmospheric air, and insects) that can enter the PBR and mix with the microalgal culture. The entire PBR was designed to be sealed except for the 0.7 cm holes found along the body of the PBR. The cylindrical rods of 0.7 cm are placed 1 cm vertical from the surface of both platforms to promote mixing of microalgal cells and minimise sedimentation. The stop block in the lower platform would serve as a way to position the sloping platforms properly onto the retention tank. The wall height of both platforms are 8 cm, taken to be 2 cm greater than the highest baffle height of 6 cm. The allowance of 2 cm helps to ensure that the culture does not come in contact with the transparent covers, and the culture is still close to any external light source placed above the transparent covers.

In Figure 27, the retention tank was designed with the net positive suction head available ( $NPSH_a$ ) of the pump in consideration, which is a Hailea HX6530 model centrifugal pump (Hailea Group Co., Ltd, RaoPing County, GuangDong Province, China). The centrifugal pump can be used as an external pump or a submerged pump. Although the net positive suction head required ( $NPSH_r$ ) of the

pump is not given by the manufacturer, but considering that a submerged pump must be fully underwater for it to operate properly and efficiently, it is thought that the  $NPSH_a$  of the retention tank will have to be greater than the height of the pump. Given that the maximum height of the pump is 17 cm, the minimum culture height in the retention tank must be above 17 cm. From the dimensions of the retention tank in Figure 27, the maximum volume of the retention tank is 16.5 L. From the dimensions of the upper platform in Figure 25 and lower platform in Figure 26, the total working volume of both platforms during steady-state operation is close to 6 L. If an initial culture volume of 13 L is prepared, the remaining culture volume in the retention tank during steady-state operation would be close to 7 L, which translates to a culture height of 23 cm. The 1" outlet valve of the retention tank is located 2 cm from the bottom of the tank (Figure 27). After deducting the vertical height of the centre point of the outlet valve (3.27 cm), the final culture height with respect to the pump's centre point is roughly 20 cm. The centre point of the tank outlet valve is in line with the centre point of the impellers of centrifugal pump. The final culture height of 20 cm satisfies the 17 cm head estimation. The total volume and dimensions of the retention tank were chosen (as in Figure 27) so that the maximum volume (16.5 L) exceeds the operation volume (13 L) by a factor of about 1.2 and the final culture height (20 cm) exceeds the estimated head required by the pump (17 cm).

At the start of the semi-batch TLC PBR, the microalgal culture would be pumped from the retention tank to the sloping platforms above. This indicates that the centrifugal pump is the heart of the operation, and choosing a suitable pump takes priority. For this design, Hailea HX6530 centrifugal pump was selected. Hailea HX6530 centrifugal pump has a rated pump capacity of 1750 L/h. The hose inlet diameter to the upper platform (as shown in Figure 25 as the hole to install 1" valve) was chosen to be 1" (2.54 cm) so that the culture velocity was not excessively high. By using the following equation, the culture inlet velocity was calculated to be 0.99 m/s.

$$v = \frac{Q}{A} \quad (17)$$

Where  $v, Q, A$  refer to the velocity of the fluid, volume flow rate of the fluid, and cross-sectional area of the pipe.

As microalgae are best cultivated in liquid medium which are properly mixed and aerated, Bernoulli's equation is important in the calculation of steady-state fluid flow across baffles in the PBR. Bernoulli's equation is represented as:

$$P_1 + \frac{1}{2}\rho v_1^2 + \rho g h_1 = P_2 + \frac{1}{2}\rho v_2^2 + \rho g h_2 \quad (18)$$

Where  $P_1, v_1, h_1$  refer to the pressure, velocity, and height of the fluid at point 1, while  $P_2, v_2, h_2$  refer to the pressure, velocity, and height of the fluid at point 2.

The equation of continuity states that for an incompressible fluid flowing across an enclosure with different cross-sectional area, its mass flow rate is the same across all cross-sections. The equation of continuity is used to calculate overflow rate of fluid over the baffles. The equation of continuity is represented as:

$$\rho_1 A_1 v_1 = \rho_2 A_2 v_2 \quad (19)$$

Where  $\rho_1, A_1, v_1$  refer to the density of the fluid, cross-sectional area of the enclosure, and velocity of the fluid at point 1, while  $\rho_2, A_2, v_2$  refer to the density of the fluid, cross-sectional area of the enclosure, and velocity of the fluid at point 2.

### 4.4.3. CFD simulation of initial concept

#### 4.4.3.1. Drawing of upper and lower platforms in ANSYS

ANSYS CFX was used for the CFD analysis of the semi-closed TLC PBR to study fluid flow patterns and mixing in the PBR. ANSYS DesignModeler software was employed to draw the required geometry for the PBR. When drawing in DesignModeler, it is often better to represent the object or domain of interest in simple ways. For

instance, in this study, rectangular blocks were drawn to model the real-life PBR, and all the blocks were joined into a single body. The property of the body was then changed to fluid domain (Figure 28). In light of the high fluid inlet velocity in the upper platform, an inlet tube was simulated as well (shown in Figure 30). In real-life, the inlet tube could be made using rubber tube with larger internal diameters than the upper platform inlet diameter.

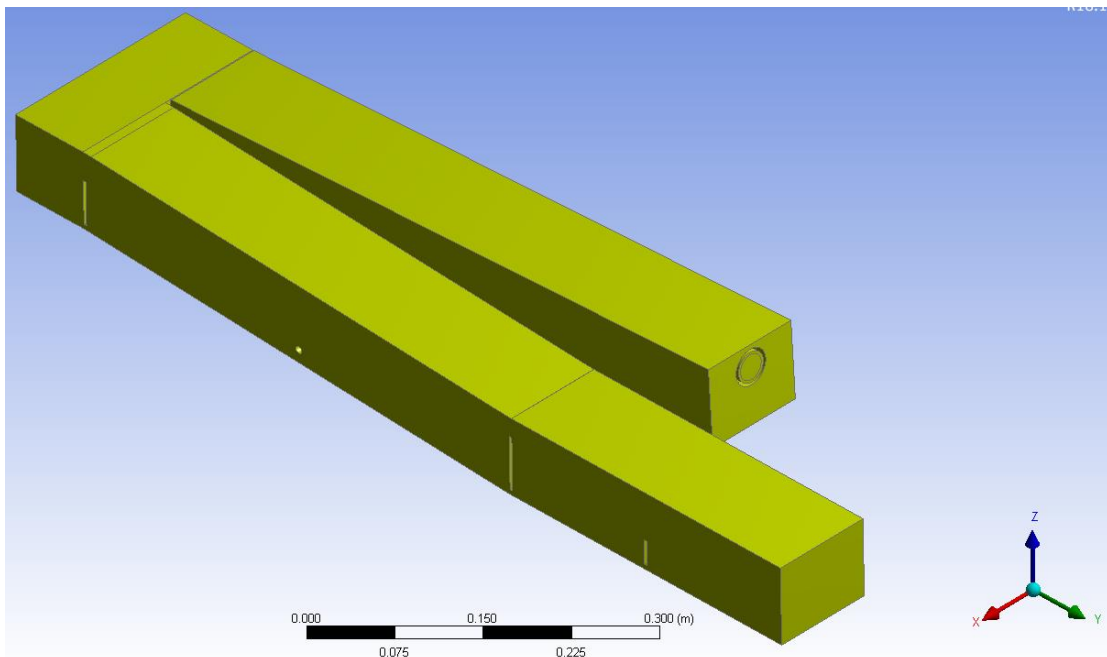


Figure 28 – Drawing of initial concept of semi-closed thin layer cascade photobioreactor in ANSYS DesignModeler

#### 4.4.3.2. Meshing of drawing in ANSYS

The mesh was done using ANSYS Meshing software. Under Mesh > Sizing, the options “relevance centre” and “span angle centre” were changed from the default values of “medium” to “fine”. Changing these settings increased the mesh quality of the upper and lower platform, as shown in Figure 29. These settings gave a total number of nodes and elements of 45,580 and 237,602. The rest of the options were left at their default settings. In Figure 30, upon selecting the drawing in Meshing, the areas of interest became highlighted in green. The geometry and features that was drawn in DesignModeler became clear this way.



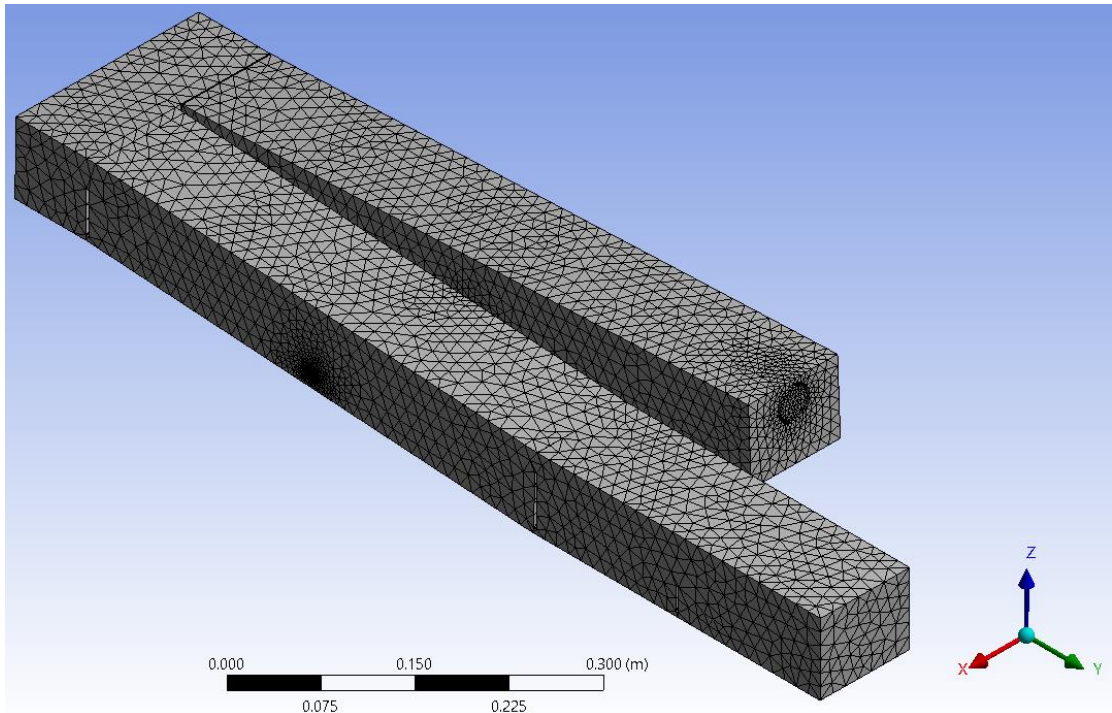


Figure 29 – Meshing of initial concept of semi-closed thin layer cascade photobioreactor in ANSYS Meshing

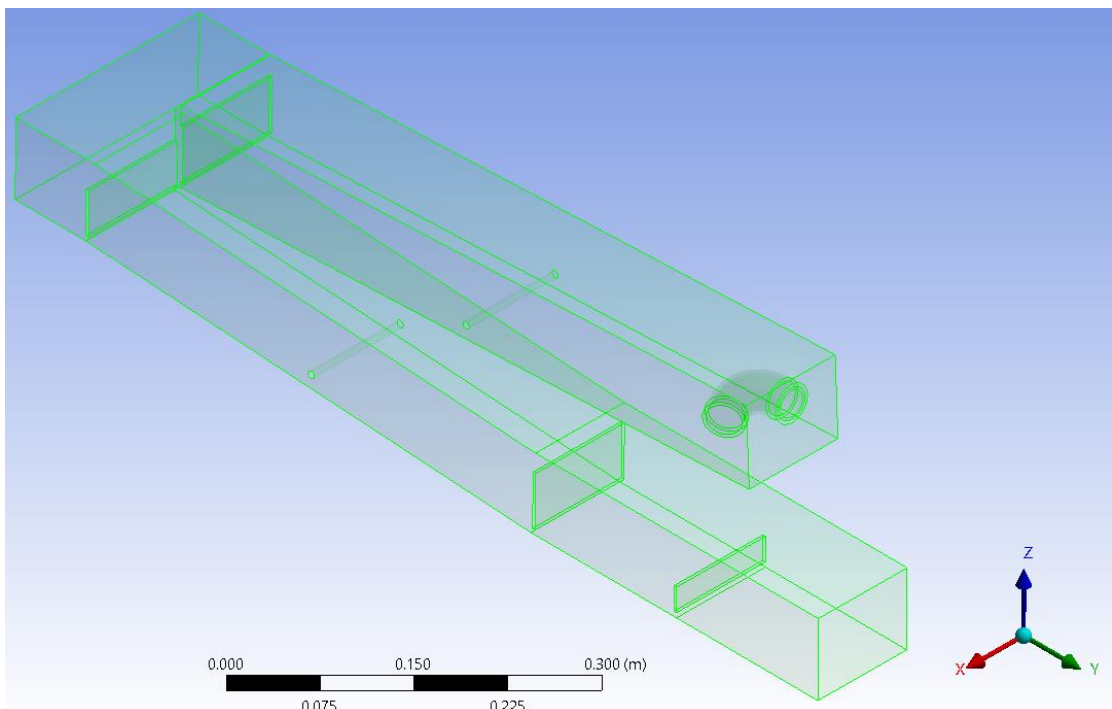


Figure 30 – Green highlight of initial concept of semi-closed thin layer cascade photobioreactor in ANSYS Meshing

#### 4.4.3.3. Setup of simulation in ANSYS

The simulation setup was done in ANSYS CFX-Pre software. The simulation was run as steady state. This was because the culture volume was expected to reach a maximum and steady state (controlled by the height of the rectangular baffles) as the time of operation proceeded. The PBR drawing was divided into 4 different groups, namely FreeTop (Figure 31a), Outlet (Figure 31b), Walls (Figure 31c), and WaterInlet (Figure 31d). The “FreeTop” here referred to the covers of the PBR, in this case the top surfaces of the drawing, and all the top surfaces were treated as an opening. An opening-type boundary condition allows easier calculation and convergence for the program since air could move freely in and out of the top surfaces, as shown by the double-directional blue arrows in Figure 31a. The “Outlet” condition was set at 0 atmosphere (atm) static pressure and was marked by black arrows exiting the lowest part of the lower platform in Figure 31b. The outlet condition ensured that air or water only flowed out of the lower platform. The “Walls” condition was set to no-slip walls and smooth walls. This meant that fluid flow very close to the walls of the system would experience zero flow, and the fluid velocity would recover as the fluid moved away from the walls. The “WaterInlet” condition was set as 0.485 kg/s of water flow, which was a conversion done by using 1,750 L/h capacity of the pump and water density of 997 kg/m<sup>3</sup> at 25°C. Only the specified fluid (in this case water) could enter the “WaterInlet” boundary, and this was marked by the black arrow pointing into the system in Figure 31d.

The entire PBR system was configured to contain only air and water. This was because the PBR was thought to have only air and culture during operation. The culture was thought to be mostly water as even highly-dense microalgal cultures contain only a maximum of 30 g/L dry biomass in autotrophic cultures (Perez-Garcia et al., 2011). If there were 30 g/L of microalgal biomass present in water, that would only increase the total density of the fluid system (water + microalgal cells) by 3%. This density increase of 3% was thought to be negligible when running the simulation. In the simulation, both air and water were simulated

at 25°C, with gravity acting in the negative Z-direction (the compass could be found in the lower right corner of Figure 31). The PBR system was run as a multiphase homogenous model. According to the user guide within ANSYS, if in a multiphase system, each fluid has distinct profiles but share an interphase region, homogenous model is recommended for faster convergence.

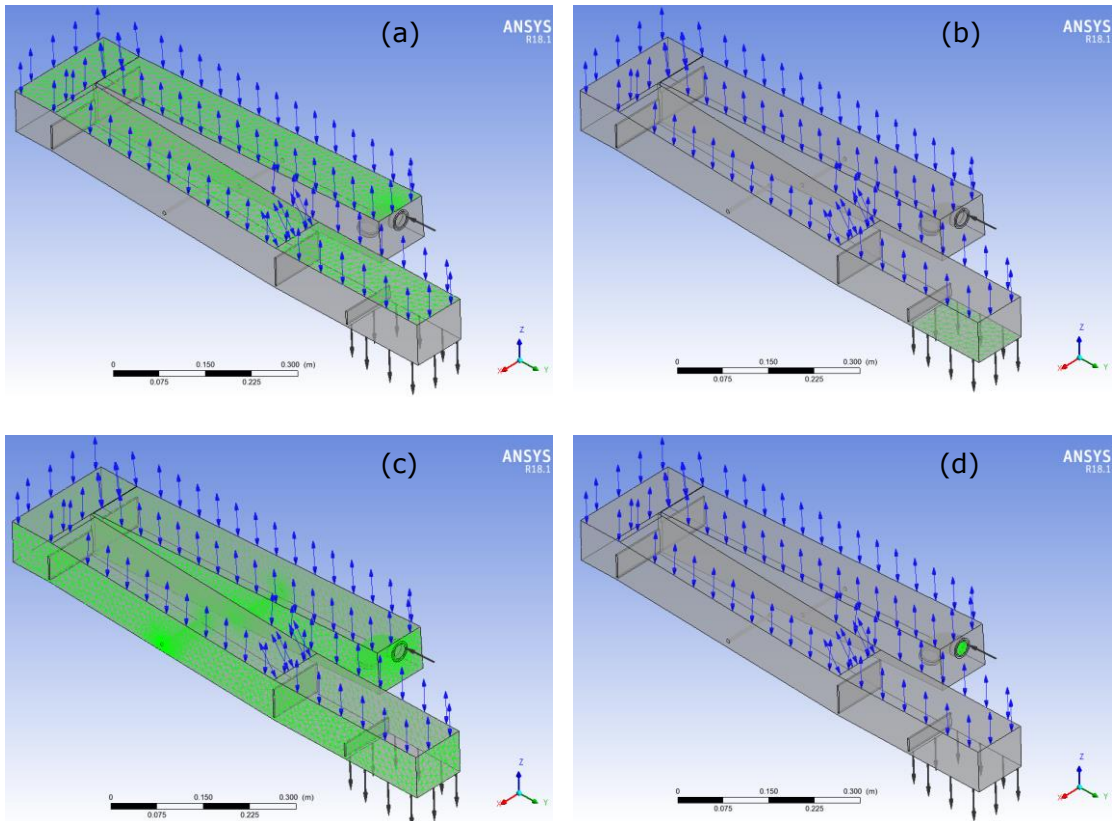


Figure 31 – The four main boundaries in ANSYS CFX-Pre, namely (a) FreeTop, (b) Outlet, (c) Walls, (d) WaterInlet

The initial conditions set at the start of the simulation was 100% air volume fraction and 0% water volume fraction. The “mesh adaption” function was also used to refine the mesh at areas affected by the adaption criteria specified. In this case, the adaption criterion was set as “water volume fraction”. This would help to solve for clear boundaries between air and water volume fractions in the simulation results.

#### 4.4.3.4. Results of simulation in ANSYS

As shown in Figure 32, there was a clear distinction between water volume fraction and air volume fraction from the simulation results. This showed that mesh adaption was very helpful in calculating and segregating the water and air fractions in the PBR. From Figure 33a, it could be seen that water inlet velocity was very high, but was slowed significantly upon exiting the inlet tube. Although most of the water flow region in the upper platform had velocities of around 0.25 m/s, there was still significant areas with close to zero flow, such as areas close to the opening of the rubber tube, behind the rubber tube, and close to the bottom of the upper platform. These areas would result in microalgal cells sedimentation if not treated properly. The water velocity in the transition basin was around 0.25 m/s, and close to zero flow near the bottom of the basin. In Figure 33b, although the water velocity was mostly around 0.25 m/s and reached more than 0.5 m/s when overflowing across the baffles, the close to zero flow near the bottom of the lower platform would still pose an issue for cell sedimentation.

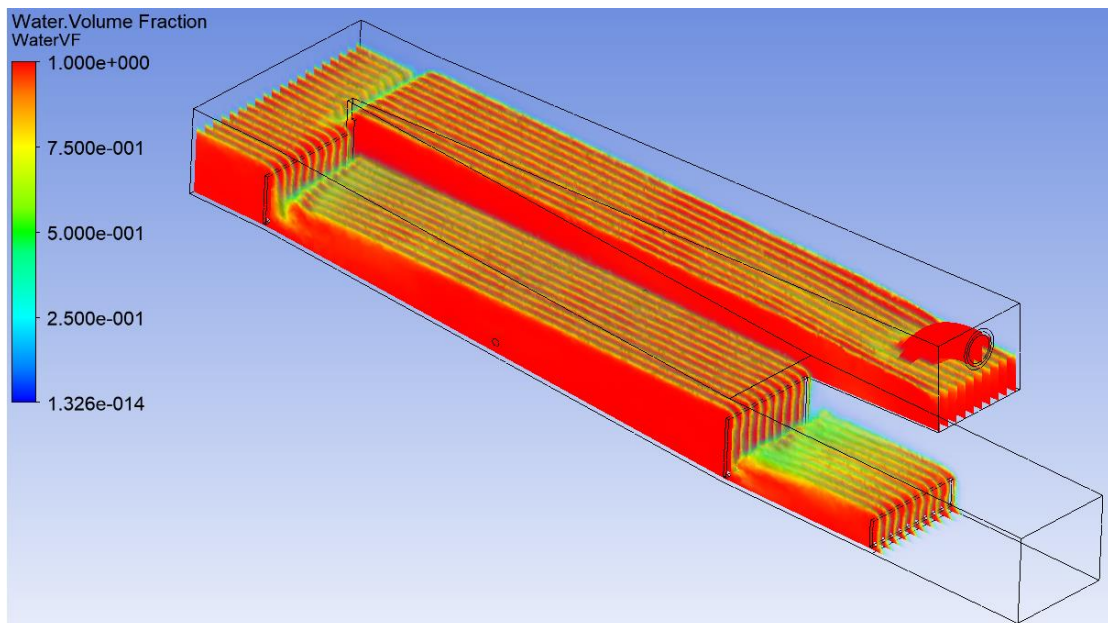


Figure 32 – A clear representation of water volume fraction in ANSYS CFD-Post

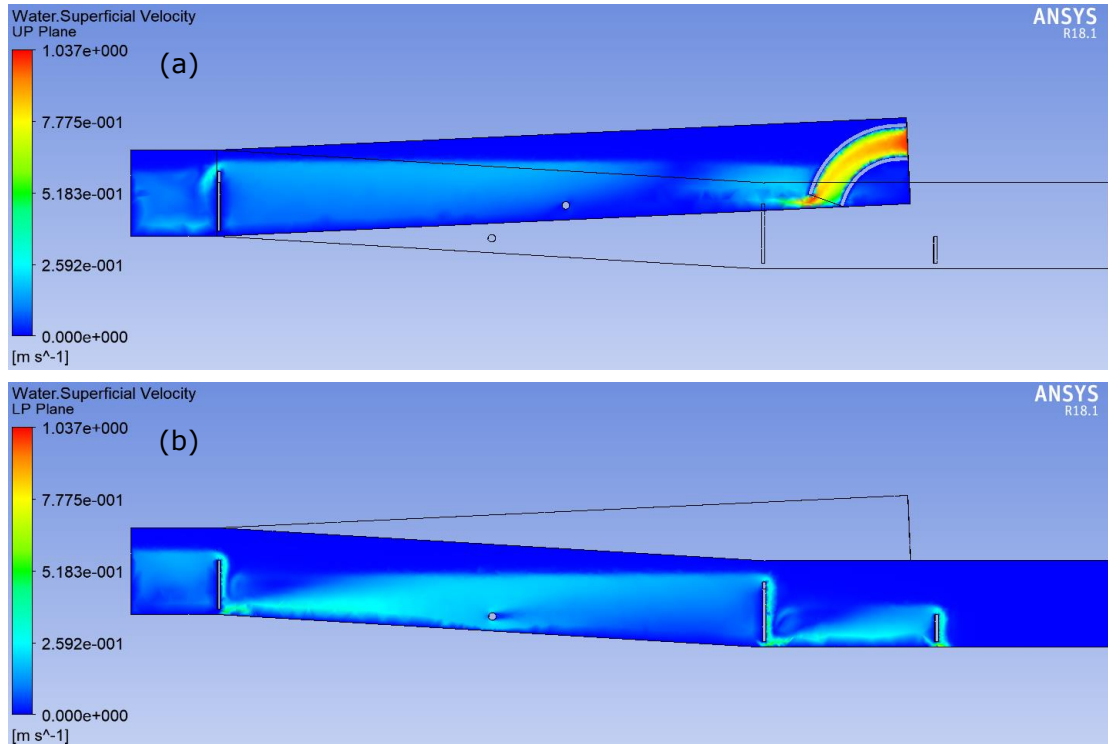


Figure 33 – Water velocity of (a) the upper platform and (b) the lower platform in ANSYS CFD-Post

#### 4.4.4. Improvement of the initial concept of semi-closed thin layer cascade photobioreactor

To solve the issue of zero flow near the bottom of the sloping platforms and behind the inlet tube, the initial concept was proposed to be improved by adding more mixing rods in both upper and lower platforms (as shown in Figure 34). The addition of mixing rods was thought to aid in increasing water velocities near the bottom of the platforms, thereby minimising cell sedimentation. The opening of the inlet tube was elevated slightly so that its water output was aimed more towards the centre of the upper platform rather than towards the bottom of the platform. Altering the inlet tube was thought to aid mixing in the upper platform. A portion of the PBR below the inlet tube was also cut away to minimise the area where stagnant flow occurred behind the inlet tube.

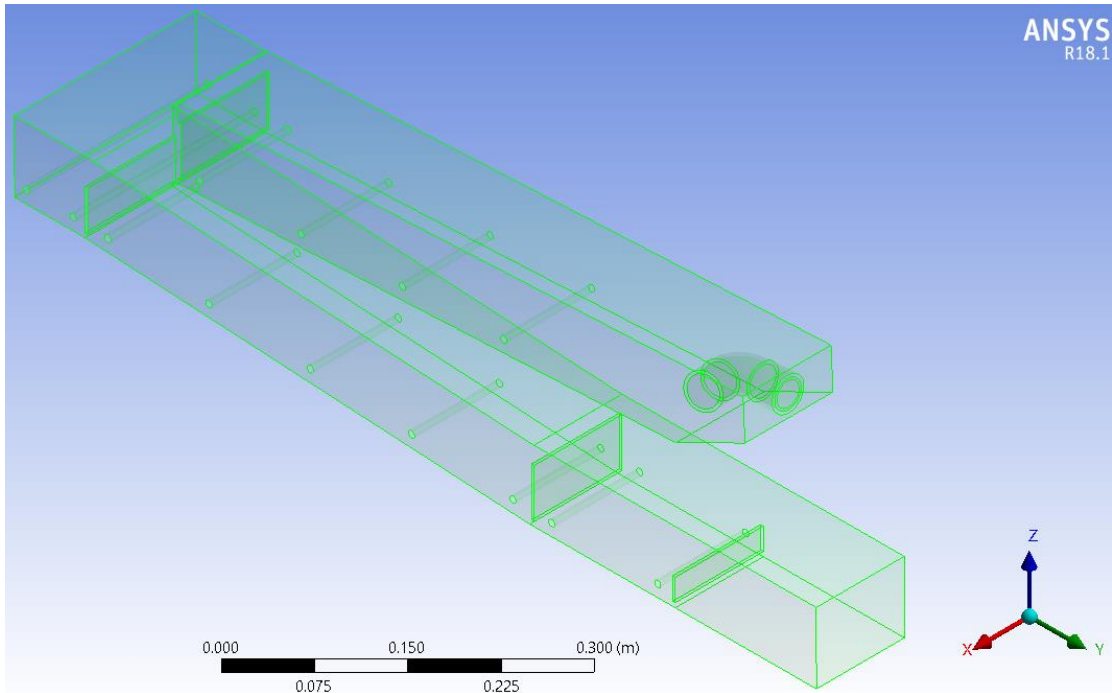


Figure 34 – Improved concept design by addition of more mixing rods, slight elevation of the opening of inlet tube, and cutting away of portions of the photobioreactor below the inlet tube (to minimise the stagnant flow behind the inlet tube)

#### 4.4.4.1. Meshing and setup of the proposed improvements in ANSYS

The meshing of the improved PBR was done using the default settings of “medium” value in both the “relevance centre” and “span angle centre” functions. This was because the addition of mixing rods increased the complexity of the PBR, and this would lead to large numbers of nodes and elements for the simulation to run. This would increase the run-time of the simulation and burden on the computer. With the mesh settings on “medium”, the total number of nodes and elements were 54,435 and 282,246. If the mesh settings were on “fine”, the total number of nodes and elements would jump to 256,135 and 1,381,483. The medium mesh could be used to first obtain good results, after which the mesh could be refined to a higher quality and solved to find out if the simulation results were sensitive to mesh quality. The medium mesh of the new PBR is shown in Figure 35. In CFX-Pre, all the parameters of the simulation remain unchanged from the previous run.

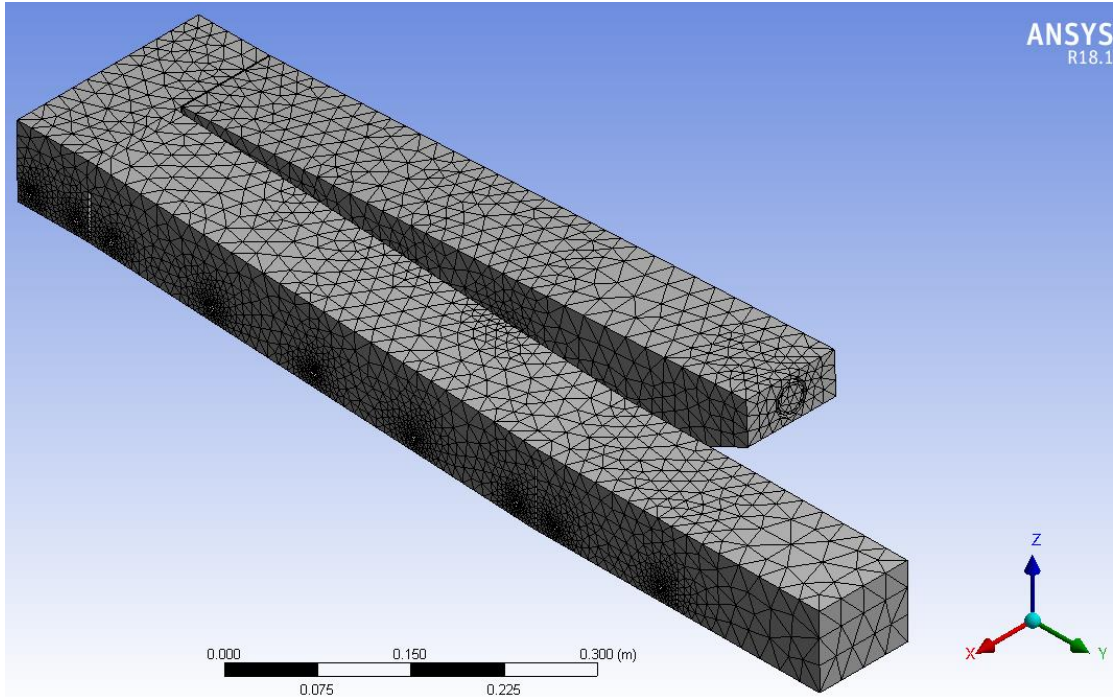


Figure 35 – Mesh of the improved photobioreactor concept design

#### 4.4.4.2. Simulation results of the proposed improvements in ANSYS

As seen in Figure 36a, the elevated inlet tube and four mixing rods in the upper platform caused a rise in water velocity close to the bottom regions of the upper platform. Similar to the results in Section 4.4.3.4, the middle region of the upper platform still experienced close to zero flow. The reason for this could be due to the direction of water from the inlet tube, which pushed water further near the bottom region rather than the top region of the upper platform. From Figure 36a and Figure 36b, the inclusion of two mixing rods in the transition basin had encouraged higher water velocities in the bottom region near the upper plate. In the region before the lower plate, the inner region of the transition basin showed zero flow. This could be due to the direction of water flow down into the sloping region of the lower platform. However, the increased water velocities in the transition basin could promote circulation of microalgal cells and reduce sedimentation. In Figure 36b, the addition of mixing rods in the lower sloping platform and lower basin had increased the water velocities near the bottom of both areas in the lower platform.

Mixing would become better since the higher velocity of water would circulate any microalgal cells and return the cells back into the retention tank. The microalgal cells could restart their travel through the TLC PBR system. The improved PBR system had performed satisfactorily in preventing microalgal cell sedimentation by having considerable water velocities throughout the water-filled regions in the PBR. Therefore, the improved concept design was chosen for a mesh independence study in the next section.

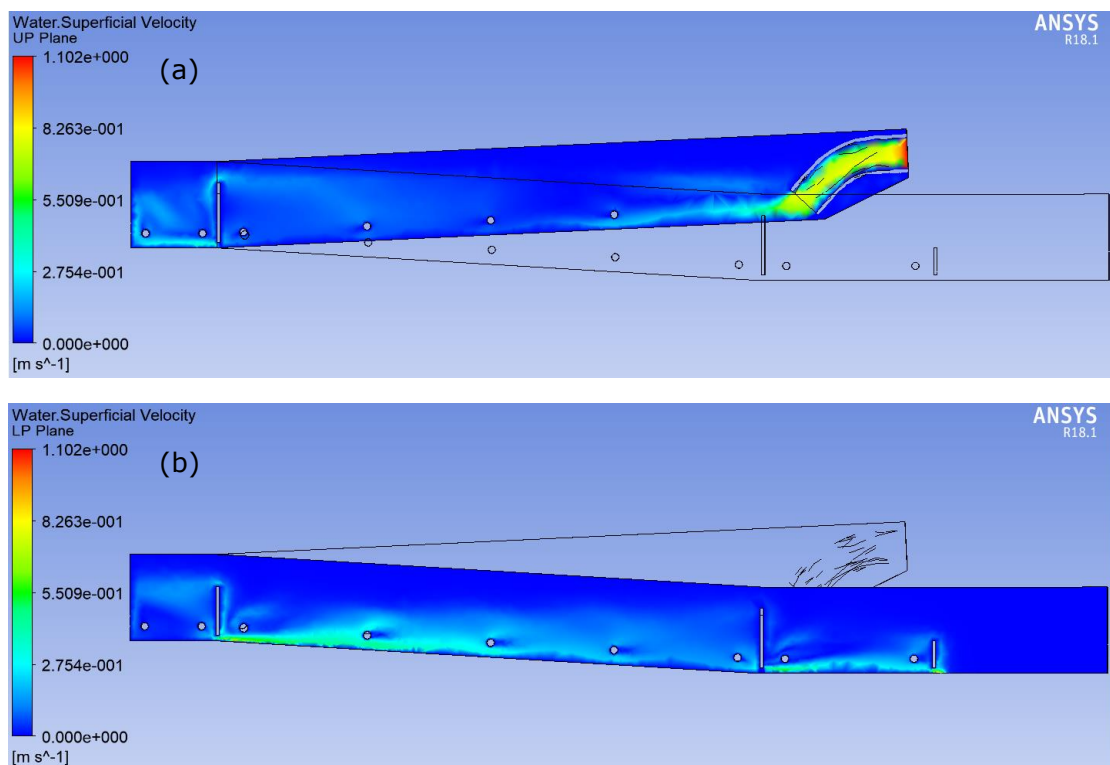


Figure 36 – Simulation results of the improved photobioreactor concept design where (a) represents the upper platform and (b) represents the lower platform

#### 4.4.4.3. Mesh independence study of improved PBR concept design

A mesh independence study was conducted on the improved PBR concept design to determine whether the simulation results in Section 4.4.4.2 were sensitive to mesh quality. The mesh quality of the improved PBR design was enhanced so that the total number of nodes and elements of the new mesh was increased by about



two-fold compared to the previous mesh, as seen in Figure 37. The total number of nodes and elements of the new mesh became 105,442 and 542,073. The simulation results shown in Figure 38 was similar to the results in Figure 36. The only difference between the two simulation results was the zero velocity flow at the middle two mixing rods in upper platform in Figure 38. However, this difference was not significant as the water velocity in the same region in Figure 36 was also approaching zero flow. Therefore, the medium mesh produced reliable simulation results and the results were not sensitive to mesh refinement.

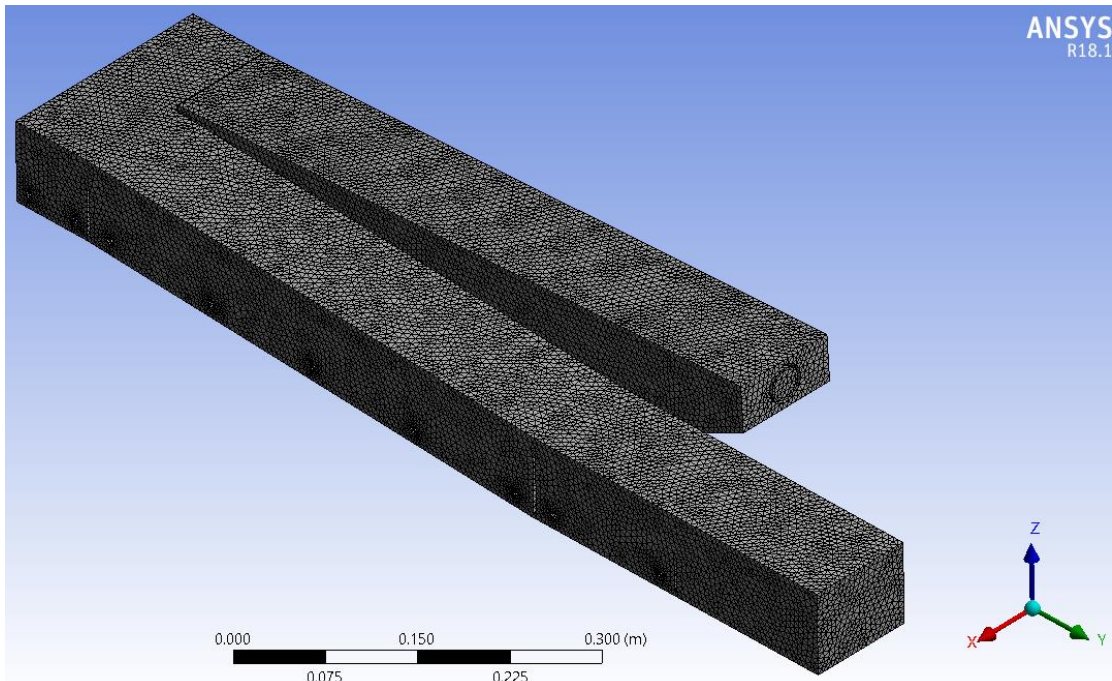


Figure 37 – Refined mesh of improved photobioreactor concept design for mesh independence study

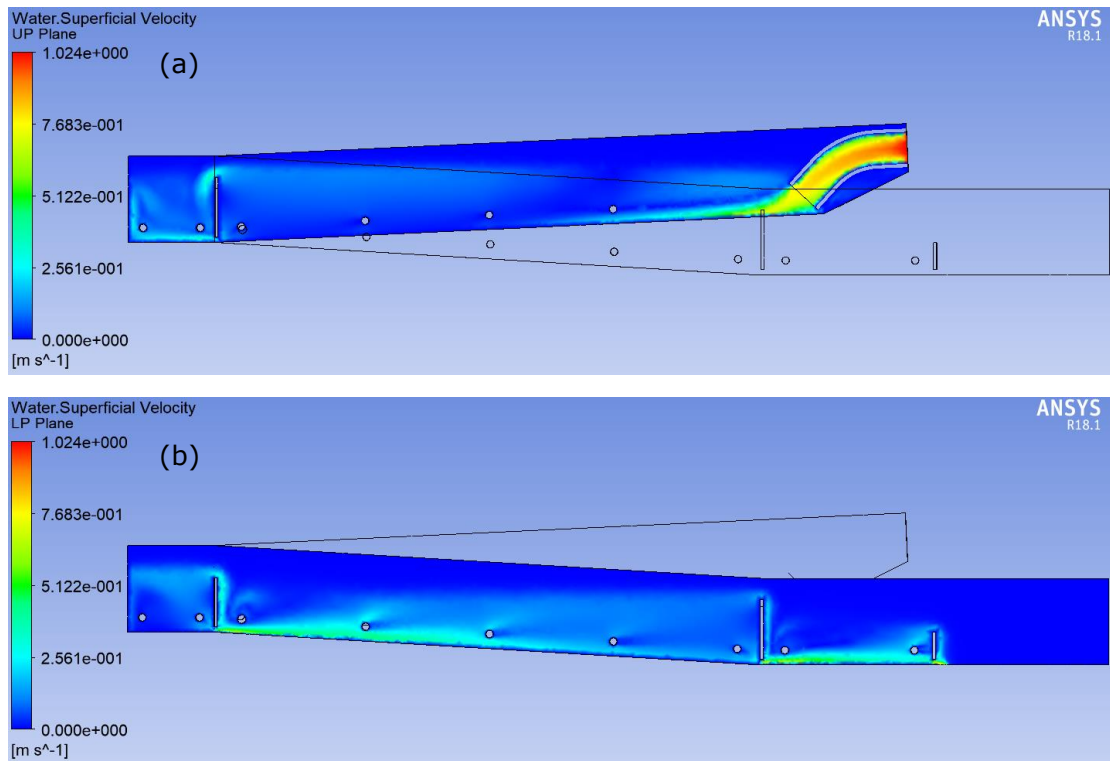


Figure 38 – Simulation results of improved photobioreactor concept design with refined mesh where (a) represents the upper platform and (b) represents the lower platform

#### 4.4.4.4. Effects of dense microalgal cultures on simulation results

At the start of cultivation, the properties of the microalgal culture closely resembles the properties of water at the same temperature. However, when the culture has been grown for a period of time, the concentration of microalgal cells increased exponentially. The proliferation of microalgal cells would cause the properties of the water system to change. Two properties of the water system that are directly altered are density and viscosity (Petkov and Bratkova, 1996). At room temperature of 25°C, the density and viscosity of water are 997 kg/m<sup>3</sup> and 8.9 x 10<sup>-4</sup> Pa.s respectively. When the microalgal culture has matured, the density of the water system would increase by the dry mass of the microalgal biomass suspended in the culture, up to a maximum of about 30 g/L dry weight of microalgal biomass (Perez-Garcia et al., 2011). For green and blue microalgae species, such as

*Scenedesmus* sp. and *Spirulina* sp., the viscosity of the culture could be increased to 0.9 – 1.2 mPa.s at the end of cultivation. In the case of microalgae species that secrete polysaccharides into the surrounding medium, such as the red microalga *Porphyridium* sp., the viscosity of the water system could increase higher to 1.8 – 2.6 mPa.s at the end of cultivation (Petkov and Bratkova, 1996). Hence, in this section, the effects of dense microalgal cultures on the simulation results were investigated. During the setup of the simulation model in ANSYS CFX-Pre, a new fluid model named “Culture” was added and used to replace “Water” in the simulation. The “Culture” fluid stream had properties identical to “Water”, but had its density and viscosity values changed to match two different microalgal cultures, the moderate viscosity culture and high viscosity culture. Under the moderate viscosity culture, the density and viscosity were set to 1,027 kg/m<sup>3</sup> and 1.2 x 10<sup>-3</sup> Pa.s. A maximum microalgal biomass of 30 g/L was used in the density calculation. On the other hand, under the high viscosity culture, the density remained at 1,027 kg/m<sup>3</sup> but the viscosity was increased to 2.6 x 10<sup>-3</sup> Pa.s. The greater biomass concentration and viscosity values were utilised in order to increase the extent of changes that would occur in the simulation results.

Figure 39 and Figure 40 illustrated the simulation results of moderate viscosity and high viscosity microalgal cultures by ANSYS. However, when compared with the simulation results that used “Water” stream in Figure 36, there were no significant changes in the culture fluid velocities or fluid flow patterns in Figure 39 and Figure 40. This implied that the density and viscosity changes brought upon by the maturation of microalgal cultures did not affect the physical properties of the entire water system in any significant manner.

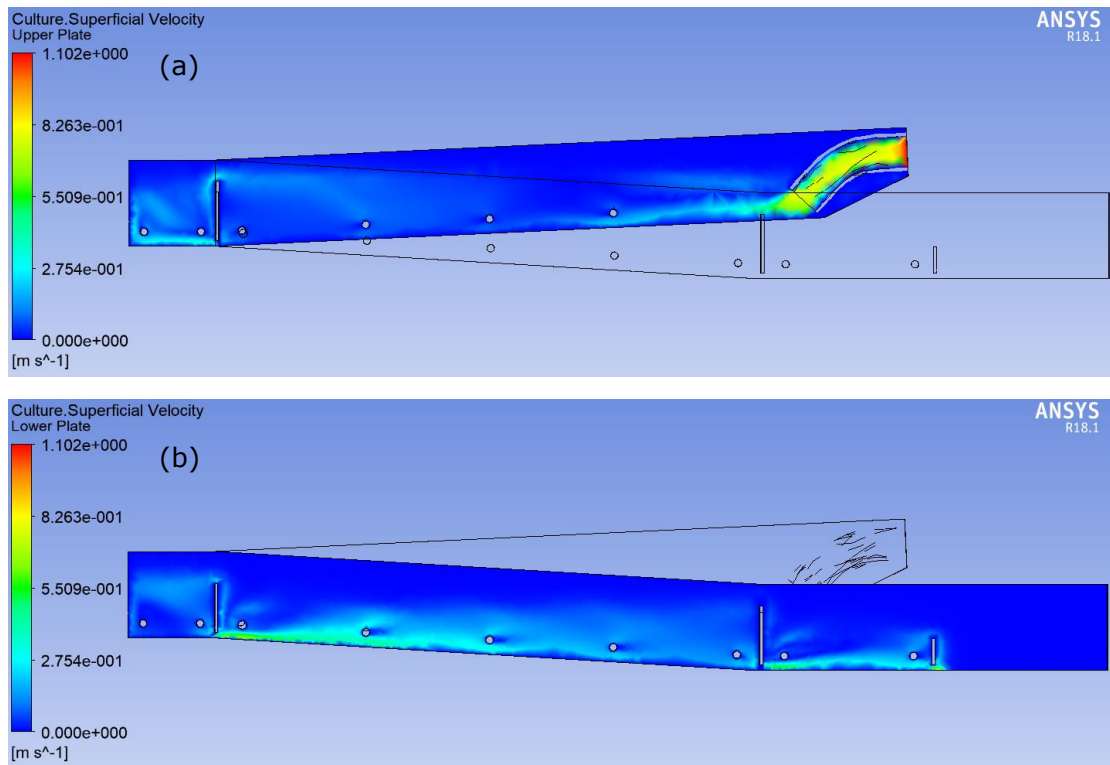


Figure 39 – Simulation results of improved concept design with moderate viscosity ( $1.2 \times 10^{-3}$  Pa.s) microalgal culture where (a) represents the upper platform and (b) represents the lower platform

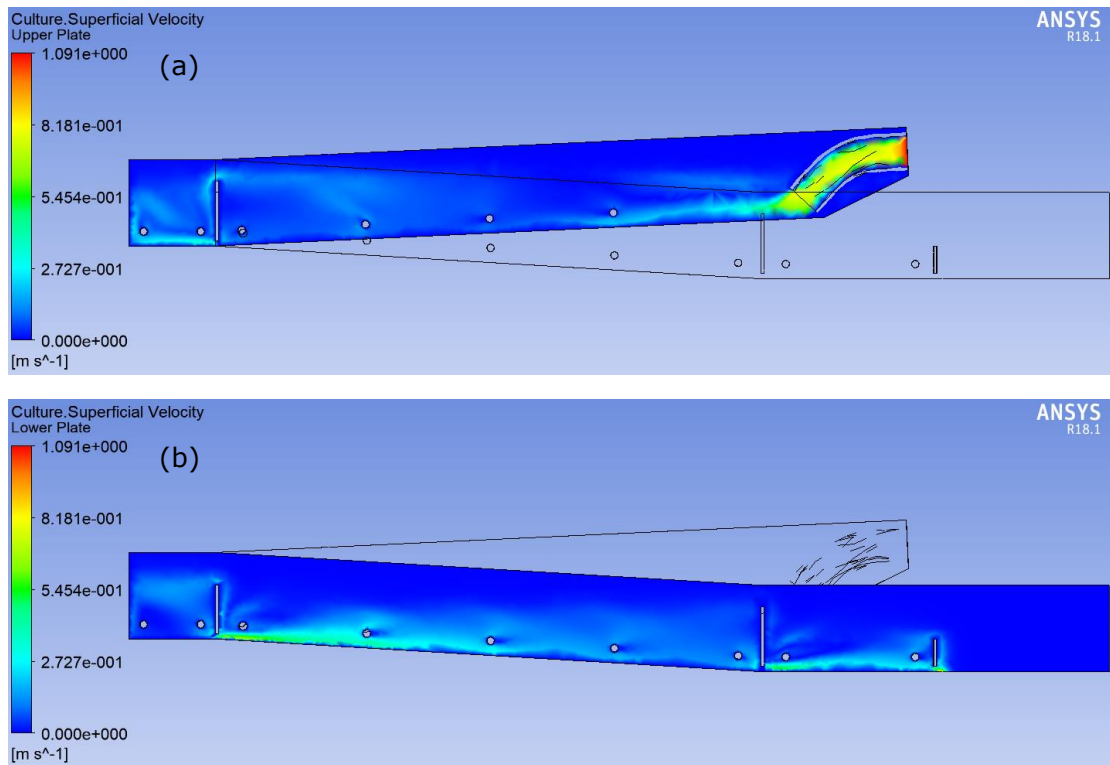


Figure 40 – Simulation results of improved concept design with high viscosity ( $2.6 \times 10^{-3} \text{ Pa}\cdot\text{s}$ ) microalgal culture where (a) represents the upper platform and (b) represents the lower platform

# CHAPTER 5

## CONCLUSIONS

In the area of protein production, the microalgae species *Chlorella sorokiniana* CY1 and *Chlorella vulgaris* ESP-31 had proven to be potential producers of protein for feed purposes in the aquaculture industry. Given a short cultivation time of 2 days, the biomass and protein production capabilities of both *Chlorella sorokiniana* CY1 and *Chlorella vulgaris* ESP-31 could be considered remarkable. It was observed that both species could still withstand and flourish under high light intensity of 1000  $\mu\text{mol}/\text{m}^2/\text{s}$  when cultured in 1 L laboratory bottles. Despite these advantages, the protein contents of both species were mediocre. The improvement of protein contents in both species would be the main focus of future studies, followed by the assessment of scaling up to larger photobioreactors. Upon scaling up, design of experiments (DOE) software would be useful in reducing the number of experiments and determining the optimum conditions more quickly. Another future work would be a study of the effects of feeding small fish and shrimp species using a mixed diet of fish feed and protein-rich microalgal biomass. A characterisation study involving the amino acid profile of the microalgal biomass would prove useful in monitoring the health of the small fish and shrimp species.

Apart from producing proteins from microalgae, another important product from microalgae is biodiesel. Among the five microalgal strains tested, the best oil producing strain was *Chlamydomonas* sp. Tai-03, achieving high oil content and oil productivity of 28.6% and 124.1 mg/L/d respectively. The shorter chain FAMES produced (palmitic acid, oleic acid and linoleic acid) are suitable for biodiesel production. Nitrate concentration was the main parameters affecting the lipid

accumulation in *Chlamydomonas* sp. Tai-03. A low nitrate concentration (25% of the original one) caused nitrogen starvation to occur earlier, thereby enhancing the lipid productivity. The influences of light intensity and initial cell concentration on maximum lipid accumulation in Tai-03 strain were still significant, but less substantial compared to the concentration of nitrate.

In a follow-up study, the microalga *Chlamydomonas* sp. Tai-03 was further optimised by altering the CO<sub>2</sub> concentration and medium replacement ratio (MRR) under semi-batch operation. The optimum condition was observed as 5% CO<sub>2</sub> concentration using semi-batch operation with 25% MRR where *Chlamydomonas* sp. Tai-03 was successfully cultured for two replacement cycles. *Chlamydomonas* sp. Tai-03 bounced back to peak biomass growth in only 1 day after both replacement cycles, achieving high mean biomass and lipid productivities of  $1.23 \pm 0.02$  g/L/d and  $239.6 \pm 24.8$  mg/L/d, and moderate mean lipid content of  $19.4 \pm 2.0\%$ . This rapid growth pattern implies that after the first 8 days of batch culture, 25% of *Chlamydomonas* sp. Tai-03 culture could be harvested daily for biodiesel production. This study has demonstrated that by combining MRR treatment with suitable microalgal strains, this culture method could be applied to produce not only lipids, but also other valuable products such as carbohydrates, proteins, enzymes, and carotenoids. This operation mode could also enhance the efficiency of microalgal biorefineries to produce a wide range of microalgal-derived products. Following this study, future works would involve the study of long-term behaviour and stability of *Chlamydomonas* sp. Tai-03 cultures under 25% MRR operation.

Computational fluid dynamics (CFD) analysis of the proposed semi-closed thin layer cascade (TLC) photobioreactor (PBR) had shown that sufficient mixing and water velocities could be achieved using the improved concept design. The addition of mixing rods strategically placed in the PBR were able to induce mixing near the bottom of both the upper and lower platforms, which would sweep up any cells sediment and circulate the microalgal cells through the PBR system. The installation of the inlet tube and removal of a portion of the upper platform behind

the inlet tube had served to reduce the stagnant regions in the upper platform. Satisfactory results of CFD analysis of the improved design concept had demonstrated the potential benefits of utilising this PBR for cultivation larger volumes of microalgal cultures. This design concept could become useful as a hybrid photobioreactor design that could be used in both indoor and outdoor conditions. Future works following this PBR study would involve implementing and testing other innovative methods to further improve the efficiency of this system. The PBR system could also be fabricated and tested to better understand the mechanism and performance of the system in real-life. This would provide valuable insights into the future designs of PBR with better considerations and advanced features.



# REFERENCES

---

- Baba M & Shiraiwa Y 2012. Chapter 15 - High-CO<sub>2</sub> response mechanisms in microalgae. *In: Najafpour M (ed.) Advances in Photosynthesis - Fundamental Aspects.* IntechOpen, pp. 299-320. DOI: <https://doi.org/10.5772/1385>
- Bahadar A & Bilal Khan M 2013. Progress in energy from microalgae: A review. *Renewable and Sustainable Energy Reviews*, 27, pp. 128-148. DOI: <https://doi.org/10.1016/j.rser.2013.06.029>
- Barbosa MJ, Janssen M, Ham N, Tramper J & Wijffels RH 2003. Microalgae cultivation in air - lift reactors: Modeling biomass yield and growth rate as a function of mixing frequency. *Biotechnology and Bioengineering*, 82, no. 2, pp. 170-179. DOI: <https://doi.org/10.1002/bit.10563>
- Batterton JC & Van Baalen C 1971. Growth responses of blue-green algae to sodium chloride concentration. *Archiv für Mikrobiologie*, 76, no. 2, pp. 151-165. DOI: <https://doi.org/10.1007/bf00411789>
- Becker E 2007. Micro-algae as a source of protein. *Biotechnology Advances*, 25, no. 2, pp. 207-210. DOI: <https://doi.org/10.1016/j.biotechadv.2006.11.002>
- Borowitzka MA 1999. Commercial production of microalgae: ponds, tanks, tubes and fermenters. *Journal of Biotechnology*, 70, no. 1, pp. 313-321. DOI: [https://doi.org/10.1016/S0079-6352\(99\)80123-4](https://doi.org/10.1016/S0079-6352(99)80123-4)
- Borowitzka MA & Moheimani NR 2013. Open Pond Culture Systems. *In: Borowitzka MA & Moheimani NR (eds.) Algae for Biofuels and Energy.* Dordrecht, Netherlands, Springer, pp. 133-152. DOI: [https://doi.org/10.1007/978-94-007-5479-9\\_8](https://doi.org/10.1007/978-94-007-5479-9_8)
- Brennan L & Owende P 2010. Biofuels from microalgae—a review of technologies for production, processing, and extractions of biofuels and co-products. *Renewable and Sustainable Energy Reviews*, 14, no. 2, pp. 557-577. DOI: <https://doi.org/10.1016/j.rser.2009.10.009>
- Breuer G, Lamers PP, Martens DE, Draaisma RB & Wijffels RH 2012. The impact of nitrogen starvation on the dynamics of triacylglycerol accumulation in nine microalgae strains. *Bioresource Technology*, 124, pp. 217-226. DOI: <https://doi.org/10.1016/j.biortech.2012.08.003>
- Breuer G, Lamers PP, Martens DE, Draaisma RB & Wijffels RH 2013. Effect of light intensity, pH, and temperature on triacylglycerol (TAG) accumulation induced by nitrogen starvation in *Scenedesmus obliquus*. *Bioresource Technology*, 143, pp. 1-9. DOI: <https://doi.org/10.1016/j.biortech.2013.05.105>

## References

- Brown MR, Jeffrey SW, Volkman JK & Dunstan GA 1997. Nutritional properties of microalgae for mariculture. *Aquaculture*, 151, no. 1-4, pp. 315-331. DOI: [https://doi.org/10.1016/S0044-8486\(96\)01501-3](https://doi.org/10.1016/S0044-8486(96)01501-3)
- Cardozo KHM et al. 2007. Metabolites from algae with economical impact. *Comparative Biochemistry and Physiology Part C: Toxicology & Pharmacology*, 146, no. 1-2, pp. 60-78. DOI: <https://doi.org/10.1016/j.cbpc.2006.05.007>
- Carlozzi P 2008. Closed photobioreactor assessments to grow, intensively, light dependent microorganisms: a twenty-year Italian outdoor investigation. *The Open Biotechnology Journal*, 2, pp. 63-72. DOI: <https://doi.org/10.2174/1874070700802010063>
- Carvalho AP, Meireles LA & Malcata FX 2006. Microalgal reactors: a review of enclosed system designs and performances. *Biotechnology Progress*, 22, no. 6, pp. 1490-1506. DOI: <https://doi.org/10.1021/bp060065r>
- Cheah WY, Show PL, Chang J-S, Ling TC & Juan JC 2015. Biosequestration of atmospheric CO<sub>2</sub> and flue gas-containing CO<sub>2</sub> by microalgae. *Bioresource Technology*, 184, pp. 190-201. DOI: <https://doi.org/10.1016/j.biortech.2014.11.026>
- Cheirsilp B & Torpee S 2012. Enhanced growth and lipid production of microalgae under mixotrophic culture condition: Effect of light intensity, glucose concentration and fed-batch cultivation. *Bioresource Technology*, 110, pp. 510-516. DOI: <http://dx.doi.org/10.1016/j.biortech.2012.01.125>
- Chen C-Y, Chang J-S, Chang H-Y, Chen T-Y, Wu J-H & Lee W-L 2013. Enhancing microalgal oil/lipid production from *Chlorella sorokiniana* CY1 using deep-sea water supplemented cultivation medium. *Biochemical Engineering Journal*, 77, pp. 74-81. DOI: <https://doi.org/10.1016/j.bej.2013.05.009>
- Chen C-Y, Chang Y-H & Chang H-Y 2016. Outdoor cultivation of *Chlorella vulgaris* FSP-E in vertical tubular-type photobioreactors for microalgal protein production. *Algal Research*, 13, pp. 264-270. DOI: <https://doi.org/10.1016/j.algal.2015.12.006>
- Chen C-Y, Lee P-J, Tan CH, Lo Y-C, Huang C-C, Show PL, Lin C-H & Chang J-S 2015. Improving protein production of indigenous microalga *Chlorella vulgaris* FSP-E by photobioreactor design and cultivation strategies. *Biotechnology Journal*, 10, no. 6, pp. 905-914. DOI: <https://doi.org/10.1002/biot.201400594>
- Chen C-Y, Yeh K-L, Aisyah R, Lee D-J & Chang J-S 2011. Cultivation, photobioreactor design and harvesting of microalgae for biodiesel production: A critical review. *Bioresource Technology*, 102, no. 1, pp. 71-81. DOI: <http://dx.doi.org/10.1016/j.biortech.2010.06.159>
- Chen C-Y, Yeh K-L, Su H-M, Lo Y-C, Chen W-M & Chang J-S 2010. Strategies to enhance cell growth and achieve high - level oil production of a *Chlorella*

## References

- vulgaris* isolate. *Biotechnology Progress*, 26, no. 3, pp. 679-686. DOI: <https://doi.org/10.1002/btpr.381>
- Chen F & Johns MR 1991. Effect of C/N ratio and aeration on the fatty acid composition of heterotrophic *Chlorella sorokiniana*. *Journal of Applied Phycology*, 3, no. 3, pp. 203-209. DOI: <https://doi.org/10.1007/BF00003578>
- Chen L, Liu T, Zhang W, Chen X & Wang J 2012. Biodiesel production from algae oil high in free fatty acids by two-step catalytic conversion. *Bioresource Technology*, 111, pp. 208-214. DOI: <http://dx.doi.org/10.1016/j.biortech.2012.02.033>
- Chisti Y 2007. Biodiesel from microalgae. *Biotechnology Advances*, 25, no. 3, pp. 294-306. DOI: <https://doi.org/10.1016/j.biotechadv.2007.02.001>
- Chisti Y 2016. Large-scale production of algal biomass: raceway ponds. *Algae Biotechnology*. Springer, pp. 21-40. DOI: [https://doi.org/10.1007/978-3-319-12334-9\\_2](https://doi.org/10.1007/978-3-319-12334-9_2)
- Chisti Y & Moo-Young M 1993. Improve the Performance of Airlift Reactors. *Chemical Engineering Progress*, pp. 39.
- Chiu S-Y, Kao C-Y, Chen C-H, Kuan T-C, Ong S-C & Lin C-S 2008. Reduction of CO<sub>2</sub> by a high-density culture of *Chlorella* sp. in a semicontinuous photobioreactor. *Bioresource technology*, 99, no. 9, pp. 3389-3396. DOI: <https://doi.org/10.1016/j.biortech.2007.08.013>
- Chojnacka K & Marquez-Rocha F-J 2004. Kinetic and stoichiometric relationships of the energy and carbon metabolism in the culture of microalgae. *Biotechnology*, 3, no. 1, pp. 21-34. DOI: <https://doi.org/10.3923/biotech.2004.21.34>
- Christenson L & Sims R 2011. Production and harvesting of microalgae for wastewater treatment, biofuels, and bioproducts. *Biotechnology Advances*, 29, no. 6, pp. 686-702. DOI: <https://doi.org/10.1016/j.biotechadv.2011.05.015>
- Chu W-L, Phang S-M & Goh S-H 1996. Environmental effects on growth and biochemical composition of *Nitzschia inconspicua* Grunow. *Journal of Applied Phycology*, 8, no. 4-5, pp. 389-396. DOI: <https://doi.org/10.1007/BF02178582>
- Coleman JR & Colman B 1981. Inorganic carbon accumulation and photosynthesis in a blue-green alga as a function of external pH. *Plant Physiology*, 67, no. 5, pp. 917-921. DOI: <https://doi.org/10.1104/pp.67.5.917>
- Collos Y, Mornet F, Sciandra A, Waser N, Larson A & Harrison P 1999. An optical method for the rapid measurement of micromolar concentrations of nitrate in marine phytoplankton cultures. *Journal of Applied Phycology*, 11, no. 2, pp. 179-184. DOI: <https://doi.org/10.1023/A:1008046023487>

## References

- Costa JAV & de Morais MG 2014. Chapter 1 - An Open Pond System for Microalgal Cultivation. *In: Pandey A, Lee D-J, Chisti Y & Soccol CR (eds.) Biofuels from Algae*. Amsterdam, Elsevier, pp. 1-22. DOI: <https://doi.org/10.1016/B978-0-444-59558-4.00001-2>
- Dasgupta CN, Gilbert JJ, Lindblad P, Heidorn T, Borgvang SA, Skjanes K & Das D 2010. Recent trends on the development of photobiological processes and photobioreactors for the improvement of hydrogen production. *International Journal of Hydrogen Energy*, 35, no. 19, pp. 10218-10238. DOI: <https://doi.org/10.1016/j.ijhydene.2010.06.029>
- Davis R, Aden A & Pienkos PT 2011. Techno-economic analysis of autotrophic microalgae for fuel production. *Applied Energy*, 88, no. 10, pp. 3524-3531. DOI: <https://doi.org/10.1016/j.apenergy.2011.04.018>
- Degen J, Uebele A, Retze A, Schmid-Staiger U & Trösch W 2001. A novel airlift photobioreactor with baffles for improved light utilization through the flashing light effect. *Journal of Biotechnology*, 92, no. 2, pp. 89-94. DOI: [https://doi.org/10.1016/S0168-1656\(01\)00350-9](https://doi.org/10.1016/S0168-1656(01)00350-9)
- Dipak P & Lele S 2005. Carotenoid production from microalga, *Dunaliella salina*. *Indian Journal of Biotechnology*, 4, no. 8, pp. 476-483.
- Dodds WK & Whiles MR 2010. Chapter 13 - Carbon. *In: Dodds WK & Whiles MR (eds.) Freshwater Ecology - Concepts and Environmental Applications of Limnology*. Academic Press, pp. 323-343. DOI: <https://doi.org/10.1016/C2009-0-01718-8>
- Doucha J & Lívanský K 1995. Novel outdoor thin-layer high density microalgal culture system: Productivity and operational parameters. *Algological Studies/Archiv für Hydrobiologie, Supplement Volumes*, 76, pp. 129-147.
- Doucha J & Lívanský K 2014. High density outdoor microalgal culture. *In: Bajpai R, Prokop A & Zappi M (eds.) Algal Biorefineries*. Springer, pp. 147-173. DOI: [https://doi.org/10.1007/978-94-007-7494-0\\_6](https://doi.org/10.1007/978-94-007-7494-0_6)
- Douskova I, Doucha J, Machat J, Novak P, Umysova D, Vitova M & Zachleder V 2008. Microalgae as a means for converting flue gas CO<sub>2</sub> into biomass with high content of starch. Proceedings of the International Conference: Bioenergy: Challenges and Opportunities, 6th/9th April, 2008 Guimarães, Portugal. Citeseer.
- Dragone G, Fernandes BD, Vicente AA & Teixeira JA 2010. Third generation biofuels from microalgae. *In: Méndez-Vilas A (ed.) Current research, technology and education topics in applied microbiology and microbial biotechnology*. Badajoz, Spain, Formatex Research Center, pp. 1355-1366.
- Du W, Li W, Sun T, Chen X & Liu D 2008. Perspectives for biotechnological production of biodiesel and impacts. *Applied Microbiology and Biotechnology*, 79, no. 3, pp. 331-337. DOI: <https://doi.org/10.1007/s00253-008-1448-8>

## References

- Erkelens M, Ball AS & Lewis DM 2014. The influences of the recycle process on the bacterial community in a pilot scale microalgae raceway pond. *Bioresource Technology*, 157, pp. 364-367. DOI: <https://doi.org/10.1016/j.biortech.2014.02.056>
- Fábregas J, Maseda A, Domínguez A, Ferreira M & Otero A 2002. Changes in the cell composition of the marine microalga, *Nannochloropsis gaditana*, during a light: dark cycle. *Biotechnology Letters*, 24, no. 20, pp. 1699-1703. DOI: <https://doi.org/10.1023/A:1020661719272>
- Falkowski PG & Raven JA 2007. *Aquatic Photosynthesis*. Princeton University Press.
- Fernández FGA, Sevilla JMF & Grima EM 2013. Photobioreactors for the production of microalgae. *Reviews in Environmental Science and Bio/Technology*, 12, no. 2, pp. 131-151. DOI: <https://doi.org/10.1016/B978-0-08-101023-5.00001-7>
- Fidalgo JP, Cid A, Torres E, Sukenik A & Herrero C 1998. Effects of nitrogen source and growth phase on proximate biochemical composition, lipid classes and fatty acid profile of the marine microalga *Isochrysis galbana*. *Aquaculture*, 166, no. 1, pp. 105-116. DOI: [https://doi.org/10.1016/S0044-8486\(98\)00278-6](https://doi.org/10.1016/S0044-8486(98)00278-6)
- Fisheries and Aquaculture Department (FAO) 2010. *The State of World Fisheries and Aquaculture*. Rome.
- Fisheries and Aquaculture Department (FAO) 2018. *The State of World Fisheries and Aquaculture - Meeting the sustainable development goals*. Rome.
- Fukuda H, Kondo A & Noda H 2001. Biodiesel fuel production by transesterification of oils. *Journal of Bioscience and Bioengineering*, 92, no. 5, pp. 405-416. DOI: [https://doi.org/10.1016/S1389-1723\(01\)80288-7](https://doi.org/10.1016/S1389-1723(01)80288-7)
- Fuls J, Hawkins CS & Hugo FJC 1984. Tractor engine performance on sunflower oil fuel. *Journal of Agricultural Engineering Research*, 30, pp. 29-35. DOI: [https://doi.org/10.1016/S0021-8634\(84\)80003-7](https://doi.org/10.1016/S0021-8634(84)80003-7)
- Gardner RD, Lohman E, Gerlach R, Cooksey KE & Peyton BM 2013. Comparison of CO<sub>2</sub> and bicarbonate as inorganic carbon sources for triacylglycerol and starch accumulation in *Chlamydomonas reinhardtii*. *Biotechnology and Bioengineering*, 110, no. 1, pp. 87-96. DOI: <https://doi.org/10.1002/bit.24592>
- Goldman JC, Dennett MR & Riley CB 1982. Effect of nitrogen - mediated changes in alkalinity on pH control and CO<sub>2</sub> supply in intensive microalgal cultures. *Biotechnology and Bioengineering*, 24, no. 3, pp. 619-631. DOI: <https://doi.org/10.1002/bit.260240308>
- Goldrick S, Ştefan A, Lovett D, Montague G & Lennox B 2015. The development of an industrial-scale fed-batch fermentation simulation. *Journal of Biotechnology*, 193, pp. 70-82. DOI: <https://doi.org/10.1016/j.jbiotec.2014.10.029>

## References

- Goyal HB, Seal D & Saxena RC 2008. Bio-fuels from thermochemical conversion of renewable resources: a review. *Renewable and Sustainable Energy Reviews*, 12, no. 2, pp. 504-517. DOI: <https://doi.org/10.1016/j.rser.2006.07.014>
- Griffiths MJ, van Hille RP & Harrison STL 2012. Lipid productivity, settling potential and fatty acid profile of 11 microalgal species grown under nitrogen replete and limited conditions. *Journal of Applied Phycology*, 24, no. 5, pp. 989-1001. DOI: <https://doi.org/10.1007/s10811-011-9723-y>
- Grobbelaar JU, Nedbal L, Tichy L & Setlik L 1995. Variation in some photosynthetic characteristics of microalgae cultured in outdoor thin-layered sloping reactors. *Journal of Applied Phycology*, 7, no. 2, pp. 175-184. DOI: <https://doi.org/10.1007/bf00693065>
- Guccione A, Biondi N, Sampietro G, Rodolfi L, Bassi N & Tredici MR 2014. *Chlorella* for protein and biofuels: from strain selection to outdoor cultivation in a Green Wall Panel photobioreactor. *Biotechnology for Biofuels*, 7, no. 1, pp. 84. DOI: <https://doi.org/10.1186/1754-6834-7-84>
- Guedes AC, Sousa-Pinto I & Malcata FX 2015. Application of microalgae protein to aquafeed. *Handbook of Marine Microalgae*. Elsevier, pp. 93-125. DOI: <https://doi.org/10.1016/B978-0-12-800776-1.00008-X>
- Gupta PL, Lee S-M & Choi H-J 2015. A mini review: photobioreactors for large scale algal cultivation. *World Journal of Microbiology and Biotechnology*, 31, no. 9, pp. 1409-1417. DOI: <https://doi.org/10.1007/s11274-015-1892-4>
- Guschina IA & Harwood JL 2009. Algal lipids and effect of the environment on their biochemistry. In: Arts MT, T BM & Kainz MJ (eds.) *Lipids in Aquatic Ecosystems*. Springer, pp. 1-24. DOI: [https://doi.org/10.1007/978-0-387-89366-2\\_1](https://doi.org/10.1007/978-0-387-89366-2_1)
- Halim R, Danquah MK & Webley PA 2012. Extraction of oil from microalgae for biodiesel production: A review. *Biotechnology Advances*, 30, no. 3, pp. 709-732. DOI: <http://dx.doi.org/10.1016/j.biotechadv.2012.01.001>
- Halim R, Gladman B, Danquah MK & Webley PA 2011. Oil extraction from microalgae for biodiesel production. *Bioresource Technology*, 102, no. 1, pp. 178-185. DOI: <https://doi.org/10.1016/j.biortech.2010.06.136>
- Hallenbeck PC, Grogger M, Mraz M & Veverka D 2015. The use of Design of Experiments and Response Surface Methodology to optimize biomass and lipid production by the oleaginous marine green alga, *Nannochloropsis gaditana* in response to light intensity, inoculum size and CO<sub>2</sub>. *Bioresource Technology*, 184, pp. 161-168. DOI: <https://doi.org/10.1016/j.biortech.2014.09.022>
- Hama S, Tamalampudi S, Fukumizu T, Miura K, Yamaji H, Kondo A & Fukuda H 2006. Lipase localization in *Rhizopus oryzae* cells immobilized within biomass support particles for use as whole-cell biocatalysts in biodiesel-fuel production. *Journal of Bioscience and Bioengineering*, 101, no. 4, pp. 328-333. DOI: <https://doi.org/10.1263/jbb.101.328>

## References

- Hamed I 2016. The Evolution and Versatility of Microalgal Biotechnology: A Review. *Comprehensive Reviews in Food Science and Food Safety*, 15, no. 6, pp. 1104-1123. DOI: <https://doi.org/10.1111/1541-4337.12227>
- Hansen PJ 2002. Effect of high pH on the growth and survival of marine phytoplankton: implications for species succession. *Aquatic Microbial Ecology*, 28, no. 3, pp. 279-288. DOI: <https://doi.org/10.3354/ame028279>
- Hardy RW & Tacon AGJ 2002. Chapter 16 - Fish meal: historical uses, production trends and future outlook for sustainable supplies. In: Stickney RR & McVey JP (eds.) *Responsible Marine Aquaculture*. UK, CABI Publishing, pp. 311-325.
- Harwood JL 1998. Involvement of chloroplast lipids in the reaction of plants submitted to stress. In: Siegenthaler P-A & Murata N (eds.) *Lipids in Photosynthesis: Structure, Function and Genetics*. Springer, pp. 287-302. DOI: [https://doi.org/10.1007/0-306-48087-5\\_15](https://doi.org/10.1007/0-306-48087-5_15)
- Heaven S, Milledge J & Zhang Y 2011. Comments on 'Anaerobic digestion of microalgae as a necessary step to make microalgal biodiesel sustainable'. *Biotechnology Advances*, 29, no. 1, pp. 164-167. DOI: <http://dx.doi.org/10.1016/j.biotechadv.2010.10.005>
- Heining M, Sutor A, Stute SC, Lindenberger CP & Buchholz R 2014. Internal illumination of photobioreactors via wireless light emitters: a proof of concept. *Journal of Applied Phycology*, 27, no. 1, pp. 59-66. DOI: <https://doi.org/10.1007/s10811-014-0290-x>
- Heredia-Arroyo T, Wei W, Ruan R & Hu B 2011. Mixotrophic cultivation of *Chlorella vulgaris* and its potential application for the oil accumulation from non-sugar materials. *Biomass and Bioenergy*, 35, no. 5, pp. 2245-2253. DOI: <https://doi.org/10.1016/j.biombioe.2011.02.036>
- Ho S-H, Chen C-NN, Lai Y-Y, Lu W-B & Chang J-S 2014. Exploring the high lipid production potential of a thermotolerant microalga using statistical optimization and semi-continuous cultivation. *Bioresource Technology*, 163, pp. 128-135. DOI: <https://doi.org/10.1016/j.biortech.2014.04.028>
- Ho S-H, Chen C-Y & Chang J-S 2012. Effect of light intensity and nitrogen starvation on CO<sub>2</sub> fixation and lipid/carbohydrate production of an indigenous microalga *Scenedesmus obliquus* CNW-N. *Bioresource Technology*, 113, pp. 244-252. DOI: <https://doi.org/10.1016/j.biortech.2011.11.133>
- Ho S-H, Chen C-Y, Lee D-J & Chang J-S 2011. Perspectives on microalgal CO<sub>2</sub>-emission mitigation systems—a review. *Biotechnology Advances*, 29, no. 2, pp. 189-198. DOI: <https://doi.org/10.1016/j.biotechadv.2010.11.001>
- Ho S-H, Li P-J, Liu C-C & Chang J-S 2013. Bioprocess development on microalgae-based CO<sub>2</sub> fixation and bioethanol production using *Scenedesmus obliquus* CNW-N. *Bioresource Technology*, 145, pp. 142-149. DOI: <http://dx.doi.org/10.1016/j.biortech.2013.02.119>

## References

- Ho S-H, Nakanishi A, Ye X, Chang J-S, Chen C-Y, Hasunuma T & Kondo A 2015. Dynamic metabolic profiling of the marine microalga *Chlamydomonas* sp. JSC4 and enhancing its oil production by optimizing light intensity. *Biotechnology for Biofuels*, 8, no. 1, pp. 48. DOI: <https://doi.org/10.1186/s13068-015-0226-y>
- Huang G, Chen F, Wei D, Zhang X & Chen G 2010. Biodiesel production by microalgal biotechnology. *Applied Energy*, 87, no. 1, pp. 38-46. DOI: <https://doi.org/10.1016/j.apenergy.2009.06.016>
- Huang Q, Jiang F, Wang L & Yang C 2017. Design of photobioreactors for mass cultivation of photosynthetic organisms. *Engineering*, 3, no. 3, pp. 318-329. DOI: <https://doi.org/10.1016/J.ENG.2017.03.020>
- James GO, Hocart CH, Hillier W, Price GD & Djordjevic MA 2013. Temperature modulation of fatty acid profiles for biofuel production in nitrogen deprived *Chlamydomonas reinhardtii*. *Bioresource Technology*, 127, pp. 441-447. DOI: <https://doi.org/10.1016/j.biortech.2012.09.090>
- James SC & Boriah V 2010. Modeling algae growth in an open-channel raceway. *Journal of Computational Biology*, 17, no. 7, pp. 895-906. DOI: <https://doi.org/10.1089/cmb.2009.0078>
- Javanmardian M & Palsson BO 1991. High-density photoautotrophic algal cultures: design, construction, and operation of a novel photobioreactor system. *Biotechnology and Bioengineering*, 38, no. 10, pp. 1182-1189. DOI: <https://doi.org/10.1002/bit.260381010>
- Ji M-K, Yun H-S, Park Y-T, Kabra AN, Oh I-H & Choi J 2015. Mixotrophic cultivation of a microalga *Scenedesmus obliquus* in municipal wastewater supplemented with food wastewater and flue gas CO<sub>2</sub> for biomass production. *Journal of Environmental Management*, 159, pp. 115-120. DOI: <https://doi.org/10.1016/j.jenvman.2015.05.037>
- Ju ZY, Deng D-F & Dominy W 2012. A defatted microalgae (*Haematococcus pluvialis*) meal as a protein ingredient to partially replace fishmeal in diets of Pacific white shrimp (*Litopenaeus vannamei*, Boone, 1931). *Aquaculture*, 354, pp. 50-55. DOI: <https://doi.org/10.1016/j.aquaculture.2012.04.028>
- Juneja A, Ceballos RM & Murthy GS 2013. Effects of environmental factors and nutrient availability on the biochemical composition of algae for biofuels production: a review. *Energies*, 6, no. 9, pp. 4607-4638. DOI: <https://doi.org/10.3390/en6094607>
- Kaewpintong K, Shotipruk A, Powtongsook S & Pavasant P 2007. Photoautotrophic high-density cultivation of vegetative cells of *Haematococcus pluvialis* in airlift bioreactor. *Bioresource Technology*, 98, no. 2, pp. 288-295. DOI: <https://doi.org/10.1016/j.biortech.2006.01.011>
- Kakinuma M, Coury DA, Kuno Y, Itoh S, Kozawa Y, Inagaki E, Yoshiura Y & Amano H 2006. Physiological and biochemical responses to thermal and salinity stresses in a sterile mutant of *Ulva pertusa* (Ulvales, Chlorophyta). *Marine*



## References

- Biology*, 149, no. 1, pp. 97-106. DOI: <https://doi.org/10.1007/s00227-005-0215-y>
- Kao C-Y, Chen T-Y, Chang Y-B, Chiu T-W, Lin H-Y, Chen C-D, Chang J-S & Lin C-S 2014. Utilization of carbon dioxide in industrial flue gases for the cultivation of microalga *Chlorella* sp. *Bioresource Technology*, 166, pp. 485-493. DOI: <https://doi.org/10.1016/j.biortech.2014.05.094>
- Karmakar A, Karmakar S & Mukherjee S 2010. Properties of various plants and animals feedstocks for biodiesel production. *Bioresource Technology*, 101, no. 19, pp. 7201-7210. DOI: <http://dx.doi.org/10.1016/j.biortech.2010.04.079>
- Kasim NS, Tsai T-H, Gunawan S & Ju Y-H 2009. Biodiesel production from rice bran oil and supercritical methanol. *Bioresource Technology*, 100, no. 8, pp. 2399-2403. DOI: <https://doi.org/10.1016/j.biortech.2008.11.041>
- Khalil ZI, Asker MMS, El-Sayed S & Kobbia IA 2010. Effect of pH on growth and biochemical responses of *Dunaliella bardawil* and *Chlorella ellipsoidea*. *World Journal of Microbiology and Biotechnology*, 26, no. 7, pp. 1225-1231. DOI: <https://doi.org/10.1007/s11274-009-0292-z>
- Khan SA, Hussain MZ, Prasad S & Banerjee UC 2009. Prospects of biodiesel production from microalgae in India. *Renewable and Sustainable Energy Reviews*, 13, no. 9, pp. 2361-2372. DOI: <https://doi.org/10.1016/j.rser.2009.04.005>
- Kiron V, Phromkunthong W, Huntley M, Archibald I & De Scheemaker G 2012. Marine microalgae from biorefinery as a potential feed protein source for Atlantic salmon, common carp and whiteleg shrimp. *Aquaculture Nutrition*, 18, no. 5, pp. 521-531. DOI: <https://doi.org/10.1111/j.1365-2095.2011.00923.x>
- Knothe G 2008. "Designer" Biodiesel: Optimizing Fatty Ester Composition to Improve Fuel Properties†. *Energy & Fuels*, 22, no. 2, pp. 1358-1364. DOI: <https://doi.org/10.1021/ef700639e>
- Krichnavaruk S, Loataweesup W, Powtongsook S & Pavasant P 2005. Optimal growth conditions and the cultivation of *Chaetoceros calcitrans* in airlift photobioreactor. *Chemical Engineering Journal*, 105, no. 3, pp. 91-98. DOI: <https://doi.org/10.1016/j.cej.2004.10.002>
- Krichnavaruk S, Powtongsook S & Pavasant P 2007. Enhanced productivity of *Chaetoceros calcitrans* in airlift photobioreactors. *Bioresource Technology*, 98, no. 11, pp. 2123-2130. DOI: <https://doi.org/10.1016/j.biortech.2006.08.010>
- Kris-Etherton PM, Grieger JA & Etherton TD 2009. Dietary reference intakes for DHA and EPA. *Prostaglandins Leukot Essent Fatty Acids*, 81, no. 2-3, pp. 99-104. DOI: <https://doi.org/10.1016/j.plefa.2009.05.011>

## References

- Kumar K, Dasgupta CN, Nayak B, Lindblad P & Das D 2011. Development of suitable photobioreactors for CO<sub>2</sub> sequestration addressing global warming using green algae and cyanobacteria. *Bioresource Technology*, 102, no. 8, pp. 4945-4953. DOI: <http://dx.doi.org/10.1016/j.biortech.2011.01.054>
- Lau PS, Tam NFY & Wong YS 1995. Effect of algal density on nutrient removal from primary settled wastewater. *Environmental Pollution*, 89, no. 1, pp. 59-66. DOI: [https://doi.org/10.1016/0269-7491\(94\)00044-E](https://doi.org/10.1016/0269-7491(94)00044-E)
- Lee Y-K 2001. Microalgal mass culture systems and methods: their limitation and potential. *Journal of Applied Phycology*, 13, no. 4, pp. 307-315. DOI: <https://doi.org/10.1023/A:1017560006941>
- Lepage G & Roy CC 1984. Improved recovery of fatty acid through direct transesterification without prior extraction or purification. *Journal of Lipid Research*, 25, no. 12, pp. 1391-1396.
- Li C, Yang H, Li Y, Cheng L, Zhang M, Zhang L & Wang W 2013. Novel bioconversions of municipal effluent and CO<sub>2</sub> into protein riched *Chlorella vulgaris* biomass. *Bioresource Technology*, 132, pp. 171-177. DOI: <https://doi.org/10.1016/j.biortech.2012.12.017>
- Lin Q, Gu N & Lin J 2012. Effect of ferric ion on nitrogen consumption, biomass and oil accumulation of a *Scenedesmus rubescens*-like microalga. *Bioresource Technology*, 112, pp. 242-247. DOI: <http://dx.doi.org/10.1016/j.biortech.2012.02.097>
- Liu C-H, Chang C-Y, Liao Q, Zhu X, Liao C-F & Chang J-S 2013. Biohydrogen production by a novel integration of dark fermentation and mixotrophic microalgae cultivation. *International Journal of Hydrogen Energy*, 38, no. 35, pp. 15807-15814. DOI: <http://dx.doi.org/10.1016/j.ijhydene.2013.05.104>
- Liu W, Ming Y, Li P & Huang Z 2012. Inhibitory effects of hypo-osmotic stress on extracellular carbonic anhydrase and photosynthetic efficiency of green alga *Dunaliella salina* possibly through reactive oxygen species formation. *Plant Physiology and Biochemistry*, 54, pp. 43-48. DOI: <https://doi.org/10.1016/j.plaphy.2012.01.018>
- Lowry OH, Rosebrough NJ, Farr AL & Randall RJ 1951. Protein measurement with the Folin phenol reagent. *Journal of Biological Chemistry*, 193, pp. 265-275.
- Lynch DV & Thompson GA 1982. Low temperature-induced alterations in the chloroplast and microsomal membranes of *Dunaliella salina*. *Plant Physiology*, 69, no. 6, pp. 1369-1375. DOI: <https://doi.org/10.1104/pp.69.6.1369>
- Maeda K, Owada M, Kimura N, Omata K & Karube I 1995. CO<sub>2</sub> fixation from the flue gas on coal-fired thermal power plant by microalgae. *Energy Conversion and Management*, 36, no. 6, pp. 717-720. DOI: [https://doi.org/10.1016/0196-8904\(95\)00105-M](https://doi.org/10.1016/0196-8904(95)00105-M)

## References

- Masojidek J, Koblizek M & Torzillo G 2013. Chapter 2 - Photosynthesis in Microalgae. In: Richmond A & Hu Q (eds.) *Handbook of Microalgal Culture: Biotechnology and Applied Phycology*. 2nd ed., pp. 20-39. DOI: <https://doi.org/10.1002/9781118567166.ch2>
- Masojidek J, Kopecký J, Giannelli L & Torzillo G 2011. Productivity correlated to photobiochemical performance of *Chlorella* mass cultures grown outdoors in thin-layer cascades. *Journal of Industrial Microbiology & Biotechnology*, 38, no. 2, pp. 307-317. DOI: <https://doi.org/10.1007/s10295-010-0774-x>
- Masojidek J & Prášil O 2010. The development of microalgal biotechnology in the Czech Republic. *Journal of Industrial Microbiology & Biotechnology*, 37, no. 12, pp. 1307-1317. DOI: <https://doi.org/10.1007/s10295-010-0802-x>
- Masojidek J, Sergejevová M, Malapascua JR & Kopecký J 2015. Thin-Layer Systems for Mass Cultivation of Microalgae: Flat Panels and Sloping Cascades. In: Prokop A, Bajpai RK & Zappi ME (eds.) *Algal Biorefineries: Volume 2: Products and Refinery Design*. Cham, Switzerland, Springer International Publishing, pp. 237-261. DOI: [https://doi.org/10.1007/978-3-319-20200-6\\_7](https://doi.org/10.1007/978-3-319-20200-6_7)
- Mata TM, Martins AA & Caetano NS 2010. Microalgae for biodiesel production and other applications: a review. *Renewable and Sustainable Energy Reviews*, 14, no. 1, pp. 217-232. DOI: <https://doi.org/10.1016/j.rser.2009.07.020>
- Mirón AS, Garcia M-CC, Camacho FG, Grima EM & Chisti Y 2002. Growth and biochemical characterization of microalgal biomass produced in bubble column and airlift photobioreactors: studies in fed-batch culture. *Enzyme and Microbial Technology*, 31, no. 7, pp. 1015-1023. DOI: [https://doi.org/10.1016/S0141-0229\(02\)00229-6](https://doi.org/10.1016/S0141-0229(02)00229-6)
- Miron AS, Gomez AC, Camacho FG, Grima EM & Chisti Y 1999. Comparative evaluation of compact photobioreactors for large-scale monoculture of microalgae. *Journal of Biotechnology*, 70, no. 1, pp. 249-270. DOI: [https://doi.org/10.1016/S0168-1656\(99\)00079-6](https://doi.org/10.1016/S0168-1656(99)00079-6)
- Monkonsit S, Powtongsook S & Pavasant P 2011. Comparison between airlift photobioreactor and bubble column for *Skeletonema costatum* cultivation. *Engineering Journal*, 15, no. 4, pp. 53-64. DOI: <https://doi.org/10.4186/ej.2011.15.4.53>
- Nakamura Y & Miyachi S 1982. Effect of temperature on starch degradation in *Chlorella vulgaris* 11h cells. *Plant and Cell Physiology*, 23, no. 2, pp. 333-341. DOI: <https://doi.org/10.1093/oxfordjournals.pcp.a076354>
- Nakanishi A, Aikawa S, Ho S-H, Chen C-Y, Chang J-S, Hasunuma T & Kondo A 2014. Development of lipid productivities under different CO<sub>2</sub> conditions of marine microalgae *Chlamydomonas* sp. JSC4. *Bioresource Technology*, 152, pp. 247-252. DOI: <http://dx.doi.org/10.1016/j.biortech.2013.11.009>
- Napolitano GE 1994. The Relationship of Lipids with Light and Chlorophyll Measurements in Freshwater Algae and Periphyton. *Journal of Phycology*,

## References

- 30, no. 6, pp. 943-950. DOI: <https://doi.org/10.1111/j.0022-3646.1994.00943.x>
- Nascimento IA, Marques SSI, Cabanelas ITD, Pereira SA, Druzian JI, de Souza CO, Vich DV, de Carvalho GC & Nascimento MA 2013. Screening Microalgae Strains for Biodiesel Production: Lipid Productivity and Estimation of Fuel Quality Based on Fatty Acids Profiles as Selective Criteria. *BioEnergy Research*, 6, no. 1, pp. 1-13. DOI: <https://doi.org/10.1007/s12155-012-9222-2>
- Naylor RL et al. 2009. Feeding aquaculture in an era of finite resources. *Proceedings of the National Academy of Sciences*, 106, no. 36, pp. 15103-15110. DOI: <https://doi.org/10.1073/pnas.0905235106>
- Nishida I & Murata N 1996. Chilling sensitivity in plants and cyanobacteria: the crucial contribution of membrane lipids. *Annual Review of Plant Biology*, 47, no. 1, pp. 541-568. DOI: <https://doi.org/10.1146/annurev.arplant.47.1.541>
- Nurachman Z et al. 2012. Oil productivity of the tropical marine diatom *Thalassiosira* sp. *Bioresource Technology*, 108, pp. 240-244. DOI: <http://dx.doi.org/10.1016/j.biortech.2011.12.082>
- Ogbonna JC, Soejima T & Tanaka H 1999. An integrated solar and artificial light system for internal illumination of photobioreactors. *Journal of Biotechnology*, 70, no. 1, pp. 289-297. DOI: [https://doi.org/10.1016/S0079-6352\(99\)80121-0](https://doi.org/10.1016/S0079-6352(99)80121-0)
- Oncel S & Sukan FV 2008. Comparison of two different pneumatically mixed column photobioreactors for the cultivation of *Artrospira platensis* (*Spirulina platensis*). *Bioresource Technology*, 99, no. 11, pp. 4755-4760. DOI: <https://doi.org/10.1016/j.biortech.2007.09.068>
- Ono E & Cuello JL 2003. Selection of optimal microalgae species for CO<sub>2</sub> sequestration. Proceedings of Second Annual Conference on Carbon Sequestration, 2003 Alexandria, VA, USA. Citeseer.
- Pal D, Khozin-Goldberg I, Cohen Z & Boussiba S 2011. The effect of light, salinity, and nitrogen availability on lipid production by *Nannochloropsis* sp. *Applied Microbiology and Biotechnology*, 90, no. 4, pp. 1429-1441. DOI: <https://doi.org/10.1007/s00253-011-3170-1>
- Pancha I, Chokshi K, George B, Ghosh T, Paliwal C, Maurya R & Mishra S 2014. Nitrogen stress triggered biochemical and morphological changes in the microalgae *Scenedesmus* sp. CCNM 1077. *Bioresource Technology*, 156, pp. 146-154. DOI: <https://doi.org/10.1016/j.biortech.2014.01.025>
- Pancha I, Chokshi K, Maurya R, Trivedi K, Patidar SK, Ghosh A & Mishra S 2015. Salinity induced oxidative stress enhanced biofuel production potential of microalgae *Scenedesmus* sp. CCNM 1077. *Bioresource Technology*, 189, pp. 341-348. DOI: <https://doi.org/10.1016/j.biortech.2015.04.017>

## References

- Park JBK, Craggs RJ & Shilton AN 2011. Wastewater treatment high rate algal ponds for biofuel production. *Bioresource Technology*, 102, no. 1, pp. 35-42. DOI: <https://doi.org/10.1016/j.biortech.2010.06.158>
- Patil PD, Gude VG, Mannarswamy A, Deng S, Cooke P, Munson-McGee S, Rhodes I, Lammers P & Nirmalakhandan N 2011. Optimization of direct conversion of wet algae to biodiesel under supercritical methanol conditions. *Bioresource Technology*, 102, no. 1, pp. 118-122. DOI: <https://doi.org/10.1016/j.biortech.2010.06.031>
- Perez-Garcia O, Escalante FM, de-Bashan LE & Bashan Y 2011. Heterotrophic cultures of microalgae: metabolism and potential products. *Water research*, 45, no. 1, pp. 11-36. DOI: <https://doi.org/10.1016/j.watres.2010.08.037>
- Petkov GD & Bratkova SG 1996. Viscosity of algal cultures and estimation of turbulence in devices for the mass culture of microalgae. *Algological Studies/Archiv für Hydrobiologie, Supplement Volumes*, 81, pp. 99-104.
- Posten C 2009. Design principles of photo - bioreactors for cultivation of microalgae. *Engineering in Life Sciences*, 9, no. 3, pp. 165-177. DOI: <https://doi.org/10.1002/elsc.200900003>
- Prado JM, Veggi PC & Meireles MAA 2014. Supercritical Fluid Extraction Of Lemon Verbena (*Aloysia triphylla*): Process Kinetics and Scale-Up, Extract Chemical Composition and Antioxidant Activity, and Economic Evaluation. *Separation Science and Technology*, 49, no. 4, pp. 569-579. DOI: <https://doi.org/10.1080/01496395.2013.862278>
- Price C 1965. A membrane method for determination of total protein in dilute algal suspensions. *Analytical Biochemistry*, 12, no. 2, pp. 213-218. DOI: [https://doi.org/10.1016/0003-2697\(65\)90084-9](https://doi.org/10.1016/0003-2697(65)90084-9)
- Putt R, Singh M, Chinnasamy S & Das KC 2011. An efficient system for carbonation of high-rate algae pond water to enhance CO<sub>2</sub> mass transfer. *Bioresource Technology*, 102, no. 3, pp. 3240-3245. DOI: <https://doi.org/10.1016/j.biortech.2010.11.029>
- Qiang H, Zarmi Y & Richmond A 1998. Combined effects of light intensity, light-path and culture density on output rate of *Spirulina platensis* (Cyanobacteria). *European Journal of Phycology*, 33, no. 2, pp. 165-171. DOI: <https://doi.org/10.1080/09670269810001736663>
- Rana KJ, Siriwardena S & Hasan MR 2009. *Impact of rising feed ingredient prices on aquafeeds and aquaculture production*. Food and Agriculture Organization of the United Nations (FAO).
- Raven JA, Cockell CS & De La Rocha CL 2008. The evolution of inorganic carbon concentrating mechanisms in photosynthesis. *Philosophical Transactions of the Royal Society B: Biological Sciences*, 363, no. 1504, pp. 2641-2650. DOI: <https://doi.org/10.1098/rstb.2008.0020>

## References

- Razzak SA, Hossain MM, Lucky RA, Bassi AS & de Lasa H 2013. Integrated CO<sub>2</sub> capture, wastewater treatment and biofuel production by microalgae culturing—A review. *Renewable and Sustainable Energy Reviews*, 27, pp. 622-653. DOI: <https://doi.org/10.1016/j.rser.2013.05.063>
- Renaud SM, Thinh L-V, Lambrinidis G & Parry DL 2002. Effect of temperature on growth, chemical composition and fatty acid composition of tropical Australian microalgae grown in batch cultures. *Aquaculture*, 211, no. 1-4, pp. 195-214. DOI: [https://doi.org/10.1016/S0044-8486\(01\)00875-4](https://doi.org/10.1016/S0044-8486(01)00875-4)
- Roessler PG 1990. Environmental control of glycerolipid metabolism in microalgae: commercial implications and future research directions. *Journal of Phycology*, 26, no. 3, pp. 393-399. DOI: <https://doi.org/10.1111/j.0022-3646.1990.00393.x>
- Rorrer GL & Cheney DP 2004. Bioprocess engineering of cell and tissue cultures for marine seaweeds. *Aquacultural Engineering*, 32, no. 1, pp. 11-41. DOI: <https://doi.org/10.1016/j.aquaeng.2004.03.007>
- Ross AB, Biller P, Kubacki ML, Li H, Lea-Langton A & Jones JM 2010. Hydrothermal processing of microalgae using alkali and organic acids. *Fuel*, 89, no. 9, pp. 2234-2243. DOI: <https://doi.org/10.1016/j.fuel.2010.01.025>
- Saka S & Kusdiana D 2001. Biodiesel fuel from rapeseed oil as prepared in supercritical methanol. *Fuel*, 80, no. 2, pp. 225-231. DOI: [http://dx.doi.org/10.1016/S0016-2361\(00\)00083-1](http://dx.doi.org/10.1016/S0016-2361(00)00083-1)
- Sathish A & Sims RC 2012. Biodiesel from mixed culture algae via a wet lipid extraction procedure. *Bioresource Technology*, 118, pp. 643-647. DOI: <http://dx.doi.org/10.1016/j.biortech.2012.05.118>
- Šetlík I, Šust V & Málek I 1970. Dual Purpose Open Circulation Units for Large Scale Culture of Algae in Temperate Zones. I. Basic Design Considerations and Scheme of a Pilot Plant. *Algological Studies/Archiv für Hydrobiologie, Supplement Volumes*, 1, pp. 111-164.
- Seyfabadi J, Ramezanzpour Z & Khoeyi ZA 2011. Protein, fatty acid, and pigment content of *Chlorella vulgaris* under different light regimes. *Journal of Applied Phycology*, 23, no. 4, pp. 721-726. DOI: <https://doi.org/10.1007/s10811-010-9569-8>
- Singh A, Pant D, Olsen SI & Nigam PS 2012. Key issues to consider in microalgae based biodiesel production. *Energy Education Science Technology Part A: Energy Science and Research*, 29, no. 1, pp. 687-700.
- Singh RN & Sharma S 2012. Development of suitable photobioreactor for algae production—A review. *Renewable and Sustainable Energy Reviews*, 16, no. 4, pp. 2347-2353. DOI: <https://doi.org/10.1016/j.rser.2012.01.026>
- Singh SP & Singh P 2015. Effect of temperature and light on the growth of algae species: A review. *Renewable and Sustainable Energy Reviews*, 50, pp. 431-444. DOI: <https://doi.org/10.1016/j.rser.2015.05.024>

## References

- Slocombe SP, Ross M, Thomas N, McNeill S & Stanley MS 2013. A rapid and general method for measurement of protein in micro-algal biomass. *Bioresource Technology*, 129, pp. 51-57. DOI: <https://doi.org/10.1016/j.biortech.2012.10.163>
- Sorokin C & Krauss RW 1958. The Effects of Light Intensity on the Growth Rates of Green Algae. *Plant Physiology*, 33, no. 2, pp. 109.
- Suh IS & Lee C-G 2003. Photobioreactor engineering: design and performance. *Biotechnology and Bioprocess Engineering*, 8, no. 6, pp. 313-321. DOI: <https://doi.org/10.1007/BF02949274>
- Sun X, Cao Y, Xu H, Liu Y, Sun J, Qiao D & Cao Y 2014. Effect of nitrogen-starvation, light intensity and iron on triacylglyceride/carbohydrate production and fatty acid profile of *Neochloris oleoabundans* HK-129 by a two-stage process. *Bioresource Technology*, 155, pp. 204-212. DOI: <https://doi.org/10.1016/j.biortech.2013.12.109>
- Sun Z, Dou X, Wu J, He B, Wang Y & Chen Y-F 2015. Enhanced lipid accumulation of photoautotrophic microalgae by high-dose CO<sub>2</sub> mimics a heterotrophic characterization. *World Journal of Microbiology and Biotechnology*, 32, no. 1, pp. 9. DOI: <https://doi.org/10.1007/s11274-015-1963-6>
- Tacon AGJ & Metian M 2009. Fishing for feed or fishing for food: increasing global competition for small pelagic forage fish. *Ambio*, 38, no. 6, pp. 294-302. DOI: <https://doi.org/10.1579/08-A-574.1>
- Taher H, Al-Zuhair S, Al-Marzouqi AH, Haik Y, Farid M & Tariq S 2014. Supercritical carbon dioxide extraction of microalgae lipid: Process optimization and laboratory scale-up. *The Journal of Supercritical Fluids*, 86, pp. 57-66. DOI: <http://dx.doi.org/10.1016/j.supflu.2013.11.020>
- Takagi M & Yoshida T 2006. Effect of salt concentration on intracellular accumulation of lipids and triacylglyceride in marine microalgae *Dunaliella* cells. *Journal of Bioscience and Bioengineering*, 101, no. 3, pp. 223-226. DOI: <https://doi.org/10.1263/jbb.101.223>
- Takahashi S & Badger MR 2011. Photoprotection in plants: a new light on photosystem II damage. *Trends in Plant Science*, 16, no. 1, pp. 53-60. DOI: <https://doi.org/10.1016/j.tplants.2010.10.001>
- Tan CH, Chen C-Y, Show PL, Ling TC, Lam HL, Lee D-J & Chang J-S 2016. Strategies for enhancing lipid production from indigenous microalgae isolates. *Journal of the Taiwan Institute of Chemical Engineers*, 63, pp. 189-194. DOI: <https://doi.org/10.1016/j.jtice.2016.02.034>
- Tang D, Han W, Li P, Miao X & Zhong J 2011a. CO<sub>2</sub> biofixation and fatty acid composition of *Scenedesmus obliquus* and *Chlorella pyrenoidosa* in response to different CO<sub>2</sub> levels. *Bioresource Technology*, 102, no. 3, pp. 3071-3076. DOI: <https://doi.org/10.1016/j.biortech.2010.10.047>

## References

- Tang H, Abunasser N, Garcia MED, Chen M, Simon Ng KY & Salley SO 2011b. Potential of microalgae oil from *Dunaliella tertiolecta* as a feedstock for biodiesel. *Applied Energy*, 88, no. 10, pp. 3324-3330. DOI: <http://dx.doi.org/10.1016/j.apenergy.2010.09.013>
- Thompson Jr GA 1996. Lipids and membrane function in green algae. *Biochimica et Biophysica Acta (BBA)-Lipids and Lipid Metabolism*, 1302, no. 1, pp. 17-45. DOI: [https://doi.org/10.1016/0005-2760\(96\)00045-8](https://doi.org/10.1016/0005-2760(96)00045-8)
- Tjahjono AE, Hayama Y, Kakizono T, Terada Y, Nishio N & Nagai S 1994. Hyper-accumulation of astaxanthin in a green alga *Haematococcus pluvialis* at elevated temperatures. *Biotechnology Letters*, 16, no. 2, pp. 133-138. DOI: <https://doi.org/10.1007/BF01021659>
- Tran D-T, Chen C-L & Chang J-S 2013. Effect of solvents and oil content on direct transesterification of wet oil-bearing microalgal biomass of *Chlorella vulgaris* ESP-31 for biodiesel synthesis using immobilized lipase as the biocatalyst. *Bioresource Technology*, 135, pp. 213-221. DOI: <http://dx.doi.org/10.1016/j.biortech.2012.09.101>
- Tran D-T, Yeh K-L, Chen C-L & Chang J-S 2012. Enzymatic transesterification of microalgal oil from *Chlorella vulgaris* ESP-31 for biodiesel synthesis using immobilized *Burkholderia* lipase. *Bioresource Technology*, 108, pp. 119-127. DOI: <http://dx.doi.org/10.1016/j.biortech.2011.12.145>
- Ugwu CU & Aoyagi H 2012. Microalgal Culture Systems: An Insight into their Designs, Operation and Applications. *Biotechnology*, 11, no. 3, pp. 127. DOI: <https://doi.org/10.3923/biotech.2012.127.132>
- Ugwu CU, Aoyagi H & Uchiyama H 2008. Photobioreactors for mass cultivation of algae. *Bioresource Technology*, 99, no. 10, pp. 4021-4028. DOI: <https://doi.org/10.1016/j.biortech.2007.01.046>
- Vizcaíno AJ et al. 2014. Effects of the microalga *Scenedesmus almeriensis* as fishmeal alternative in diets for gilthead sea bream, *Sparus aurata*, juveniles. *Aquaculture*, 431, pp. 34-43. DOI: <https://doi.org/10.1016/j.aquaculture.2014.05.010>
- Vonshak A & Guy R 1992. Photoadaptation, photoinhibition and productivity in the blue - green alga, *Spirulina platensis* grown outdoors. *Plant, Cell & Environment*, 15, no. 5, pp. 613-616. DOI: <https://doi.org/10.1111/j.1365-3040.1992.tb01496.x>
- Wang B, Lan CQ & Horsman M 2012. Closed photobioreactors for production of microalgal biomasses. *Biotechnology Advances*, 30, no. 4, pp. 904-912. DOI: <https://doi.org/10.1016/j.biotechadv.2012.01.019>
- Wei L et al. 2019. Knockdown of carbonate anhydrase elevates *Nannochloropsis* productivity at high CO<sub>2</sub> level. *Metabolic Engineering*. DOI: <https://doi.org/10.1016/j.ymben.2019.03.004>



## References

- Westerhoff P, Hu Q, Esparza - Soto M & Vermaas W 2010. Growth parameters of microalgae tolerant to high levels of carbon dioxide in batch and continuous - flow photobioreactors. *Environmental Technology*, 31, no. 5, pp. 523-532. DOI: <https://doi.org/10.1080/09593330903552078>
- Xie T, Xia Y, Zeng Y, Li X & Zhang Y 2017. Nitrate concentration-shift cultivation to enhance protein content of heterotrophic microalga *Chlorella vulgaris*: over-compensation strategy. *Bioresource Technology*, 233, pp. 247-255. DOI: <https://doi.org/10.1016/j.biortech.2017.02.099>
- Xin L, Hong-ying H & Yu-ping Z 2011. Growth and lipid accumulation properties of a freshwater microalga *Scenedesmus* sp. under different cultivation temperature. *Bioresource Technology*, 102, no. 3, pp. 3098-3102. DOI: <https://doi.org/10.1016/j.biortech.2010.10.055>
- Xiong W, Li X, Xiang J & Wu Q 2008. High-density fermentation of microalga *Chlorella protothecoides* in bioreactor for microbio-diesel production. *Applied Microbiology and Biotechnology*, 78, no. 1, pp. 29-36. DOI: <https://doi.org/10.1007/s00253-007-1285-1>
- Xu L, Weathers PJ, Xiong XR & Liu CZ 2009. Microalgal bioreactors: challenges and opportunities. *Engineering in Life Sciences*, 9, no. 3, pp. 178-189. DOI: <https://doi.org/10.1002/elsc.200800111>
- Yadavalli R, S RR & Rao CS 2014. Lipid Productivity In *Chlorella Pyrenoidosa* Under Nitrogen Starvation: Energy Evaluation Of An Internally Illuminated Bubble Column Photo Bioreactor. *Asian Journal of Microbiology, Biotechnology and Environmental Sciences*, 16, no. 1, pp. 245-251.
- Yeh KL & Chang JS 2011. Nitrogen starvation strategies and photobioreactor design for enhancing lipid content and lipid production of a newly isolated microalga *Chlorella vulgaris* ESP - 31: Implications for biofuels. *Biotechnology Journal*, 6, no. 11, pp. 1358-1366. DOI: <https://doi.org/10.1002/biot.201000433>
- Yen HW, Ho SH, Chen CY & Chang JS 2015. CO<sub>2</sub>, NO<sub>x</sub> and SO<sub>x</sub> removal from flue gas via microalgae cultivation: A critical review. *Biotechnology Journal*, 10, no. 6, pp. 829-839. DOI: <https://doi.org/10.1002/biot.201400707>
- Zeebe RE & Wolf-Gladrow D 2001. *CO<sub>2</sub> in Seawater: Equilibrium, Kinetics, Isotopes*. In: Halpern D (ed.) Elsevier Oceanography Series. Elsevier, pp. 360.
- Zhan J, Rong J & Wang Q 2017. Mixotrophic cultivation, a preferable microalgae cultivation mode for biomass/bioenergy production, and bioremediation, advances and prospect. *International Journal of Hydrogen Energy*, 42, no. 12, pp. 8505-8517. DOI: <https://doi.org/10.1016/j.ijhydene.2016.12.021>
- Zhang K, Miyachi S & Kurano N 2001. Evaluation of a vertical flat-plate photobioreactor for outdoor biomass production and carbon dioxide bio-fixation: effects of reactor dimensions, irradiation and cell concentration on the biomass productivity and irradiation utilization efficiency. *Applied Microbiology and Biotechnology*, 55, no. 4, pp. 428-433. DOI: <https://doi.org/10.1007/s002530000550>

## References

- Zhang Q, Wang T & Hong Y 2014. Investigation of initial pH effects on growth of an oleaginous microalgae *Chlorella* sp. HQ for lipid production and nutrient uptake. *Water Science and Technology*, 70, no. 4, pp. 712-719. DOI: <https://doi.org/10.2166/wst.2014.285>
- Zhao B & Su Y 2014. Process effect of microalgal-carbon dioxide fixation and biomass production: a review. *Renewable and Sustainable Energy Reviews*, 31, pp. 121-132. DOI: <https://doi.org/10.1016/j.rser.2013.11.054>
- Zou N & Richmond A 1999. Effect of light-path length in outdoor flat plate reactors on output rate of cell mass and of EPA in *Nannochloropsis* sp. *Journal of Biotechnology*, 70, no. 1, pp. 351-356. DOI: [https://doi.org/10.1016/S0079-6352\(99\)80127-1](https://doi.org/10.1016/S0079-6352(99)80127-1)